

DISSERTATION

submitted to the
Combined Faculty of Natural Sciences and Mathematics
of the Ruprecht-Karls-University of Heidelberg, Germany
for the degree of
Doctor of Natural Sciences

Presented by
Rachana Eshwaran, Master of Biological Sciences
born in: Bangalore, India
Oral examination: 12th April, 2022

**Investigation of the potential role of glucosamine
in experimental diabetic retinopathy**

Referees: Prof. Dr. Thomas Wieland

PD Dr. Yuxi Feng

Acknowledgements

This thesis is the culmination of four years of learning, improvement, and hard-work, that would have been impossible without the help of incredible people guiding me through this journey.

I am very thankful to Prof. Dr. Thomas Wieland for giving me the opportunity to work in his lab, glittering with several talented scientists always eager in the pursuit of knowledge. I am also grateful to him for all his insightful comments that helped me bring this project to completion, and his encouragement in broadening the mind through a variety of sources.

To my supervisor PD Dr. Yuxi Feng, I am incredibly thankful for being a wonderful mentor, providing support and encouragement throughout the difficulties encountered, and reigning in my enthusiasm with her experience. I am grateful for her expert advice and for helping foster an incredible scientific environment rife with collaboration, teamwork, and constant scientific curiosity.

A special mention goes out to Heike Rauscher, who always stood by my side during animal experiments. I am also very appreciative of all the technicians in the lab, Doris, Tina, Sabine, and Heinz, who ran the lab smoothly and helped vastly improve my German speaking skills.

I would also like to acknowledge the support from DIAMICOM and Prof. Dr. Hans-Peter Hammes, whose excitement about the diabetic field is truly contagious. The Autumn and Spring Schools helped transfer and develop knowledge about diabetic complications while fostering both scientific and personal connections with other members. Similarly, I would also like to acknowledge HBIGS, whose mentoring opportunities helped me hone not only my scientific but also my project management and business skills.

A crucial part of my memories in the lab and during the PhD have been the wonderful colleagues I was blessed to work alongside. Through long days in the lab broken by raucous lunch breaks to picnics, bike rides, fictional fantasy discussions, and food and more food, I will forever cherish my times with Anu, Joost, Santosh, Philip, Hongpeng, Yohanes, Nan, Pan, Atif, and Timo, who made the hard times much easier to get through.

Throughout my academic journey, I have always been incredibly overwhelmed with support from my family and friends. My parents and my brother have constantly been my champions, and I am forever grateful for their cheers. I am also incredibly thankful to Tim Heckmann for being by my side, celebrating my victories and tirelessly listening to my tribulations. A huge thank you also goes out to Akanksha Roy and Grusha Mathias for sharing stories of their misfortunes in their PhDs with me to make me feel better about my own, and for always being there for both mindless gossip and heartfelt conversations.

Table of Contents

Acknowledgements.....	iii
Table of Contents.....	v
List of Figures	viii
List of Tables	ix
Summary	x
Zusammenfassung	xii
Abbreviations.....	xiv
1. Introduction.....	1
1.1. Diabetic retinopathy	1
1.1.1. Pathology and progression of diabetic retinopathy	2
1.1.2. Involvement and regulation of retinal cell types in DR	6
1.1.3. Hexosamine biosynthetic pathway (HBP)	15
1.2. Glucosamine in the HBP.....	17
1.2.1. Pharmacokinetic properties of glucosamine.....	18
1.2.2. Glucosamine in osteoarthritis	19
1.2.3. Characteristics of glucosamine.....	20
2. Aims of the study.....	23
3. Materials.....	25
3.1. Cell Culture.....	25
3.1.1. Cell isolations and cell lines	25
3.1.2. Cell Culture medium and supplements	25
3.1.3. Cell Culture reagents and enzymes	26
3.2. Buffers and chemicals	26
3.2.1. Cell culture buffers	26
3.2.2. Protein analysis buffers	27
3.2.3. Immunofluorescence buffers	28
3.2.4. Retina digestion buffers.....	28
3.3. Chemicals	29
3.4. Antibodies	31

3.4.1. Primary antibodies.....	31
3.4.2. Secondary antibodies	32
3.5. qPCR primers and master mix.....	33
3.6. Consumables	34
3.7. Kits.....	36
3.8. Apparatus	36
3.9. Software	38
4. Methods	38
4.1. <i>In vivo</i> methods.....	38
4.1.1. Maintenance of the animals.....	38
4.1.2. Analysis of metabolites.....	39
4.1.3. Optical Coherence Tomography	39
4.1.4. Electroretinogram.....	40
4.1.5. Retinal digestion and retinal morphometry analysis	40
4.1.6. Retina Whole-mount Immunofluorescence	42
4.2. <i>In vitro</i> methods	43
4.2.1. Cell culture.....	43
4.3. Protein Biochemical Methods.....	47
4.3.1. Protein extraction from cells	47
4.3.2. Protein extraction from the retina	47
4.3.3. Protein concentration estimation using BCA assay.....	48
4.3.4. Protein denaturation	49
4.3.5. Immunoblotting/Western blotting.....	49
4.4. Immunofluorescence staining.....	53
4.4.1. Seeding and fixation of cells on coverslips	53
4.4.2. Immunofluorescence staining in cells	53
4.5. ELISA for VEGF detection	54
4.6. RNA and qPCR techniques.....	54
4.6.1. RNA Isolation from retina	54
4.6.2. RNA isolation from Müller cells.....	55
4.6.3. cDNA synthesis	56
4.6.4. Actin PCR and agarose gel electrophoresis	56

4.6.5. qPCR and analysis	58
4.7. Data quantification and statistical analysis.....	59
5. Results	60
5.1. Glucosamine supplementation in mice does not alter their metabolic parameters.....	60
5.2. Glucosamine treatment increases its levels in the blood, but is non-toxic	60
5.3. Glucosamine affects neither blood glucose nor HbA1c, but induces body weight gain	63
5.4. Retinal thickness is unaltered by glucosamine	65
5.5. Glucosamine exerts a neuroprotective effect in the retina.....	67
5.6. Astrocyte coverage in the retina is unaffected by glucosamine.....	68
5.7. Müller cell activation in the diabetic retina is reduced by glucosamine	69
5.8. Glucosamine decreases activation of Müller cells and reduces the expression of VEGF <i>in vitro</i>	71
5.9. Glucosamine does not alter expression of neurotrophic factors in Müller cells.....	74
5.10. Inflammatory and angiogenic factors are not influenced at the transcriptional level by glucosamine	75
5.11. Glucosamine aggravates vascular damage in the retina	78
5.12. Glucosamine suppresses survival signaling in endothelial cells	80
6. Discussion	90
6.1. Glucosamine-induced neuroprotection and related mechanisms	90
6.2. Glucosamine-induced vascular damage and related mechanisms.....	94
6.3. Glucosamine effect on blood glucose, HbA1c, and body weight.....	97
6.4. Limitations of the study	98
7. Conclusion	99
References	100

List of Figures

<i>Figure 1: Diabetic retinopathy as a disease of the neurovascular unit.....</i>	<i>1</i>
<i>Figure 2: Biochemical processes involved in the pathology of diabetic retinopathy</i>	<i>3</i>
<i>Figure 3: Diabetic retinopathy damages the neurovascular unit.....</i>	<i>5</i>
<i>Figure 4: Angiopoietin-Tie interactions.....</i>	<i>9</i>
<i>Figure 5: Interaction between glial and vascular cells in the retina</i>	<i>14</i>
<i>Figure 6: The hexosamine biosynthesis pathway.....</i>	<i>16</i>
<i>Figure 7: Biophysical properties of glucosamine.....</i>	<i>18</i>
<i>Figure 8: Signaling pathways regulated by glucosamine.....</i>	<i>22</i>
<i>Figure 9: Standard curve of BCA assay.....</i>	<i>49</i>
<i>Figure 10: Assembly of blotting sandwich</i>	<i>52</i>
<i>Figure 11: Actin PCR.....</i>	<i>58</i>
<i>Figure 12: Metabolic parameters of the mice are not impacted by glucosamine</i>	<i>61</i>
<i>Figure 13: Glucosamine is increased in plasma after supplementation</i>	<i>62</i>
<i>Figure 14: Liver function enzymes in plasma are not influenced by glucosamine</i>	<i>63</i>
<i>Figure 15: Glucosamine does not affect blood glucose or HbA1c.....</i>	<i>64</i>
<i>Figure 16: Retinal thickness is unaffected.....</i>	<i>65</i>
<i>Figure 17: Retinal cell number and layer thickness are unaffected</i>	<i>66</i>
<i>Figure 18: Glucosamine is neuroprotective in the retina</i>	<i>68</i>
<i>Figure 19: Astrocyte coverage in the retina is unaffected</i>	<i>70</i>
<i>Figure 20: Glucosamine reduces Müller cell activation in the retina.....</i>	<i>72</i>
<i>Figure 21: Glucosamine reduces rat Müller cell activation.....</i>	<i>73</i>
<i>Figure 22: Neurotrophic factor mRNA expression is uninfluenced by glucosamine</i>	<i>76</i>
<i>Figure 23: Inflammatory factors in the retina and mouse Müller cells are not impacted by glucosamine</i>	<i>77</i>
<i>Figure 24: Angiogenic and survival factors are not influenced at transcriptional level by glucosamine....</i>	<i>78</i>
<i>Figure 25: Glucosamine aggravates vascular damage in the retina.....</i>	<i>79</i>
<i>Figure 26: Glucosamine is harmful to endothelial cells in higher concentrations</i>	<i>81</i>
<i>Figure 27: Glucosamine alters Ang2 and VEGFR2 content in HUVECs.....</i>	<i>83</i>
<i>Figure 28: Glucosamine alters Ang2 and VEGFR2 content independently of the glucose concentration... ..</i>	<i>84</i>
<i>Figure 29: Glucosamine alters Ang2 and VEGFR2 content in HUVECs.....</i>	<i>85</i>
<i>Figure 30: Glucosamine does not influence VEGF protein content or secretion</i>	<i>86</i>
<i>Figure 31: Glucosamine does not influence AKT and ERK1/2 phosphorylation</i>	<i>87</i>
<i>Figure 32: Glucosamine Glucosamine alters Ang2 and VEGFR2 content in HRMVECs.....</i>	<i>88</i>
<i>Figure 33: Glucosamine suppresses survival signaling in HRMVECs.....</i>	<i>89</i>

List of Tables

<i>Table 1: Cell isolations and cell lines</i>	25
<i>Table 2: Cell culture medium and supplements</i>	25
<i>Table 3: Cell Culture reagents and enzymes</i>	26
<i>Table 4: Cell Culture buffers</i>	26
<i>Table 5: Protein analysis buffers</i>	27
<i>Table 6: Immunofluorescence buffers</i>	28
<i>Table 7: Retina digestion buffers</i>	28
<i>Table 8: List of chemicals</i>	29
<i>Table 9: Primary antibodies</i>	31
<i>Table 10: Secondary antibodies</i>	32
<i>Table 11: qPCR primers and master mix</i>	33
<i>Table 12: Consumables</i>	34
<i>Table 13: Kits</i>	36
<i>Table 14: Apparatus</i>	36
<i>Table 15: Software</i>	38
<i>Table 16: Periodic Acid-Schiff staining</i>	41
<i>Table 17: Cell seeding for cell culture and experiments</i>	46
<i>Table 18: Lysis buffer addition based on cell density</i>	47
<i>Table 19: Gel percentage determined according to protein molecular mass</i>	50
<i>Table 20: Components and volumes for casting separating gels</i>	50
<i>Table 21: Components and volumes for casting stacking gels</i>	51
<i>Table 22: Program for cDNA synthesis in thermal cyclers</i>	56
<i>Table 22: Components and volumes for actin PCR</i>	57
<i>Table 23: Program for actin PCR in thermal cyclers</i>	57
<i>Table 24: Components and volumes for qPCR</i>	58

Summary

The hexosamine biosynthesis pathway (HBP), an offshoot of glycolysis, functions as a nutrient sensing pathway, and incorporates elements of amino acid, fatty acid, glucose, and nucleotide metabolisms. The HBP is implicated in post-translational protein modification via O-GlcNAc cycling, and plays a role in the initiation and progression of diabetic retinopathy.

Glucosamine, an intermetabolite in the HBP, is a hexose sugar that is found naturally occurring in bones and crustacean shells. It is currently widely prescribed as an oral supplement in the treatment of osteoarthritis to promote cartilage renewal and to restore normal joint function. Due to its antioxidative and anti-inflammatory properties, and its role in the HBP, the aim of this study was to investigate the role of glucosamine in an experimental model of diabetic retinopathy, and to uncover the underlying mechanism of action using cultured cell models.

The general metabolic parameters including blood glucose, HbA1c, the consumption of food and water, and the subsequent excretion of urine and feces were unaffected by glucosamine supplementation in the diet. Despite this, the non-diabetic animals treated with glucosamine exhibited a body weight gain compared to the controls.

Examination of the neuroretinal function *in vivo* via electroretinogram (ERG) showed that supplementation of glucosamine reduced the P1-wave amplitude elevated in diabetic animals, suggesting an improvement in neuroretinal function possibly via modulation of Müller cells. Moreover, cultured Müller cells treated with glucosamine demonstrated a decrease in GFAP expression, suggesting an amelioration in Müller cell function that correlates with the *in vivo* ERG results. Additionally, reduction in VEGF expression in the Müller cells upon glucosamine treatment was detected, indicating a possible impact of glucosamine on retinal vasculature.

However, glucosamine supplementation induced vascular damage in the retina, which is also a prominent characteristic in diabetic retinopathy. Unexpectedly, similar to the diabetic animals, glucosamine-treated retinas showed increased pericyte loss and acellular capillary numbers in the non-diabetic and diabetic retinas. The assessment of endothelial signaling showed a dose-dependent decrease in Ang2 and VEGFR2 protein levels upon glucosamine treatment in both

normal and high glucose conditions, suggesting that glucosamine may cause vascular damage by interfering with endothelial survival signals.

In conclusion, glucosamine can have multi-faceted effects, and any supplementation, especially in osteoarthritis patients suffering concomitantly with diabetes, should be taken with care.

Zusammenfassung

Der Hexosamin-Biosyntheseweg (HBP), eine Abzweigung der Glykolyse, verbindet als Nährstoffsensor die Aminosäure-, Fettsäure-, Glukose- und Nukleotid-stoffwechsel. Der HBP ist an der posttranslationalen Proteinmodifikation über den O-GlcNAc-Zyklus beteiligt und spielt eine Rolle bei der Initiation und dem Fortschreiten der diabetischen Retinopathie.

Glucosamin, ein Intermetabolit im HBP, ist eine Hexose, die ursprünglich in Knochen und den Schalen von Krustentieren gefunden wurde. Es wird derzeit häufig als orales Ergänzungsmittel bei der Behandlung von Osteoarthritis verwendet, um die Knorpelregenerierung und die Verbesserung der Gelenkfunktion zu fördern. Aufgrund der antioxidativen und entzündungshemmenden Eigenschaften und der Rolle von Glucosamin im HBP war das Ziel dieser Studie, die Rolle von Glucosamin in der experimentellen diabetischen Retinopathie zu untersuchen und die zugrunde liegenden Wirkmechanismen anhand von kultivierten Zellmodellen herauszufinden.

Die allgemeinen Stoffwechselfparameter von den Tieren wie Blutzucker, HbA1c, Nahrungs- und Wasseraufnahme, und die anschließende Ausscheidung von Urin und Kot wurden durch die Zugabe von Glucosamin in der Nahrung nicht beeinflusst. Jedoch zeigten die mit Glucosamin behandelten nicht diabetischen Tiere eine Körpergewichtszunahme im Vergleich zur Kontrollgruppe.

Die Untersuchung der neuroretinalen Funktion *in vivo* mittels Elektroretinogramm (ERG) zeigte, dass Glucosamin die durch Diabetes erhöhte P1-Wellen-Amplitude reduzierte, was eine verbesserte neuroretinale Funktion, möglicherweise durch eine Modulation der Müller-Zellen, hervorruft. Weiterhin zeigte sich in den mit Glucosamin behandelten Müller-Zellen *in vitro* eine Herunterregulation der GFAP-Expression, was auf eine Verbesserung der Müllerzellfunktion hinwies, und dadurch mit den ERG-Ergebnissen *in vivo* einherging. Darüber hinaus wurde eine Reduktion der VEGF-Expression in den Müllerzellen nach der Glucosaminbehandlung detektiert, was auf eine mögliche Wirkung von Glucosamin auf die retinalen Gefäße hindeutet.

Eine Glucosamin-Supplementierung induzierte hingegen Gefäßschäden in der Retina, ein Merkmal der diabetischen Retinopathie. Ähnlich wie bei den diabetischen Tieren zeigten die mit Glucosamin behandelten Retinae unerwartet einen erhöhten Perizytenverlust und eine vermehrte Anzahl an azellulären Kapillaren in nicht diabetischen Retinae. Die Analyse der endothelialen Signalwege stellte eine glukosamindosisabhängige Herunterregulation der Ang2- und VEGFR2- Expression unter normaler und hoher Glukose dar. Daher kann Glucosamin zu Gefäßschäden, wahrscheinlich durch die Inhibition der endothelialen Überlebenssignale, führen.

Zusammenfassend lässt sich die Schlussfolgerung ziehen, dass Glucosamin vielfältige Wirkungen in der Retina ausüben kann. Eine Supplementierung mit Glukosamin sollte aber, insbesondere bei Osteoarthritis-Patienten mit Diabetes, mit Vorsicht angewendet werden.

Abbreviations

ACs	Acellular capillaries
Ang	Angiopoietin
ANOVA	Analysis of variance
APS	Ammonium peroxide sulfate
BDNF	Brain derived neurotrophic factor
BM	Basement membrane
BRB	Brain retinal barrier
BSA	Bovine serum albumin
DAPI	4',6-diamidino-2-phenylindole
dH ₂ O	Distilled water
DM	Diabetes mellitus
DMEM	Dulbecco's Modified Eagles Medium
DMSO	Dimethyl sulfoxide
DNA	Deoxyribonuclein acid
DR	Diabetic retinopathy
ECBM	Endothelial cell basal medium
ECGM	Endothelial cell growth medium
ECGM MV	Microvascular endothelial cell growth medium
ECs	Endothelial cells
EDTA	Ethylenediaminetetraacetic acid
eNOS	Endothelial nitric oxide synthase 3
ERG	Electroretinogram
FCS	Fetal calf serum
FITC	Fluorescein Isothiocyanate
GDNF	Glial derived neurotrophic factor
GFAP	Glial fibrillary acidic protein
GFAT	Glutamine:fructose-6phosphae amidotransferase

GlcN	Glucosamine
HbA1c	Glycated hemoglobin
HBP	Hexosamine biosynthesis pathway
HRMVECs	Human retinal microvascular endothelial cells
HUVECs	Human umbilical vein endothelial cells
KCl	Potassium chloride
NaCl	Sodium chloride
NaHCO ₃	Sodium bicarbonate
NaOH	Sodium hydroxide
OCT	Optical Coherence Tomography
OGA	O-GlcNAcase
O-GlcNAc	O-linked N-Acetylglucosamine
OGT	O-GlcNAc transferase
PAGE	Polyacrylamide gel electrophoresis
PBS	Phosphate buffered saline
PCR	Polymerase chain reaction
PCs	Pericytes
PFA	Paraformaldehyde
rMCs	Rat Müller cells
RT	Room temperature
SDS	Sodium dodecyl sulfate
TEMED	Tetramethylethylenediamine
TBS	Tris buffered saline
UDP-GlcNAc	Uridine diphosphate N-Acetylglucosamine
VEGF	Vascular endothelial growth factor
VEGFR2	Vascular endothelial growth factor receptor 2
WB	Western Blotting

1. Introduction

1.1. Diabetic retinopathy

Diabetic retinopathy (DR) is one of the most common long-term complications of diabetes, and is the most frequent cause of blindness in working-age adults. Over 80% of patients suffering for over two decades with type 1 diabetes mellitus develop diabetic retinopathy [1]. DR and other diabetic eye complications such as diabetic macular edema are increasing threats to quality of life of diabetic patients. The visual impairment caused by DR has increased by 64 % from 1990 to 2010, accompanied by a 27 % rate of increase in blindness [2]. In its early stages, DR presents in a largely asymptomatic manner; patients with diabetes should hence undergo regular eye screenings in order to detect the complication in a timely manner. DR can initially be diagnosed based on the observation of the fundus; additionally, the diagnosis may also be based upon functional tests such as electroretinogram (ERG) and retinal blood flow [3]. Diabetic macular edema is often present at the later stages of DR, and can be observed and quantified by measuring the retinal thickness using optical coherence tomography (OCT) [2].

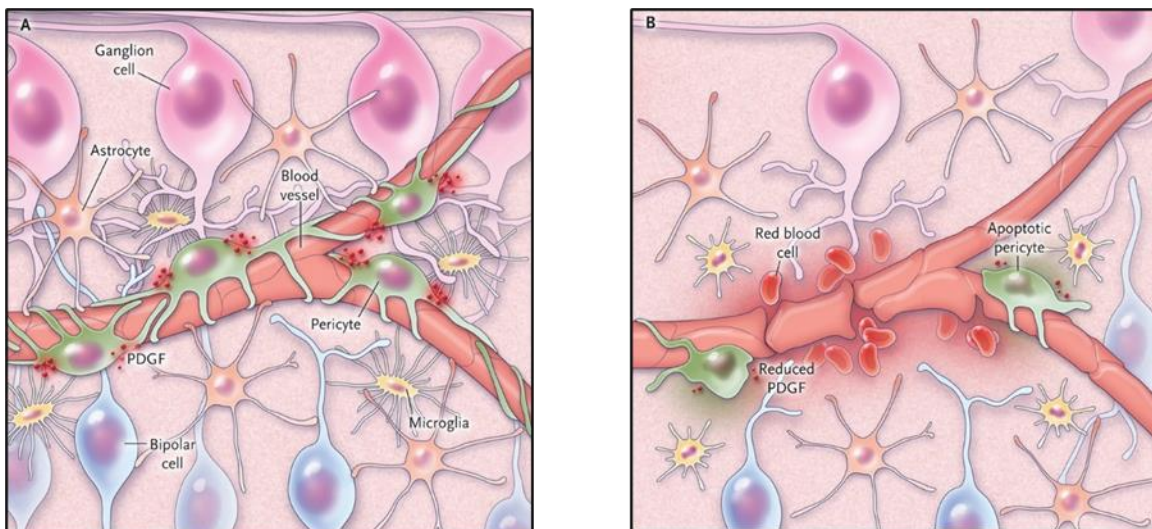


Figure 1: Diabetic retinopathy as a disease of the neurovascular unit. Graphic representation of the retinal neurovascular unit in the normal retina (left) and the diabetic retina (right) showing loss of pericytes, abnormal vessels with increased permeability, and overall reduced integrity, displaying that diabetic retinopathy causes dysfunction of the neurovascular unit. Reproduced with permission from David A. Antonetti, 2012 [4], copyright Massachusetts Medical Society.

DR is characterized by progressive alterations in the retinal microvasculature, and is influenced by several systemic features of diabetes (Fig. 1). Some of the earliest changes in DR include the loss of pericytes from the microvasculature and the subsequent loss of endothelial cells, leading to capillaries consisting of only the basement membrane that do not support blood flow, namely, acellular capillaries (ACs). This leads to increased vessel permeability and hence retina perfusion [5]. Additionally, the appearance of microaneurysms, adhesion of leucocytes, and the apoptosis of neuronal cells also signal the beginnings of DR. These pathological changes together contribute to the development of hypoxia in the retina and subsequent neo-vascularization, which is the hallmark of the late stages of DR [6].

Current therapeutic strategies to manage DR include anti-VEGF therapy to suppress/inhibit the formation of new, abnormal blood vessels, laser photocoagulation therapy, intravitreal injections of steroid agents, and vitreoretinal surgery. Most treatment paradigms focus on the treatment of advanced DR [2, 7].

1.1.1. Pathology and progression of diabetic retinopathy

The pathogenesis of DR is a complex process; several factors contribute to the pathophysiology. Chronic hyperglycemia in the retinal vasculature results in the formation and accumulation of advanced glycation end products (AGEs), neuronal dysfunction, inflammation, and oxidative stress (Fig. 2). The combination of these biochemical changes is hypothesized to lead to vascular damage in the retina [8].

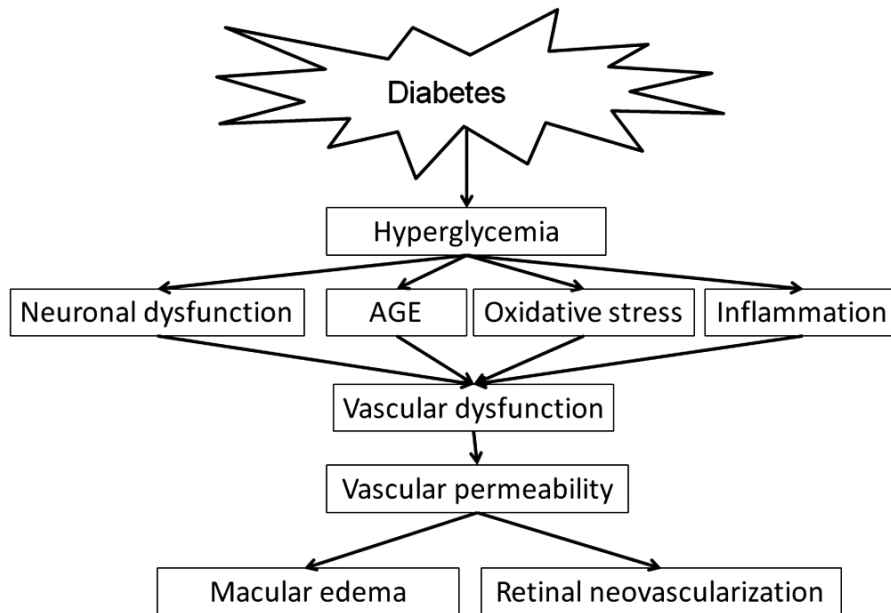


Figure 2: Biochemical processes involved in the pathology of diabetic retinopathy. Graphical representation of the cascade of events triggered by hyperglycemia in diabetes, eventually leading to diabetic retinopathy. Adapted from Shin et al, 2014 [8], and used in accordance with CC BY 4.0 license.

Non-proliferative diabetic retinopathy (NPDR) is the earliest stage of DR, and is characterized morphologically by vasoregression, or retinal vascular damage. In the diabetic retina, vasoregression begins with the loss of pericytes (PCs) from the retinal vasculature. Since the pericytes wrap around retinal capillaries and provide structural support in addition to modulating endothelial cell function, their loss leads subsequently to the loss of endothelial cells (ECs) and the formation of acellular capillaries (ACs) [3]. Biochemical and molecular changes that occur in the endothelial cells and pericytes lead to this vasoregression. Pericyte dropout is considered one of the earliest morphological changes seen in DR development, and can occur as early as 2 months after the onset of diabetes in experimental mouse and rat models [9]. It has been shown that pericyte loss in the diabetic retina is mediated via hyperglycemia-induced increase in angiotensin-2 (Ang2) secreted by ECs [10]. Additionally, the AGEs formed due to sustained hyperglycemia contribute to the expansion of the basement membrane (BM). This modification of the BM by the AGEs regulates signaling pathways mediated by platelet-derived growth factor, hence affecting the survival of pericytes [11]. Another proposed mechanism is pericyte migration,

suggesting that pericytes migrate from injured capillaries for survival, although the fate of the migrating pericytes is yet unknown [5].

DR is not only a vascular disease, but also a neuronal one. The vasculature in the retina is tied closely with the neuronal system, interconnected via the crosstalk between the closely-located cell types, forming the retinal neurovascular unit (NVU) [12]. The capillaries in the retina are made of endothelial cells and pericytes that have cell-cell contact with macroglia (Müller cells and astrocytes), neural processes, and microglia. The interactions of the neurons, glia, and vascular cells regulate the blood flow and the neuronal microenvironment [2] (Fig. 3).

Controversy has reigned since 1875 over whether DR begins with vasoregression or neuronal degeneration. While the initial leading theories suggested the commencement of DR with vascular damage, recent studies have shown that retinal neurodegeneration, characterized by neural apoptosis and reactive gliosis, is an early event in the pathogenesis of DR, and may precede or parallel the vascular damage [13, 14]. Neural apoptosis in the retina was detected prior to retinal vascular apoptosis [15]; neural apoptosis in the retina is also associated with and mediated by inflammation, oxidative stress, and the breakdown of the BRB [16].

The damage to the neurons in DR can be attributed to the activation of glial cells, such as Müller cells, which closely interact with the retinal vasculature and release growth factors such as vascular endothelial growth factor (VEGF) and neurotrophic factors such as nerve growth factor (NGF) and ciliary neurotrophic factor (CNTF) [17, 18]. DR can reduce the ability of the Müller cells to process and remove glutamate from extracellular spaces, hence increasing the total glutamate level in the retina, which can induce retinal neuronal apoptosis [19]. Reduction in retinal thickness, observed via OCT, can serve as an indicator of neurodegeneration in the retina. Apart from neuronal cell death, the process of neurodegeneration in DR can also include changes in neuronal morphology, alterations in neurotransmission, and neurotransmitter metabolism [20]. The neuronal cell death observed in DR is closely related to vascular damage, corresponding to the same regions of the retina, suggesting that there are close interactions between the neuronal and vascular components of the retina, and that this interaction is vital to the maintenance of the BRB and hence retinal function [21].

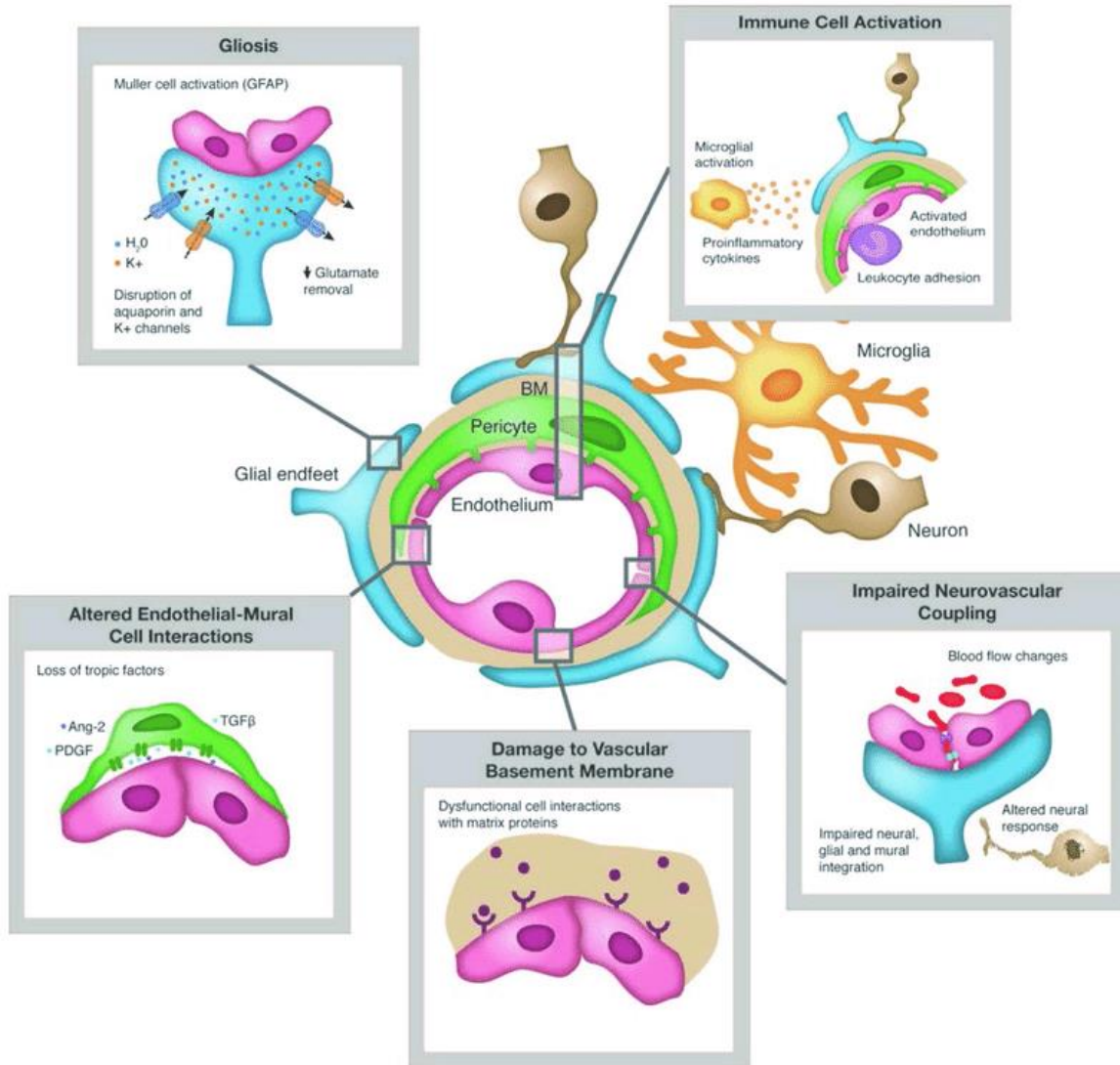


Figure 3: Diabetic retinopathy damages the neurovascular unit. Graphical representation demonstrating the damaging capacity of chronic hyperglycemia and subsequent diabetic retinopathy on the various cell types found in the neurovascular unit. Adapted from Duh et al 2017 [2], and used in accordance with CC BY 4.0 license.

In addition to hyperglycemia, evidence suggests that oxidative stress and inflammation in the retina may play a major role in the pathogenesis of DR. Upsurge in reactive oxygen species (ROS) levels in the diabetic retina leads to increased oxidative stress [22], which is further related with vascular damage and dysfunction – pericyte loss, formation of ACs, and thickening of the BM, eventually leading to increased vascular permeability and vascular leakage [23, 24]. Proinflammatory lipids, insulin dysregulation, and epigenetic changes have also been implicated

in the progression of DR [25]. Biochemical pathways such as the polyol pathway and the hexosamine pathway are involved in the pathogenesis of DR.

1.1.2. Involvement and regulation of retinal cell types in DR

The retina consists of four major cellular components that can be affected by the hyperglycemia during DR:

a) *Blood vessels*: Formed of endothelial cells and pericytes, they are responsible for the blood flow through the retina. ECs line the interior surface of the blood vessels, forming the BRB along with the basement membrane, and pericytes are mesenchymal cells that envelop the ECs and the capillaries, providing structural support and integrity to the vasculature.

b) *Glial cells*: In the retina, astrocytes and Müller cells form the glial cell component. Glial cells in the retina form physical and biochemical connections between the neuronal and vascular components in the retina, and are hence key mediators of the neurovascular dysfunction associated with DR.

c) *Neurons*: Consisting of photoreceptors, bipolar cells, horizontal cells, ganglion cells, and amacrine cells, neurons transmit electrochemical impulse to the brain for sensory processing.

d) *Microglia*: These cells respond to stress and injury in the retina, and modulate immune function in the retina by releasing cytokines and recruiting macrophages, thereby maintaining retina homeostasis.

Endothelial cells and Müller cells are the main focus in this study, and their regulation in DR will be discussed in detail in the following sections.

1.1.2.1. Endothelial cells and pericytes – how they influence DR progression

Endothelial cells and pericytes are the major vascular components in the retina, contributing towards the maintenance of the BRB along with neuronal components such as astrocytes and Müller cells. Diabetes and DR lead to the loss of vascular cells in the retina, specifically pericytes. Pericytes are critical for the maintenance of vascular integrity. They are in close contact with endothelial cells through tight junctions, adhesion junctions, gap junctions, and peg and socket contacts. Sufficient pericyte coverage in the retina is critical for maintaining the stability of endothelial tubes [26]. Pericyte dropout is hence a major destabilization factor of the retinal vasculature, and is a hallmark in early DR. Increased vascular cell apoptosis has been observed throughout the entire retinal vasculature in DR [15]. This apoptosis is thought to occur of pericytes, leaving behind pericyte ghosts, which are empty pockets in the BM that appear to have once contained pericytes [27]. Pericyte loss does not diminish the number of endothelial cells in the retinal vessels; in fact, it may even lead to increased endothelial cell proliferation, which in turn results in the formation of microaneurysms [8].

Pericyte loss in the diabetic retinal vasculature leads hence to the destabilization of the retinal vasculature, resulting in the formation of acellular capillaries (ACs), which have less than one-fourth of the normal capillary diameter. These ACs consist of only the BM without any cell nuclei, and are unable to support blood flow [28]. In this manner, the loss of pericytes can lead to reduced blood flow through the capillaries, and microaneurysms.

The loss of pericytes from the retinal microvasculature is also mediated by regulation from the endothelial cells, in particular, through the Angiopoietin-Tie (Ang-Tie) signaling pathway. **The**

Angiopoietin2-Tie2 system

The Ang-Tie signaling pathway is a vascular cell-specific receptor tyrosine kinase pathway that plays a critical role in vessel development and maintenance. The Tie receptors are expressed selectively on endothelial cells and pericytes [29], and signaling via the Ang-Tie pathway promotes endothelial cell survival, vascular stability and maturation [30]. Angiopoietin 1 (Ang1) and angiopoietin 2 (Ang2) are among the ligands that bind to the major Tie receptor, Tie2, in order to regulate vascular development and function. Although they bind with similar affinity to Tie2, they regulate the activity of Tie2 in a differential manner (Fig. 4). While Ang1 is a strong

agonist of Tie2 and leads to its phosphorylation and subsequent signaling, Ang2 can act either as an agonist or an antagonist in a context-dependent manner [31, 32]. Ang2 is expressed primarily by endothelial cells and Müller cells in the retina, and is released in response to specific stimuli [33, 34]. It was hypothesized that, based on the effects of Ang1 and Ang2 binding to the Tie2 receptor, the Ang2-Tie2 system mediates pericyte loss in DR in the retina.

Several studies have been conducted to show the effect of Ang2 in pericyte loss. In mouse models of DR, increased Ang2 levels are observed prior to the first morphological changes [35], and these elevated Ang2 levels are correlated with increased loss of pericytes [36]. Injection of recombinant Ang2 into the eyes of normal rats led to a dose-dependent increase in pericyte loss [35]. Elevated levels of Ang2 were also correlated with increased levels of proapoptotic factor BAX and decreased levels of antiapoptotic factor BCL-2, hence suggesting a role in mediating pericyte and endothelial cell apoptosis and dysfunction in DR [37]. Furthermore, studies involving OIR (oxygen-induced retinopathy) mouse models show an increase in Ang2, with the expression peaking at P17 [38, 39]. Overexpression of Ang2 in OIR mouse models also led to reduced pericyte coverage and vascular damage [40]. In retinal pericytes in the presence of TNF α , Ang2 accelerated the process of apoptosis [41]. In transgenic models of DR where Ang2 was overexpressed in both non-diabetic and STZ-induced diabetic mice, the increase in Ang2 led to a worsening in pericyte loss and acellular capillary (AC) formation.

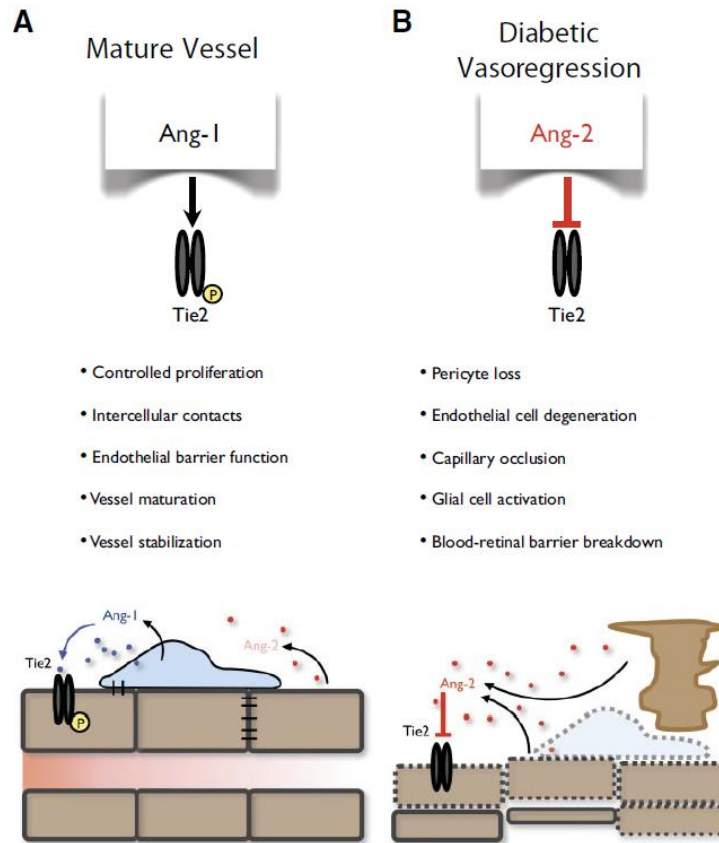


Figure 4: Angiopoietin-Tie interactions. Graphical representation of Ang1 and Ang2 signaling via Tie2 receptor in normal mature vessels and during vasoregression in diabetic retinopathy. Adapted from Hammes et. al, 2011 [5], and used with permission from American Diabetes Association.

In contrast, the heterozygous expression of Ang2 was sufficient to prevent DR-mediated PC dropout [35], and heterozygous Ang2-deficient mice even showed less age-dependent retinal vasoregression [42]. In addition, investigation of a nucleoside diphosphate kinase B (NDPK-B) deficient mouse line, in which Ang2 is upregulated due to NDPK-B deficiency, displayed reduced PC coverage and increase AC formation [43], suggesting that upregulation of Ang2 in the retina, irrelevant of the underlying mechanisms, can result in vasoregression. Additionally, in cultured human retinal endothelial cells, high glucose concentrations that mimic the hyperglycemia in diabetes lead to the upregulation of Ang2 [31, 44].

In endothelial cells, the regulation of Ang2 is thought to be regulated indirectly via hyperglycemia-induced formation of methylglyoxal. This leads to the modification of the

transcriptional co-repressor mSin3A, resulting in the recruitment of O-GlcNAc transferase (OGT) to the mSin3A-Sp3 complex. The resultant increase protein modification of O-GlcNAcylation of the transcriptional factor Sp3 decreased the binding of the complex to the repressor complex of the Ang2 promoter, hence increasing Ang2 expression [45]. Additionally, it was recently shown that increased activation of Foxo1 via O-GlcNAcylation promotes Ang2 expression [46]. In this manner, the Ang2-Tie2 system plays a crucial role in the maintenance of vascular stability in the retina.

1.2.3.1.2. The VEGF-VEGFR2 system

The process of formation of new blood vessels, angiogenesis, is a crucial mechanism in physiological states such as embryogenesis and wound healing, to pathological conditions such as DR and tumorigenesis. Endothelial cells involved in angiogenesis are regulated by a complex network of angiogenic signals that result in their activation, migration into the interstitial space, proliferation, and ultimately formation of new blood vessels [47].

Vascular endothelial growth factor (VEGF) is the primary mitogenic factor that modulates angiogenic signaling in the endothelial cells via receptor tyrosine kinase receptors (VEGFRs). Among the multiple VEGF isoforms, VEGF-A is the most significant stimulus for angiogenic and survival signaling in the retina. Binding of VEGF-A to its cognate receptor, VEGFR2, leads to its phosphorylation and subsequent activation of downstream angiogenic signaling pathways, resulting in mitogenic and survival signals in endothelial cells [48]. VEGF-VEGFR2 signaling activates the PI3K-AKT pathway, which mediates cell survival, proliferation, apoptosis, and permeability by further activating factors such as NFκB, COX-2, eNOS, mTORc1 [49], and also mediating crosstalk with the Wnt and Notch signaling pathways [50]. Moreover, endothelial cell migration via VEGF-VEGFR2 signaling is modulated by downstream signaling via p38-MAPK and AMPK involving pathways [51].

In addition to endothelial cells, VEGF is produced by several other cell types in the retina, including astrocytes, retinal pigment epithelial (RPE) cells, and Müller cells. Due to its role in vasculogenesis, VEGF is a major regulator of pathological neovascularization seen in the later stages of DR, and is involved in the regulation of endothelial and neuronal cell survival as well as

in inflammatory processes in the earlier stages of DR [52]. Recently, more studies have been conducted delving into the role of Müller cell-derived VEGF in retinal cell survival and function in DR. Müller cell-specific knockout (KO) of VEGF-A in diabetic mice resulted in a significant decrease in diabetes-induced retinal vascular leakage and inflammatory factors such as ICAM1 and TNF- α . Furthermore, acellular capillary formation in the diabetic mice was inhibited by the Müller-cell specific VEGF KO [53]. In another study, deletion of VEGFR2 in mouse Müller cells followed by diabetes induction resulted in loss of neuronal function (observed via electroretinogram) and a gradual reduction in Müller cell density and neurotrophic factors such as glial cell-derived neurotrophic factor, suggesting that VEGF-VEGFR2 signaling is required for the viability and function of neuronal and glial cells in the diabetic retina [54].

1.1.2.2. Glial cells

1.2.3.2.1. Müller cell functions

Müller cells are the primary glial cells in the retina. They span the entire depth of the retina, with their main cell body located in the inner nuclear layer and their endfeet forming the inner and outer limiting membranes of the retina [55]. In this way, they form contacts with different cell types in the retina and hence establish communication between the neuronal and vascular factions in the retina.

Müller cells are responsible for a milieu of functions in the maintenance of retinal homeostasis; they provide metabolic support and nutrition to neurons [56, 57], they modulate K⁺ channels [58] and regulate water homeostasis via Aquaporin-4 channels [59], they contribute to neuronal signaling via neurotransmitter uptake and recycling [60-62], and they release neuroactive substances such as D-serine, glutamate, and ATP [63-65]. In addition, they also synthesize and release vasoactive substances such as VEGF, Ang2, and TGF β [34, 66, 67], and scavenge free radicals in the retina to protect against oxidative stress [68, 69].

Müller cells are remarkably resistant cells in the retina that can survive most retinal injuries and are even resistant to ischemia, anoxia, and hypoglycemia [70]. Under pathological conditions, including DR, Müller cells become activated in a process known as Müller cell gliosis. In this

complex process, Müller cells induce microglial activation, vascular signal modulation, and recruitment of leukocytes into the retinal tissue. In addition, Müller cells can produce neurotrophic factors such glial-derived neuronal factor (GDNF) or brain-derived neuronal factor (BDNF), and others that can promote either survival or death of photoreceptor cells [71].

A major characteristic of Müller cell gliosis is the upregulation of glial fibrillary acidic protein (GFAP), which is an intermediate filament protein. This upregulation can be used as an early cellular marker for Müller cell activation, and is considered an indicator of retinal stress due to its sensitivity to various pathological stimuli and injuries, including photoreceptor degeneration, ischemia, and DR [72-77]. In addition, altered expression of glutamine synthase (GS), an enzyme involved in neurotransmitter recycling, is also a gliotic response in Müller cells [78]. GS is expressed specifically by Müller cells in the retina, and is used to convert glutamate to glutamine in Müller cells in the presence of ammonia, and is hence a major component of the glutamate-glutamine cycle [62, 79, 80]. In pathological conditions, including diabetic retinopathy, the GS expressed by the Müller cells is decreased, hence leading to an imbalance in the neurotransmitter recycling [77, 81].

The process of gliosis can be neuroprotective – an attempt by the cells to protect the tissue from further damage by the release of trophic factors and the recruitment of antioxidants. However, the factors released during Müller cell gliosis can have both beneficial and detrimental effects on the surrounding damaged tissue [61]. For example VEGF released during Müller cell gliosis can also induce vascular leakage and abnormal neovascularization in the retina [55].

1.2.3.2.2. Müller cell signaling in DR

In diabetic retinopathy, Müller cells are activated – seen by the upregulation of GFAP – in the early stages of the disease, even prior to the onset of vascular damage. Chronic hyperglycemia in the diabetic retina also induces Müller cell apoptosis in the retina, and *in vitro*, high glucose stimulation of Müller cells can also induce cell death, purportedly via the inactivation of the AKT survival pathway [82].

In the retina, the Müller cells work closely with the retinal vasculature. They regulate retinal blood flow [83] and support the upkeep of the blood-retinal barrier (BRB) by sheathing the

capillary endothelial cells and pericytes in the vessels using their processes, hence increasing barrier integrity. Studies show that co-culture of Müller cells with endothelial cells increases barrier integrity of the endothelial cell monoculture [84], suggesting that Müller cell dysfunction could contribute to defects in BRB function. In addition, factors such as GDNF, neurturin, and pigment epithelium-derived growth factor (PEDF) secreted by the Müller cells increase endothelial barrier integrity, which other factors such as TNF α and VEGF can contribute to its degradation [85-87].

Furthermore, Müller cells contribute to the oxidative stress in the retina during DR by increased expression of nitric oxide synthase and cyclooxygenase-2 enzymes in hyperglycemic conditions [88]. This leads to increased nitric oxide which may induce neuronal cell death [89]. Moreover, inflammation in the diabetic retina leads to altered gene expression in the Müller cells, which upregulate gene transcripts for inflammation-related proteins [90] such as IL-1 β which can affect endothelial cell viability [91].

1.2.3.2.3. Crosstalk between glial and vascular cells

Due to their close proximity, Müller cells secrete various factors that influence the function and integrity of ECs in the retina (Fig. 5). One major way is through the secretion of vascular endothelial growth factor (VEGF). Under normal conditions, Müller cells release anti-angiogenic factors such as PEDF and thrombospondin-1 which suppress proliferation of vascular endothelial cells, preventing pathogenic neovascularization. However, in DR, the expression of VEGF in the Müller cells is increased, preceding the neovascularization in the retina, suggesting that this VEGF contributes directly towards the formation of new, damaged blood vessels in the diabetic retina. Inhibition of VEGF expression in Müller cells led to a decrease in DR-related biomarkers such as the number of ACs, leukostasis, inflammation, and vascular leakage [53, 92, 93].

In addition, advanced glycation end products (AGEs) produced in the retina due to the chronic hyperglycemia in DR can activate the AGE receptors present on Müller cells [94], which further contribute towards increase in VEGF expression [95]. The VEGF, as well as other angiogenic cytokines that are released by gliotic Müller cells in the diabetic retina, also influence endothelial cells by inducing the release of matrix metalloproteases (MMPs) from them [96-98] which impair

tight junction function by proteolytic degradation of the tight junction protein occludin [99]. Furthermore, MMP secretion by endothelial cells leads to their proliferation – MMPs lead the endothelial cells to break through the BM and remove contact inhibition, thus inducing proliferation [100]. Müller cells can also stimulate vasculogenesis via the renin-angiotensin system [101, 102].

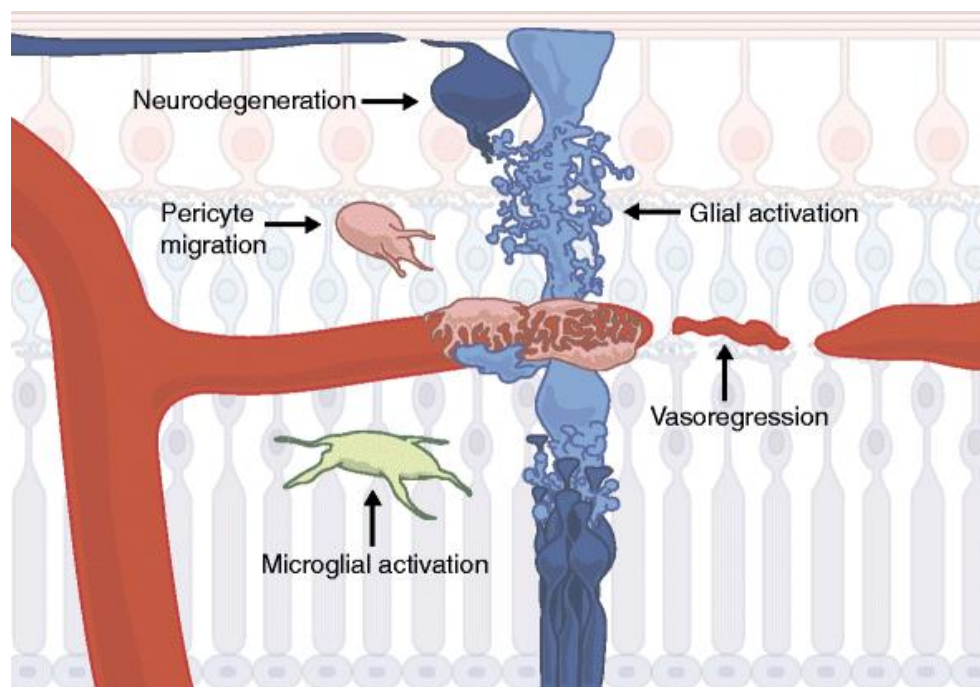


Figure 5: Interaction between glial and vascular cells in the retina. Graphical representation of the interaction between glial cells and vascular cells in the neurovascular unit during vasoregression in diabetic retinopathy. Adapted From Hammes, 2018 [106], and used with permission from Springer Nature.

While a lot of factors released by Müller cells during DR result in detrimental effects in the retina that disrupt vascular function and induce angiogenesis, the evidence accumulated so far suggests that the primary intent is to protect the Müller cells and neurons in the retina from damage due to pathological retinopathy, and the vascular damage is an unfortunate, secondary consequence. More research needs to be performed to delve into the protective nature of Müller cell-derived factors in the context of neuronal protection [103].

1.1.3. Hexosamine biosynthetic pathway (HBP)

The HBP is an offshoot of the glycolytic pathway in the cell, accounting for 2-5% of cellular glucose flux under normal conditions. Glucose is first phosphorylated to glucose-6-phosphate, then isomerized into fructose-6-phosphate, which enters the hexosamine pathway via conversion into glucosamine-6-phosphate with the help of the enzyme glutamine:fructose-6-phosphate amidotransferase and the concomitant conversion of glutamine into glucosamine which is the rate-limiting step [104, 105].

The HBP combines aspects of glucose, amino acid, fatty acid, and nucleotide metabolisms to yield the end product, uridine diphosphate-N-acetylglucosamine (UDP-GlcNAc), which is further used for protein modification by O-GlcNAcylation (Fig. 6). During this process, the GlcNAc moiety from UDP-GlcNAc is reversibly attached to the hydroxyl groups of serine and threonine residues of the target proteins via the enzyme O-GlcNAc-transferase (OGT). The moiety can be removed by the enzyme O-GlcNAcase (OGA), and this process of GlcNAc cycling and protein O-GlcNAcylation has major impacts on protein expression and regulation in the cell, including immune activation, stress response pathways, inflammation transcriptional regulation, protein trafficking, and nutrient sensing [106]. For example, O-GlcNAcylation of transcription factors such as FoxO1, Sp3, and NF- κ B influences their DNA binding ability as well as their stabilization [107], and hence has an impact on glucose metabolism, angiogenesis, and lymphocyte activation [45, 108, 109]. In addition, O-GlcNAcylation on serine and threonine residues of proteins compete with other protein modifications such as phosphorylation and ubiquitination, hence potentially inhibiting their activation or reducing the protein stability [110, 111].

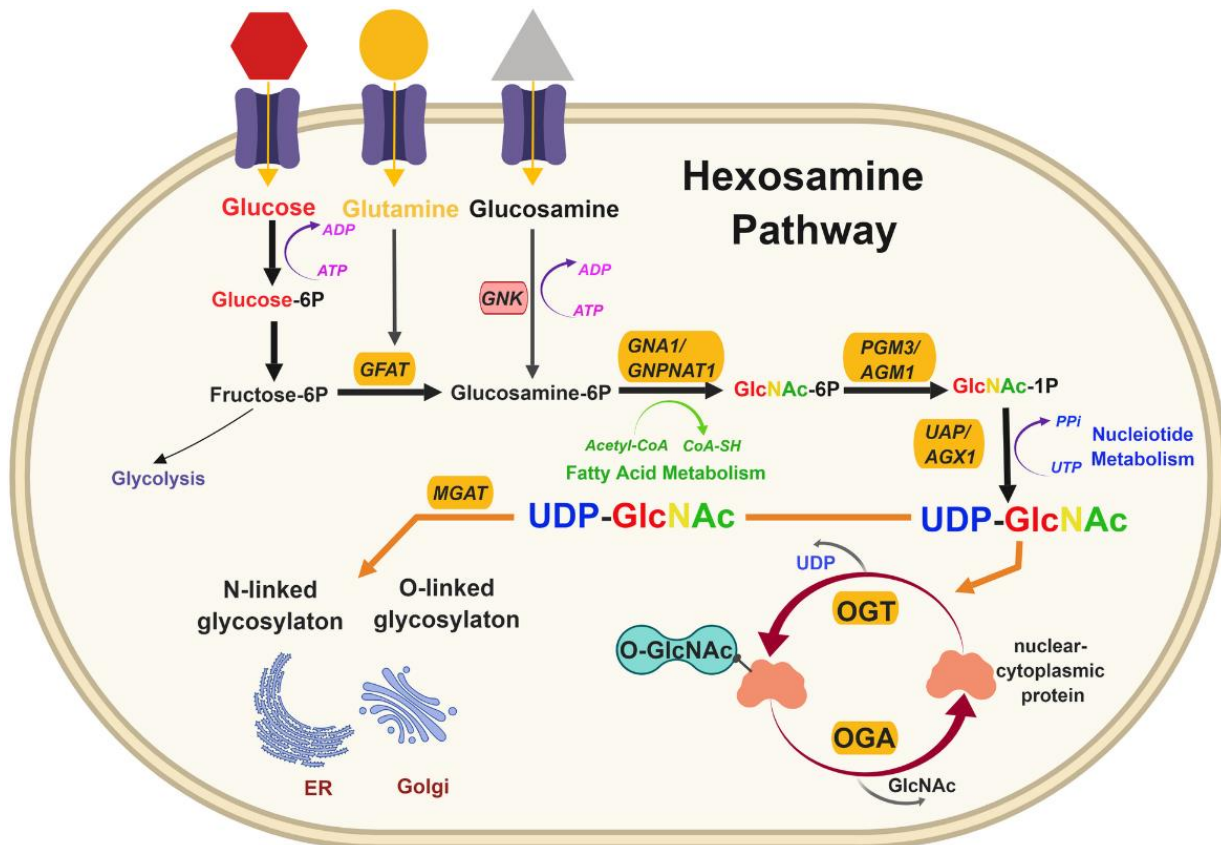


Figure 6: The hexosamine biosynthesis pathway. Illustration of the HBP in cells, displaying the role of glucosamine and the subsequent O-GlcNAc cycling pathway. Adapted from Neha Akella et. al, 2019 [112], and used in accordance with CC BY 4.0 license.

1.1.3.1. The HBP and O-GlcNAcylation in DR

The HBP is an important nutrient sensing mechanism that is involved to a great degree in glucose-induced insulin resistance [113]. In diabetic conditions, the flux through the HBP is increased, due to an upregulation in the enzyme GFAT, among others, which serves usually as the rate-limiting step; inhibition of GFAT can block glucose-induced insulin resistance [114] while contrarily, it can be increased by direct glucosamine infusion [115]. Subsequent to the increased flux to HBP, an increase in O-GlcNAcylated proteins is also observed under diabetic conditions, including specifically in the retina of diabetic mice [116]. A study done in 2014 showed that induction of O-GlcNAcylation significantly enhanced the apoptosis of retinal pericytes, a phenomenon also prevented using GlcNAc inhibitors [117]. Moreover, O-GlcNAcylation of the transcription factor

Sp1 can lead to elevated cholesterol synthesis as well as aggravate diabetic vascular damage [118]. Additionally, as mentioned before, O-GlcNAcylation results in the hyperglycemia-induced upregulation of Ang2, and hence pericyte loss in the diabetic retina [45]. In this way, the HBP plays an important role in the pathogenesis of diabetes and its complications, including DR.

1.2. Glucosamine in the HBP

Glucosamine is a hexose amino sugar naturally found in bone marrow, animal bones and crustacean shells. It is a major precursor in the synthesis of glycosylated proteins. It is an intermetabolite of the HBP, and is involved in the conversion of fructose-6-phosphate via glutamine fructose-6-phosphate amidotransferase (GFAT) into glucosamine-6-phosphate, and finally into uridine diphosphate N-acetylglucosamine (UDP-GlcNAc). It hence influences protein O-GlcNAcylation and subsequent regulation and cellular response signals.

Amino sugars such as glucosamine are synthesized in the HBP; using glutamine as an amino donor, glucosamine-6-phosphate is produced from fructose-6-phosphate [119]. However, glucosamine can also preferentially enter the HBP at a point after the enzymatic amidation by GFAT, thus bypassing the rate-limiting step of the pathway [120]. In the extracellular environment, glucosamine levels are very low, resulting in low cellular uptake in physiological conditions. However, the addition of exogenous glucosamine results in uptake by the glucose transporter into the cellular environment, where it can be phosphorylated by the enzyme hexokinase to yield glucosamine-6-phosphate and enter into the HBP [119, 121]. In this manner, the addition of exogenous glucosamine can mimic high glucose conditions in increasing the flux through the HBP, and directly increase UDP-GlcNAc and protein O-GlcNAcylation. This effect is particularly prominent in the heart in cardiomyocytes, where even a relatively low supply of glucosamine can significantly increase protein O-GlcNAcylation [122]. While acute glucosamine apparently has no effect on cardiac function, chronic exposure to glucosamine mimics diabetes-induced contractile dysfunction in isolated cardiomyocytes [123]. Furthermore, studies have shown that glucosamine (2.5mM) treated adipocytes display changes in gene expression that were distinctly different from those observed with high glucose (25mM) treatment, suggesting that glucosamine can exert effects in cells that cannot be duplicated by increased glucose flux in

the HBP [124]. Additionally, in adipocytes glucosamine has been reported to deplete ATP levels [125].

1.2.1. Pharmacokinetic properties of glucosamine

Glucosamine is a naturally occurring hexose sugar that is mainly found in bone marrow, animal bones, and crustacean shells; it is hence not a part of the everyday diet. Glucosamine can be extracted from the chitin in shellfish by enzymatic hydrolysis to yield sulfate and hydrochloride glucosamine salts used commercially as a source of exogenous glucosamine (Fig. 7). In addition, a “vegetarian” glucosamine hydrochloride salt can be procured via corn fermentation, and can be used by people that are allergic to shellfish [126].

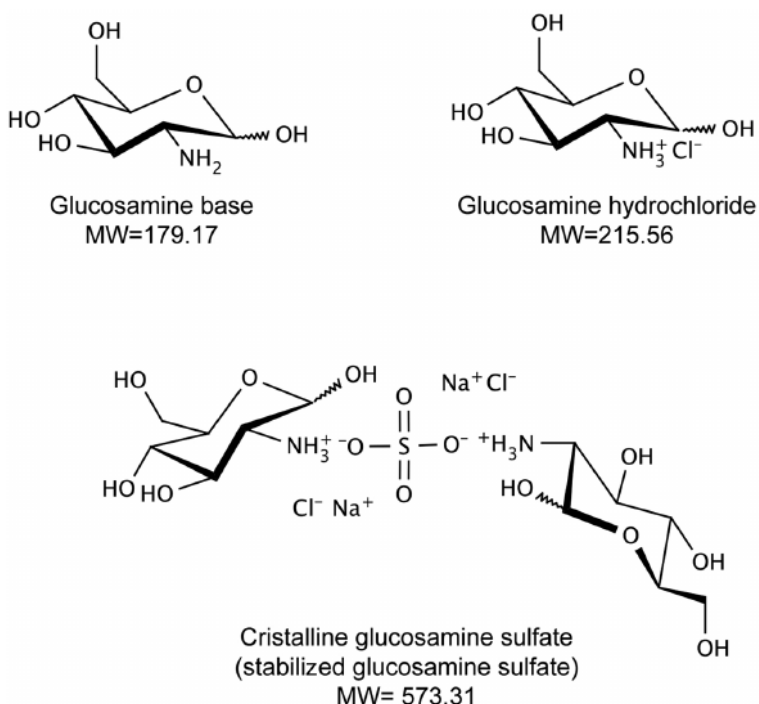


Figure 7: Biophysical properties of glucosamine. Chemical structures of glucosamine, glucosamine hydrochloride, and crystalline glucosamine sulphate demonstrating the physical and chemical properties of each form of glucosamine. Adapted from Lucio Rovati et al, 2012 [127], and used with permission from Sage Journals.

Supplementation with glucosamine is achieved by oral administration in humans, and/or via intravenous or intraperitoneal injections in experimental animal models. In humans, the most

common dosage is 1500 mg daily consumed orally, and several studies have been conducted to determine the kinetics of glucosamine and its bioavailability in the plasma [128, 129]. In a study conducted by Persiani et al in 2005, healthy human volunteers were administered 1500 mg glucosamine sulfate orally, which led to an increase in the plasma glucosamine from a baseline of 0.06 - 1.1 μM to a peak of 10 μM 3-4 hours after supplementation [130].

In rat models, the peak plasma concentrations of glucosamine were found to occur rapidly, merely 13 min after administration either orally or via i.p injection. While complete absorption of glucosamine was observed after the i.p. injection, the oral bioavailability of glucosamine was rather low, at 21% [131]. This low number is attributed to low gastrointestinal absorption, or intestinal degradation/metabolism.

Even with high doses, glucosamine supplementation is considered highly safe [132], with side effects that can range from abdominal pain, diarrhea, heartburn, and constipation to reported weight gain, nausea, vomiting, drowsiness, and headaches [133].

Glucosamine transport into mammalian cells occurs via the glucose transporters GLUT 1, 2, and 4. While GLUT1 and 4 express similar affinity towards both glucose and glucosamine, the GLUT2 affinity towards glucosamine was almost 20 times higher than for glucose; in fact, uptake of glucosamine into hepatocytes happens exclusively via the GLUT2 transporter [134]. Therefore, high concentrations of glucosamine can also competitively inhibit glucose uptake into the cell [135].

1.2.2. Glucosamine in osteoarthritis

Glucosamine-6-phosphate formed via the HBP also enters into metabolic cascades involving the formation of peptoglycans, glycolipids, and glycoproteins. Glycosaminoglycans (GAGs) form the major component of the extracellular matrix in cartilage, hence making glucosamine a building block in cartilage formation and renewal. Since osteoarthritis is characterized by inflammation of the synovial joints and subsequent degeneration of cartilage in joints, glucosamine is therefore utilized in the treatment of osteoarthritis to promote cartilage regeneration and renewal to restore normal joint function. In addition to stimulating the production of GAGs, glucosamine

also promotes the incorporation of sulfur into the cartilage [132]. Glucosamine is hence one of the most widely used oral supplements in the management of osteoarthritis. At a dose of 1500 mg daily, glucosamine sulfate can reportedly prevent joint space narrowing in the femorotibial compartment in patients with mild knee arthritis [136-138].

1.2.3. Characteristics of glucosamine

1.2.3.1. Antioxidative

During metabolic processes, reactive oxygen species (ROS) are generated. Excess ROS in tissues leads to oxidative damage and impair in tissue function, and is hence an important factor in aging and several metabolic disorders, including diabetic complications. Free ROS can be scavenged by antioxidants. Recent studies show the ability of glucosamine to boost the natural protective responses of tissues by acting as a biological response modifier and an antioxidative agent. It is an iron (Fe^{2+}) chelator, and can hence bind iron ions and remove them from oxidizable substances [139].

Depletion of glutathione, the most abundant hydrophilic antioxidant in mammalian cells, also plays a crucial role in maintenance of oxidative homeostasis via elimination of ROS. Glucosamine has been found to prevent the decrease in the cellular pool of glutathione, hence promoting its ability to prevent cellular oxidative stress [140, 141].

1.2.3.2. Anti-inflammatory

Several studies have shown the ability of glucosamine to reduce the production of inflammatory cytokines, hence reducing inflammatory responses in endothelial and synovial cells, as well as in animal models of adjuvant arthritis, inflammatory bowel disease [142], and atherosclerosis. Vascular endothelial cells are key modulators of inflammatory responses, and pathological conditions such as DR can promote the production of pro-inflammatory cytokines and impair vascular function.

Glucosamine suppressed the IL-1 β -induced production of IL-8, an inflammatory chemokine, in synovial cells [143]. In endothelial cells, glucosamine could suppress TNF α -induced production of

MCP-1 and ICAM-1 [144]. It is hypothesized that glucosamine causes these anti-inflammatory effects by increasing protein O-GlcNAcylation. For example, exogenous glucosamine supplementation has been shown to increase O-GlcNAcylation of transcription factors such as Sp1, thereby reducing its activity, and hence the expression of downstream genes, including some encoding cytokines [145].

1.2.3.3. Additional properties of glucosamine

In addition to its prominent usage in osteoarthritis treatment, glucosamine has been studied in various other pathological contexts. The first published report of the anti-cancer activity of glucosamine in 1953 showed its effectiveness in reducing Sarcoma 37 tumors in mice and thereby doubling their survival time [146]. Lowered lung and colorectal cancer risk have since also been associated with glucosamine usage [147, 148]. The proposed mechanisms of action for the observed anti-cancer effects of glucosamine include its anti-oxidative and anti-inflammatory properties, as well as its ability to inhibit HIF-1 and suppress the ubiquitin proteasome and STAT-3 signaling pathways [149] (Fig. 8). Additionally, induction of T-cell activity [150] and inhibition of N-linked glycosylation of proteins [151] have also been implicated in this ability.

Moreover, glucosamine has been found to slow down the ageing process and extend the lifespan of nematodes such as *C. elegans* and also of mice by interfering with the glycolytic process and subsequently increasing amino acid turnover [152]. The induction of autophagy in mammalian cells as well as *C. elegans* by glucosamine treatment was also postulated as a mechanism for the extended lifespan [153]. In an ex vivo model testing the effects of oral glucosamine supplementation on skin ageing, it was determined that 250 mg of glucosamine daily for 8 weeks has a significant positive effect on dermal markers associated with age [154], demonstrating another characteristic of glucosamine that warrants further research.

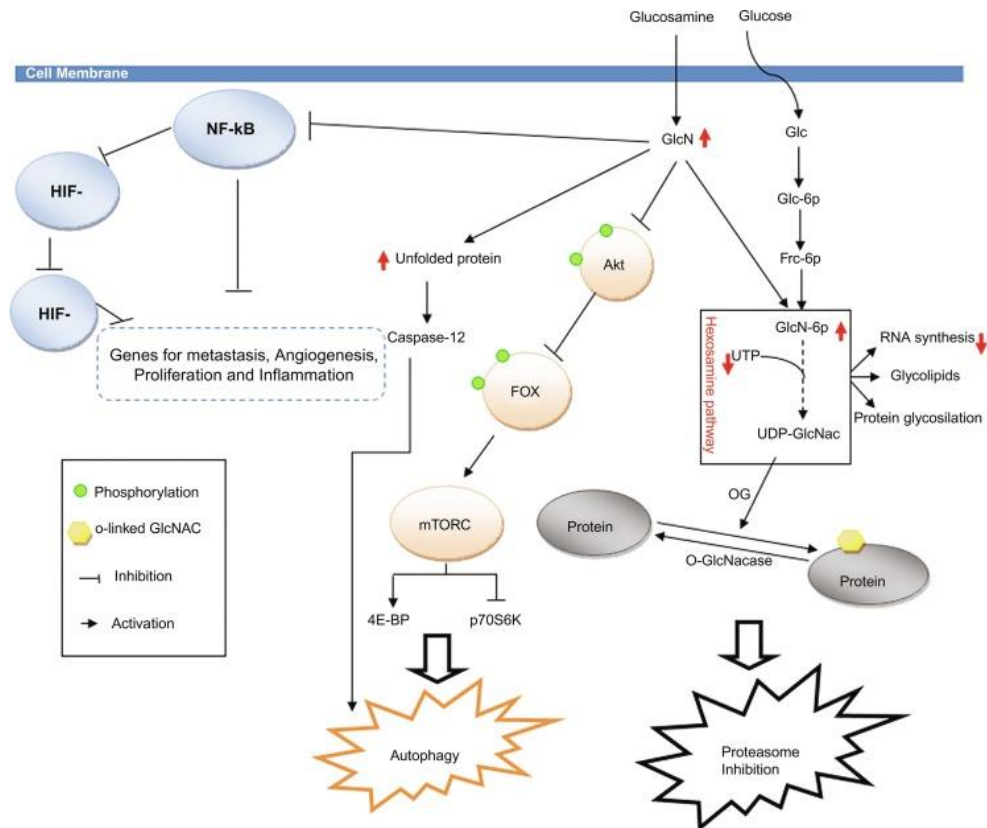


Figure 8: Signaling pathways regulated by glucosamine. Graphical representation of various signaling in the cell that can be modulated by exogenous glucosamine supply. Adapted from Zahedipour et. al, 2017 [149], and used with permission from Elsevier Masson.

The increased protein O-GlcNAcylation associated with glucosamine supplementation in animals has also been linked to improved functional recovery in hearts injured by ischemia and calcium paradox [155, 156], and can confer a protective effect against hypoxia and reoxygenation stress in isolated cardiomyocytes [157]. This suggests a contradictory role of protein O-GlcNAcylation in cardiac function compared to its regulation of diabetic retinopathy, implicating that glucosamine as well can lead to different outcomes in different tissues.

2. Aims of the study

Diabetic retinopathy is hence characterized by vascular damage and neuronal dysfunction, and is modulated by biochemical pathways, including the hexosamine pathway. Glucosamine, an intermetabolite of the hexosamine pathway, is involved in the regulation of pathological processes, such as inflammation and oxidative stress.

Being a hexose sugar and involved in the HBP, glucosamine has been examined extensively regarding its role in glucose metabolism. Increased flux through the HBP has been linked with induction of insulin resistance in both cultured cells and animal models [158-160]. Since the HBP functions in a nutrient sensing manner, it can affect metabolism in organs such as liver, muscle, fat, and β cells in the pancreas. Thus, chronic changes in HBP flux as caused by glucosamine supplementation can supposedly mimic insulin resistance caused by high fat diet [161]. In addition to the induction of insulin resistance, exposure to glucosamine was found to increase protein O-GlcNAcylation in tissues [162], an important protein modification influencing the pathology of DR.

The intersection of the signaling pathways involved in regulation of the pathological processes in DR and those influenced by glucosamine supplementation suggests that glucosamine can be involved in the modulation of DR. Moreover, the biochemical properties of glucosamine as examined in various studies suggest antioxidative and anti-inflammatory characteristics, as illustrated in the sections above.

Currently, the effect of glucosamine on the retina *in vivo* is largely unknown. This study hence endeavors to delve into the influence of glucosamine on diabetic retinopathy *in vivo*, and uncover the mechanisms of action in cultured cell models *in vitro*. Furthermore, as diabetes and osteoarthritis often occur concomitantly in elderly patients, this study also seeks to determine whether the beneficial effect of glucosamine on cartilage renewal and pain alleviation in osteoarthritis may occur alongside possible beneficial or detrimental effects on other cell or organ systems.

Therefore, the aims of the current study involved examining the impact of glucosamine on diabetic retinopathy and the various processes and cell types involved.

2.1. Aim 1:

The first part of the study focused on investigating the role of glucosamine on the retina in an animal model of experimental diabetic retinopathy. Male C57Bl/6 mice were induced with diabetes and given oral doses of glucosamine for 24 weeks in order to evaluate the biochemical effects of glucosamine on the mice, and specifically on neuronal and vascular functions involved in diabetic retinopathy.

2.2. Aim 2:

The second part of the study aimed to characterize the underlying mechanisms of action of glucosamine. Endothelial cells and Müller cells, the two major cell types involved in regulation of diabetic retinopathy-related pathological events in the retina, were cultured *in vitro*, treated with high glucose and glucosamine, and evaluated by examination of signaling molecules primarily via immunoblotting and immunofluorescence.

3. Materials

3.1. Cell Culture

3.1.1. Cell isolations and cell lines

Table 1: Cell isolations and cell lines

Cell type	Source
HUVECs	Self-isolated from umbilical cords
HRMVECs	PB-CH-160-8511; Pelobiotech
Mouse Müller cells	Self-isolated from mouse retinas
Rat Müller cells	rMC-1 cell line

3.1.2. Cell Culture medium and supplements

Table 2: Cell culture medium and supplements

Components (500ml)	Catalog number
Endothelial cell basal medium (ECBM)	C-22110; PromoCell
Endothelial supplements	C-39210; PromoCell
Endothelial cell growth media (ECGM)	ECBM + Supplements + PenStrep: 1%
Microvascular ECGM (ECGM MV)	ECBM + Hydrocortisone: 1 µg/ml, ECGS: 40 µg/ml, PenStrep: 1%, EGF: 5ng/ml
DMEM (1000 mg/ml glucose)	D-6546; Sigma-Aldrich

3.1.3. Cell Culture reagents and enzymes

Table 3: Cell Culture reagents and enzymes

Reagents	Company	Catalog Number and details
Collagenase I	Worthington	LS004194
Dispase II	Roche	04942078001
EDTA Trypsin 0.05%	Sigma-Aldrich	T3924
FCS	Sigma	F7524
Glutamine	Sigma	G7513
Penicillin/Streptomycin (PS)	Sigma	P4333

3.2. Buffers and chemicals

3.2.1. Cell culture buffers

Table 4: Cell Culture buffers

Reagents	Company	Catalog Number
PBS	Sigma-Aldrich	D-5652
Gelatin (surface coating for ECs)	Fluka	48720; 1% in PBS
Collagen (surface coating for mouse Müller cells)	Corning	354236; 1:100 in PBS

3.2.2. Protein analysis buffers

Table 5: Protein analysis buffers

Buffer	Contents
RIPA buffer	150mM NaCl; 1% Triton-X-100; 0.5% sodium deoxycholate; 0.1% SDS; 50 mM Tris; pH 8.0
Cell lysis buffer	RIPA buffer + Protease inhibitor cocktail (Roche), 1 tablet/10 ml
Ponceau S (100ml)	0.2g Ponceau; 5 ml acetic acid; 95 ml H ₂ O
Protein loading buffer (4X, 50ml)	0.125g Bromophenol Blue; 25ml Glycerol; 5ml 2-mercaptoethanol; 5 ml H ₂ O
SDS-PAGE electrophoresis buffer (5X)	0.125M Tris; 1.25M Glycine; 0.5% SDS; in H ₂ O
TBS (10X)	100mM Tris; 1.5M NaCl; pH: 7.4
TBST (1L)	100 ml 10X TBS; 10 ml 10% Tween-20; 890 ml H ₂ O
Tris buffer for stacking gel	1M Tris; pH 6.8
Tris buffer for resolving gel	1.5 M Tris; pH 8.8
WB buffer stock (10X)	32.5 g Tris; 144 g Glycine; 1000 ml H ₂ O
WB transfer buffer (1L)	100 ml 10X WB; 900 ml H ₂ O

3.2.3. Immunofluorescence buffers

Table 6: Immunofluorescence buffers

Buffer	Contents
Fixation solution	Retina: 4% PFA in PBS Cells: 4% Roti-Histofix
Permeabilization/Blocking buffer (P/B)	2.5% BSA, 0.3% Triton-X-100; in PBS
Wash buffer	1X PBS
Antibody dilution buffer	1:1 P/B and 1X PBS

3.2.4. Retina digestion buffers

Table 7: Retina digestion buffers

Buffer	Contents
Fixation solution	4% Formalin
Digestion solution	3% Trypsin (Difco, 250K98); 0.2 M Tris-HCl; pH: 7.0
Wash buffer	ddH ₂ O

3.3. Chemicals

Table 8: List of chemicals

Chemicals	Company	Catalog Number
2-Mercaptoethanol	Serva	28625
APS	Merck	1.012.010.100
Bromopheol Blue	Chroma-Gesellschaft	4F057
BSA	Sigma-Aldrich	A9647
Chloroform	Merck	2447
cOMPLete protease inhibitor cocktail	Roche	5892970001
DMSO	Sigma-Aldrich	D8418
DAPI	Life Technologies	1603428
D-(+)-Glucose	Sigma-Aldrich	SLBF1738V
Ethanol	Richter Chemie	V-126
EDTA	Roth	8040.1
Entellan	Merck	107961
Gelatin from porcine skin	BD	214340
Glucosamine	Sigma-Aldrich	G4875
Glycerol	Sigma-Aldrich	G9012

HCl	Sigma-Aldrich	H1758
KCl	Sigma-Aldrich	P9333
Mayer's Hamalaun	Roth	T865.2
Methanol	Roth	4627.5
NaCl	Sigma-Aldrich	M7439
NaHCO ₃	Sigma-Aldrich	S5761
NaOH	Merck	106498
Periodic acid	Sigma-Aldrich	P7875
PFA	Merck	1.040.031.000
PhosSTOP™	Sigma-Aldrich	4906845001
Ponceau S	Sigma-Aldrich	P-3564
Protein marker	Roth	T8512
Roti-Block	Roth	A151.1
Roti-Histofix	Roth	P087.4
Roti-Histol	Roth	6640.4
Roti-Mount FluorCare	Roth	HP19.1
Rotiphorese Gel 30	Roth	3029.1

Schiff's reagent	Roth	X900.2
SDS	Sigma-Aldrich	74255
SuperScript IV VILO Master Mix	Thermofisher	11755050
TEMED	Roth	T7024
Tris	Serva	37181
Triton-X-100	Merck	1.080.031.000
Trizol	Life Technologies	15596018
Trypsin for RD	Difco	250K98
Tween 20	Sigma-Aldrich	P-7949

3.4. Antibodies

3.4.1. Primary antibodies

Table 9: Primary antibodies

Antibody	Company; Catalog Number	Dilution
Ang2	Santa Cruz; sc-74403 (WB)	WB: 1:500
	Santa Cruz; sc-7017 (IF)	IF: 1:200
GFAP	Dako; Z0334	WB: 1:5000 IF retina: 1:500 IF rMCs: 1:200

O-GlcNAc	Abcam; ab2739	1:2000
γ-Tubulin	Sigma-Aldrich; T5168	1:5000
VEGF	Abcam; ab46154	1:10000
VEGFR2	Cell Signaling; 55B11	1:1000

3.4.2. Secondary antibodies

Table 10: Secondary antibodies

Antibody	Company; Catalog Number	Dilution
Donkey anti-goat FITC conjugate	Acris; R1254F	1:200
Goat anti-mouse Alexa Fluor 594	Life technologies;	1:200
Goat anti-rabbit peroxidase	Sigma-Aldrich; A9169	1:20000
Rabbit anti-mouse peroxidase	Sigma-Aldrich; A9044	1:20000
Rabbit anti-goat peroxidase	Sigma-Aldrich; A8919	1:20000
Swine anti-rabbit FITC conjugate	Dako; F0205	1:20

3.5. qPCR primers and master mix

Table 11: qPCR primers and master mix

Reagents/Primers	Company	Catalog Number
TaqMan™ Fast Advanced Master Mix	Thermo Fisher Scientific	4444557
GoScript™ Reverse Transcription system	Promega	A5001
Cyclophilin F	Thermo Fisher Scientific	Mm01273726_m1
BDNF	Thermo Fisher Scientific	Mm01334042_m1
GDNF	Thermo Fisher Scientific	Mm00599849_m1
GFAP	Thermo Fisher Scientific	Mm01253033_m1
Il1-β	Thermo Fisher Scientific	Mm00434228_m1
Il-6	Thermo Fisher Scientific	Mm00446190_m1
TNF-α	Thermo Fisher Scientific	Mm00443258_m1

ICAM-1	Thermo Fisher Scientific	Mm00516023_m1
Ang2 (ANGPT2)	Thermo Fisher Scientific	Mm00545822_m1
VEGFR2 (KDR)	Thermo Fisher Scientific	Mm01222421_m1
VEGF	Thermo Fisher Scientific	Mm00437306_m1

3.6. Consumables

Table 12: Consumables

Consumables	Company	Catalog Number
3-way stopcock	BD Connecta TM	394600
Cell counting chamber	Marienfeld	0640010
Cell culture plate (6 well, 12 well, 24 well)	Sarstedt	83.3920, 83.3921, 83.3922
Cell culture dish (6 cm, 10 cm, 15 cm)	Sarstedt	83.3901, 83.3902, 83.3903
Cell culture flask (T25, T75)	Sarstedt	83.3910.002, 83.3911.002
Cell scraper	Sarstedt	83.1830
Cover slips	Carl Roth GmbH	41021070

Gel combs	BioRad	1653359
Cryotubes	Sarstedt	72.377
Eppendorf tubes (1.5 ml, 2 ml)	Eppendorf	0030, 120.086
Pipette tips (1000 μ l, 200 μ l, 10 μ l)	Eppendorf	70.760.002, 70.1130, 70.762
Falcon tubes (15 ml, 50 ml)	Sarstedt	62.554.502, 62.547.254
Microscope objective slides	R. Langenbrinck	03-0002 2642672
Nitrocellulose membrane	Häberle	6267735
Pipettes (5 ml, 10 ml, 25 ml)	Sarstedt	86.1253.001, 86.1254.001, 86.1685.001
Parafilm	Parafilm'M'	PM-996
Whatman filter paper	VWR	514-8013
Filtropur S 0.2	Sarstedt	31046103
Syringe	Seidel Medipool	301229
Syringe needles (21G, 25G, 27G, 30G)	BD Microlance	

3.7. Kits

Table 13: Kits

Kits	Company	Catalog Number
Lumi-Light Western Blotting	Roche	12015200001
Super-Signal West Femto Maximum Sensitivity Substrate	Thermo Scientific	34095
Human VEGF DuoSet ELISA	R&D Biosystems	DY293B-05
DuoSet Ancillary Reagent Kit 2	R&D Biosystems	DY008

3.8. Apparatus

Table 14: Apparatus

Apparatus	Company
Centrifuge	Eppendorf, Hettich
Laminar flow bench	Herasafe, Heraeus
Water bath	Thermo Scientific
Incubator (37°C, 5% CO ₂)	Memmert
Shaker	Neolab
Weighing scale	Sartorius
Pipettor	Eppendorf

Multi-step pipettor	Eppendorf
pH meter	WTW
Heating block	Thermomix comfort
Electrophoresis chamber and apparatus	BioRad
Turbo Blotting apparatus	BioRad 1704150
Voltmeter	Biometra
Gel imager	Vilber Fusion FX6
Thermal cycler	MJ Research
qPCR	Quantstudio 3, Applied biosystems
Stereo microscope	Eschenbach
Fluorescence microscope	Olympus
Confocal microscope TCS SP8	Leica
Millipore water machine	Milli-QR
-20 °C freezer	Bosch
-80 °C freezer	Hera
Envision 2102 multiplate reader	Perkin-Elmer

3.9. Software

Table 15: Software

Purpose	Company	Software
Image analysis	NCBI	ImageJ
Fluorescence microscope software	Olympus	CellSens Dimension
Confocal microscope software	Leica	LASx
Statistics	La Jolla	GraphPad Prism 6
References	Microsoft	Endnote v9

4. Methods

4.1. *In vivo* methods

4.1.1. Maintenance of the animals

The use of mice in this study was approved by the local ethics committee (Medical Faculty Mannheim, Heidelberg University, Germany). The care and experimental use of animals were in accordance with institutional guidelines and in compliance with the Association for Research in Vision and Ophthalmology (ARVO) statement. All animal experiments were approved by the local ethics committee (Regierungspräsidium Karlsruhe, Germany). The mice were housed in a separate building with artificial lighting to simulate a 12h:12h light:dark cycle. The room temperature was kept constant at 21 °C. The mice received tap water for drinking, and were fed either a normal chow diet (containing 9% fat, 33% protein, and 58% carbohydrates), or normal chow diet supplemented with 10g/kg glucosamine [152]. The mice were allowed free access to food and water. Diabetic animals were generated using a single intraperitoneal injection of

streptozotocin (145mg/kg body weight). One week after the STZ injection, the animals were started on glucosamine treatment, which was continued for six months. After six months, the animals were weighed, anesthetized with isoflurane, and euthanized using ketamine and xylazine overdose administered intraperitoneally, followed by cervical dislocation. The eyes, kidneys, liver, heart, and plasma samples were collected, flash frozen in liquid nitrogen, and stored at -80 °C for further analyses. Blood glucose, HbA1c, and the levels of amino acids and other metabolites were determined, and metabolites to determine liver and kidney function were measured.

4.1.2. Analysis of metabolites

Non-thiol containing amino acids were quantified after specific labeling with the fluorescence dye AccQ-Tag™ (Waters) according to the manufacturers protocol. The resulting derivatives were separated by reversed phase chromatography on an Acquity BEH C18 column (150 mm x 2.1 mm, 1.7 µm, Waters) connected to an Acquity H-class UPLC system and quantified by fluorescence detection (Acquity FLR detector, Waters). The column was heated to 42 °C and equilibrated with 5 column volumes of buffer A (140 mM sodium acetate pH 6.3, 7 mM triethanolamine) at a flow rate of 0.45 ml min⁻¹. Baseline separation of amino acid derivatives was achieved by increasing the concentration of acetonitrile (B) in buffer A as follows: 1 min 8% B, 7 min 9% B, 7.3 min 15% B, 12.2 min 18% B, 13.1 min 41% B, 15.1 min 80% B, hold for 2.2 min, and return to 8% B in 1.7 min. Data acquisition and processing was performed with the Empower3 software suite (Waters). Cys was determined after labeling with monobromobimane (Calbiochem) as described in Wirtz et al. [163].

4.1.3. Optical Coherence Tomography

The measurement of retinal thickness measured via optical coherence tomography (OCT) was subsequently performed using the build-in OCT of the RETImap system. Retinal thickness was measured with a spectral-domain optical coherence tomography module by quantifying the thickness at the border of the inner third to the outer two thirds of the retina in 5 locations.

4.1.4. Electroretinogram

To determine neuronal function in the retina, multifocal electroretinography was performed as described by Dutescu et al [164]. The mice were positioned 1 to 2 mm in front of a scanning laser ophthalmoscopy (SLO) device (RETImap, Roland Consult, Brandenburg an der Havel, Germany), and the potentials were collected with a DTL electrode placed at the corneal limbus. Subcutaneous silver needle electrodes were positioned at the neck of the mice, serving as reference and ground electrodes. A 90 dioptre contact lens mounted over viscous 2% methocel gel was placed on the eyes of the mice. An array of 7 equally sized hexagons was chosen, and stimulation was performed using 150 cd/m^2 and 1 cd/m^2 for the m-sequence with four dark frames in between the stimuli. An average of eight cycles for each hexagon was used for the final analyses processed with the built-in 50 Hz band filter to reduce background noise. For each animal, the average amplitude of the six hexagons around the optic nerve head was used for final analyses. mfERG recording took place under photopic conditions where, in mice, both rod and cone photoreceptors were activated. The initial negative-going N1-wave is initiated by photoreceptors, whereas the following positive-going P1-wave is generated in the inner retina, mainly by ON-bipolar cells under the influence of Müller cells.

4.1.5. Retinal digestion and retinal morphometry analysis

Frozen eyes were fixed in 4% Formalin for 48 hours at room temperature. The eyes were further placed under a microscope and dissected. The lens and vitreous were removed, and the retina was carefully extracted. The isolated retina was placed in water at $37 \text{ }^\circ\text{C}$ for 30 min, and subsequently incubated in 3% trypsin dissolved in 0.2M Tris-HCl buffer (pH 7.0) for 2.5h at $37 \text{ }^\circ\text{C}$. Post-incubation, the retina was transferred carefully to a glass object slide and washed with dH_2O droplets, dropped using a syringe directly onto the retina, until the pure retinal vasculature could be visualized under the microscope. The remaining water and detritus was sucked away using a syringe connected to a vacuum pump, and the retinal vasculature was allowed to dry onto the object slide. The vasculature was then stained using Periodic-Acid-Schiff (PAS) staining. The staining procedure was performed by immersing the slide in the solutions as follows:

Table 16: Periodic Acid-Schiff staining

Solution	Time
dH ₂ O	5 min
1% Periodic Acid	10 min
dH ₂ O	Brief immersion
Schiff's reagent	15 min
Running tap water	7 min
dH ₂ O	Brief immersion
Mayer's Hamalaun	1 min
Running tap water	7 min
dH ₂ O	Brief immersion
70% ethanol	2 min
80% ethanol	2 min
96% ethanol	2 min
100% ethanol	2 min
Roti Histol x3	5 min each
Add Entellan and cover with coverslip	

The PAS-stained slides were observed under the microscope, and photos of 40x magnification were taken. The number of acellular capillaries were quantified using an integration ocular with a grid of 100 squares. The number of squares containing acellular capillary segments were counted in 10 randomly selected microscopic fields in the middle one-third of each retina. The

pericytes and endothelial cells were quantified in a similar 10 microscopic fields in the middle third of the retina under 40x magnification. The cell numbers were recorded and normalized to the relative capillary density) number of cells per mm² of capillary area). The counting and capillary area measurement was done using image analysis software (AnalysisPro, Olympus Optical, Hamburg, Germany).

4.1.6. Retina Whole-mount Immunofluorescence

Frozen eyes were fixed in 4% paraformaldehyde for 1 hour on ice, and further washed with cold PBS and blotted dry on soft paper. The eyes were dissected by visualizing them under a microscope, and the retinas were isolated. The isolated retinas were transferred into a chilled 1.5 ml Eppendorf tube containing 1 ml PBS. The retinas were washed in PBS for 2 x 1 hour, followed by washes of 5 x 10 mins at room temperature on a shaker. Following the washes, the retinas were incubated in 200 µl of blocking and permeabilization solution [3% (w/v) BSA + 0.3% Triton-X in PBS, freshly prepared and filtered before use] for 1.5 hours at room temperature, further to which the solution was carefully removed, 50 µl of the primary antibody (diluted in 0.15% Triton-X in PBS) was added, and the retinas were incubated overnight at 4 °C. The following day, the retinas were washed with PBS – a quick rinse, followed by washes of 2 x 1 hour and 5 x 10 mins. Further, 50 µl of the secondary antibody (diluted in 0.15% Triton-X in PBS) was added, and the retinas incubated at room temperature for 1.5 hours in the dark. The retinas were further washed with PBS – a quick rinse, followed by washes of 2 x 1 hour and 5 x 10 mins, following which the retina was cut into four leaves under the microscope and transferred to a glass object slide. A few drops of Roti FluorMount were added, and the retinas were covered with coverslips and allowed to remain at 4 °C overnight before visualization under a confocal microscope (TCS SP8, Leica).

4.2. *In vitro* methods

4.2.1. Cell culture

4.2.1.1. Isolation and culture of HUVECs

HUVECs were isolated from the umbilical cords of newborn infants with the informed consent of their mothers. The isolation was performed under sterile conditions. The umbilical cords were wiped multiple times with ethanol-soaked wipes in order to rid the outside surface of blood and mucus. The cord was further examined for the presence of holes; if found, the cord was cut or clamped in order to exclude the holes. One end of the cord was clamped close and at the other end, a 3-way valve was inserted into the vein to allow bidirectional flow of fluid through the vein, identified as the largest vessel in the umbilical cord. The vein was then washed with pre-warmed DMEM supplemented with 1% Penicillin/Streptomycin (PS) until blood no longer visibly drained from it. A solution of 1X DMEM-Dispase II was prepared by dilution 10X Dispase II in appropriate volume of DMEM. This solution was then filled into the vein via the valve. The cord was then placed in a covered petri dish and into a humidified incubator at 37 °C and 5% CO₂ for 30-40 mins, following which the cord was massaged gently to dislodge the detached cells completely from the vein walls. The contents of the vein, including the detached cells, were then collected in a falcon tube containing 4 ml of FCS in order to halt the enzymatic reaction. The vein was subsequently washed once with DMEM in order to collect any remaining cells, and the flowthrough was collected in the same falcon tube. The collected suspension was centrifuged at 1000 rpm for 5 mins to obtain a cell pellet, which was further resuspended in ECGM containing 2% FCS. The cells were plated on a 1% gelatin-coated T25 flask maintained in a humidified incubator at 37 °C and 5% CO₂ for 2 h to enable the HUVECs to attach to the bottom of the flask, followed by a gentle wash and media change to remove any remaining red blood cells. The cells from one cord were placed in each flask, and regarded as one isolation. The attached HUVECs were then maintained in fresh ECGM with 2% FCS.

4.2.1.2. Culture and passaging of HUVECs and HRMVECs

The freshly isolated HUVECs in passage 0 (p0) were cultured in ECGM 2% FCS with a medium change every two days until the cells reached complete confluency, at which point they were detached from the flask using trypsin digestion. Once detached, the trypsin enzyme was neutralized by the addition of ECGM with 10% FCS. The cells were resuspended in the medium, and passaged to p1 in a 1:3 ratio into 1% gelatin-coated cell culture dishes and cultured to confluency before passaging further. All experiments were performed using cells from p1 to p4.

HRMVECs were cultured in ECGM MV in 10% FCS until the cells reached confluency, at which point they were passaged similar to the HUVECs. Experiments in HRMVECs were performed using cells from p7 to p10.

4.2.1.3. Isolation of murine retinal Müller cells

Male mice at postnatal day 8-12 were anesthetized by placing them in an isoflurane chamber and immediately sacrificed. The eyes were rapidly enucleated into DMEM supplemented with 200mM L-glutamine and 1% PS (henceforth known as DMEM-Gln), and stored overnight in the dark. The following day, each eye was placed in 0.5 ml of DMEM containing 0.1% trypsin and 70U/ml (0.264 mg/ml) collagenase I, and incubated at 37 °C for 1 h. Post-incubation, the eyes were placed in a petri dish containing DMEM supplemented with 10% FCS to stop the enzymatic reaction. Working in sterile conditions under a microscope, the eyes were gently dissected using sterilized instruments until the retinas were visible as a cloudy white layer within. The retinas were carefully extricated from the rest of the eyes, and placed in a small petri dish containing a minimum amount of DMEM with 10% FCS. The retinas were mechanically dissociated with a 1 ml pipette followed by a 200 µl pipette, and the resultant suspension was plated on a cell culture dish coated with 1% collagen in fresh DMEM supplemented with 200mM L-glutamine, 1% PS, and 10% FCS. The cells were placed in a humidified incubator at 37 °C and 5% CO₂, and left undisturbed without a medium change for 5-6 days to allow the Müller cells to adhere to the bottom of the cell culture dishes. Subsequently, the medium was replaced with fresh DMEM with L-glutamine, PS, and 10% FCS every two days until the cells reach confluency about 4 to 8 days

after their initial appearance. The cells were characterized via immunofluorescence to look for Müller cell-specific markers such as GFAP, GS, and CRALBP, and used from p1-p5 in experiments.

4.2.1.4. Culture and passaging of Müller cells

Müller cells of all origins were cultured in DMEM medium supplemented with 200mM L-Glutamine and 1% PS (DMEM-Gln), and with the addition of 10% FCS. The murine-derived retinal Müller cells were plated in cell culture dishes coated with 1% collagen in PBS, and the rat-derived Müller cells were plated in cell culture flasks without coating. All the cells were cultured in a humidified incubator at 37 °C and 5% CO₂ and allowed to reach confluency. Once confluent, the cells were detached from the flask using trypsin digestion, and resuspended in DMEM-Gln with 10% FCS to stop the enzymatic reaction. They were further centrifuged at 1000 rpm for 5 min to obtain a cell pellet, which was subsequently resuspended in DMEM-Gln with 10% FCS. The cell suspension was passaged into cell culture flasks (pre-coated with 1% collagen for the murine Müller cells) in a 1:3 ratio and cultured to confluency before use in experiments.

4.2.1.5. Freezing and thawing of cells

HUVECs at p0 or p1, HRMVECs, and Müller cells were detached from the cell culture dishes via trypsin digestion and resuspended in either ECGM/ECGM MV (for HUVECs and HRMVECs, respectively) or DMEM-Gln containing 10% FCS to stop the enzymatic reaction. The cells were then pelleted by centrifugation at 1000 rpm for 5 min. The pellet was further resuspended in 3 ml of chilled ECGM/ECGM MV or DMEM-Gln supplemented with 10% FCS and 10% DMSO. Each cell suspension was divided equally between two sterile cryotubes, and placed rapidly in a pre-chilled isopropanol reservoir. The reservoir was then placed at -80 °C overnight. The following day, the cryotubes were transferred to a liquid nitrogen tank and stored at -196 °C.

To thaw the cells, the cryotube containing the required isolation was extricated from the liquid nitrogen tank and thawed rapidly in a water bath maintained at 37 °C. Once the cells were partially thawed, they were resuspended in 10 ml of pre-warmed ECGM/ECGM MV or DMEM-Gln with 10% FCS until fully thawed, and centrifuged at 1000 rpm for 5 min to obtain a cell pellet. The pellet was further resuspended in ECGM/ECGM MV or DMEM-Gln with 10% FCS, and the cells were plated on to 1% gelatin/collagen-coated cell culture dishes and maintained in a

humidified incubator at 37 °C and 5% CO₂. The culture media was replaced the following day to remove traces of DMSO, and the cells were cultured to confluency before use in experiments.

4.2.1.6. Stimulation of endothelial and Müller cells

HUVECs at p1-3, HRMVECs at p7-10, and Müller cells (p1-5 for murine Müller cells, and up to p13 for rat Müller cells) were seeded into cell culture plates according to cell numbers mentioned in Table 17. The cells were allowed to attach and grow overnight. On the following day, the cells were starved using 0.5% FCS in ECGM/ECGM MV or DMEM-Gln media for HUVECs/HRMVECs and Müller cells, respectively. After a 24h starvation period, the cells were further stimulated with high glucose (HG) and/or glucosamine. HG treatment was done using 30mM glucose by dissolving appropriate amount of D-Glucose (G7021 Sigma-Aldrich) in 0.5% ECGM/ECGM MV or DMEM-Gln. The solution was then incubated in a 37 °C water bath for 15 min, filtered through a 0.2µm filter, and added to the cells in appropriate volumes. For glucosamine stimulation, a stock solution of glucosamine hydrochloride (G4758 Sigma-Aldrich) was prepared in either 0.5% ECGM/ECGM MV or DMEM-Gln, and appropriate amounts according to the required concentrations in the experiments were diluted into media and added to the cells. HG and glucosamine treatment was performed for 24h, following which the cells were harvested in protein lysis buffer.

Table 17: Cell seeding for cell culture and experiments

Dish/Plate	Surface area per well/dish (mm ²)	Number of cells per well/dish	Volume of medium per well/dish (ml)
4-well chamber slide	170	50,000	0.5
24-well	200	50,000	0.5
12-well	401	100,000	1
6-well	962	200,000	2
6 cm	2827	500,000	4
10 cm	7854	1,000,000	8

4.3. Protein Biochemical Methods

4.3.1. Protein extraction from cells

The procedures were performed on ice. The cells were washed thrice with ice-cold PBS, following which chilled RIPA buffer was added to the cells according to volumes displayed in Table 18. Upon adding the RIPA buffer, the cells were lysed and harvested from the dish using a cell scraper. The collected suspension was transferred to a cooled 1.5ml Eppendorf tube and incubated on ice for 15 min, following which the samples were centrifuged at 13000 rpm for 15 min at 4°C. The supernatants were then carefully transferred into fresh tubes. The amount of protein present in the sample was then quantified, and the protein lysate was further diluted accordingly.

Table 18: Lysis buffer addition based on cell density

Dish/Plate	Surface area per well/dish (mm ²)	Number of cells per well/dish	Volume of RIPA buffer per well/dish (μl)
24-well	200	50,000	50
12-well	401	100,000	100
6-well	962	200,000	150
6 cm	2827	500,000	400

4.3.2. Protein extraction from the retina

All procedures were performed on ice. The retina from a frozen and unfixed eye was extracted quickly under the microscope and placed in a 1.5 ml Eppendorf tube containing 120 μl of ice-cold RIPA buffer. The retina was homogenized thoroughly by passing the suspension through syringe needles of decreasing diameters (22G, 25G, 27G, 30G). The homogenized lysate was then centrifuged at 13000 rpm for 30 min at 4 °C. The supernatant was then transferred to a fresh Eppendorf tube, and the protein concentration was measured before usage in further experiments.

4.3.3. Protein concentration estimation using BCA assay

In order to determine the concentration of protein in the cell lysates, bicinchoninic acid (BCA) assay was performed. The assay is a colorimetric technique which utilizes the reducing capacity of $\text{CuSO}_4 \cdot 5\text{H}_2\text{O}$. The peptide bonds present in the proteins reduce the copper ion in $\text{CuSO}_4 \cdot 5\text{H}_2\text{O}$ which then chelates to bicinchoninic acid, resulting in a color change from green to purple. The protein amount in the samples is directly proportional to the optical density (OD) of the final product detected at 565 nm.

The assay was conducted on clear, flat-bottomed plates. To obtain a standard curve as shown below, BSA in concentrations of 0, 0.25, 0.5, 1.0, and 2.0 $\mu\text{g/ml}$ was used. 10 μl of whole or diluted protein lysate was pipetted in duplicates into the wells. The BCA solution was prepared as follows:

- BCA A: Dissolve 3.420g Na_2CO_3 , 0.800g NaOH, 0.132g Na K-tartrate.4 H_2O in 40ml H_2O , adjust the pH to 11.25 with NaHCO_3 and bring up the final volume to 50 ml with H_2O
- BCA B: Dissolve 0.2g $\text{BCA} \cdot \text{Na}_2$ in 5 ml H_2O
- BCA C: Dissolve 0.2g $\text{CuSO}_4 \cdot 5\text{H}_2\text{O}$ in 5 ml H_2O
- Final BCA solution: 50% BCA A + 48% BCA B + 2% BCA C

100 μl of the BCA solution was added to each sample in the plate; the plate was then covered and incubated at 60 °C for 30 min, following which the OD was read using a spectrometer at 595 nm. A standard curve was created using a linear regression of the OD values plotted against the known concentrations of BSA, and was used to calculate the protein amounts in the unknown samples. The protein amounts in all the samples were equalized with RIPA buffer, and the lysates were further stored or denatured for use in experiments.

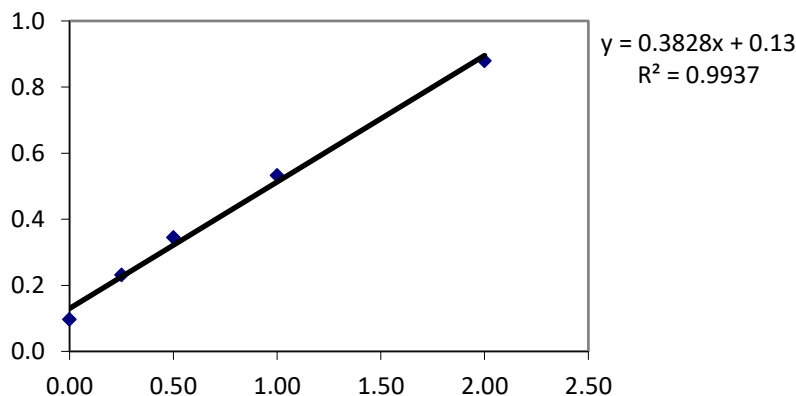


Figure 9: Standard curve of BCA assay. Example of a standard curve of BCA assay, generated using samples of BSA of increasing, known concentrations, and the corresponding optical density (OD) obtained using the assay.

4.3.4. Protein denaturation

Prior to immunoblotting, the protein lysates were denatured using 4X Laemmli buffer (SDS loading buffer) with glycerol and boiled at 95 °C for 5 min on a heating block or thermal cycler. The samples were then cooled on ice and stored at -20 °C until further analysis.

4.3.5. Immunoblotting/Western blotting

4.3.5.1. SDS-polyacrylamide gel electrophoresis (SDS-PAGE)

SDS-PAGE is a technique utilized to separate proteins by mass along an electrical gradient. The matrix is polyacrylamide-based, and the polypeptides travel along the gel through the electricity gradient that separates the peptides according to their size, since the largest migrate the slowest.

4.3.5.2. Gel casting

Polyacrylamide gels used in SDS-PAGE consist of a stacking and separating gel, which differ in pH in order to align the polypeptides prior to their separation. The polyacrylamide percentage in the gels is determined by the size of the target protein (Table 19); the reagents required for the preparation of the gels are shown in Tables 20 and 21. First, cleaned glass plates are held together on a gel-casting stand, creating a 1mm thick gap between them. The separating gel solution was prepared, and pipetted carefully into the gap between the glass plates up to 75% full. The gel was

then layered with a thin film of isopropanol to prevent drying, and allowed to polymerize for 20-30 minutes. After polymerization, the isopropanol was removed, and the stacking gel solution prepared and pipetted on top of the separating gel. A gel comb was used to create wells in the stacking gel for loading protein samples. The stacking gel was then allowed to polymerize for 15 min. The gel was used immediately or stored covered in a damp paper towel in a Ziploc bag at 4 °C until use.

Table 19: Gel percentage determined according to protein molecular mass

Protein mass (kDa)	Gel percentage (%)
< 25	15
25 – 50	12
50 – 120	10
120 – 250	6 – 8

Table 20: Components and volumes for casting separating gels

Components	6%	8%	10%	12%	15%
dH ₂ O	5.3	4.6	4.0	3.3	2.3
1.5 M Tris (pH 8.8)	2.5	2.5	2.5	2.5	2.5
30% polyacrylamide	2.0	2.7	3.3	4.0	5.0
10% SDS	0.1	0.1	0.1	0.1	0.1
10% APS	0.1	0.1	0.1	0.1	0.1
TEMED	0.008	0.006	0.004	0.004	0.004

Table 21: Components and volumes for casting stacking gels

Components	4%	5%
dH ₂ O	7.2	6.8
1.5 M Tris (pH 8.8)	1.3	1.7
30% polyacrylamide	1.25	1.25
10% SDS	0.1	0.1
10% APS	0.1	0.1
TEMED	0.01	0.01

4.3.5.3. Gel loading and running

The polymerized polyacrylamide gel was mounted on a gel cassette and placed in an electrophoresis chamber with 1x SDS running buffer, ensuring that the gels are fully immersed in the buffer. The combs forming the wells of the gel were subsequently removed, and the denatured protein lysates were loaded in appropriate volumes into the wells using a long loading pipette. The flanking wells were utilized for loading the protein marker. The electrophoresis chamber was then connected to a power source, and a voltage of 90V was applied until the proteins crossed the stacking gel, at which point the voltage was increased to 120V in order to separate the proteins according to their molecular size. The electrophoresis procedure was halted when the bromophenol blue dye staining the lysates reached the end of the separating gel. The proteins were subsequently transferred to a nitrocellulose membrane.

4.3.5.4. Protein transfer onto a nitrocellulose membrane

Further to SDS-PAGE, the proteins were transferred onto a nitrocellulose membrane using a fast, semi-dry transfer technique. The materials required for the transfer were pre-soaked in transfer buffer (100 ml 1X transfer buffer + 300 ml H₂O + 100 ml 100% Ethanol). The gel was then

extricated carefully from the glass plates and placed together with the nitrocellulose membrane in a sandwich between soaked filter cloths. The sandwich was placed in the transfer chamber, and smoothed with a roller to eliminate any air bubbles trapped within. The sandwich was organized as follows: anode – filter cloth x 6 – nitrocellulose membrane – gel – filter cloth x 6 – cathode. The chamber was placed in the transfer apparatus, and a standard 30 min transfer was performed. Post-transfer, the membrane was removed from the sandwich, washed once with TBST, and stained with 0.2% Ponceau S solution to confirm successful protein transfer. Additionally, using the protein marker and Ponceau staining as guides, the membranes were cut according to the sizes of the proteins of interest. The membranes were then washed with water and TBST to remove the Ponceau staining, and blocked using Roti Block for 1 hour at room temperature.

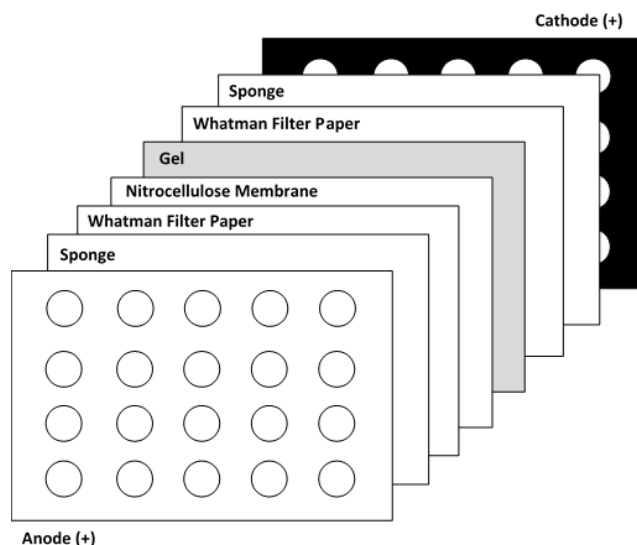


Figure 10: Assembly of blotting sandwich. Illustration of the arrangement of the transfer stack during immunoblot transfer procedure.

4.3.5.5. Antibody incubation

Following the blocking, the membranes were washed shortly in TBST and incubated with the primary antibodies specific to the protein of interest. The antibodies were diluted in TBST, and incubated with the membranes overnight at 4 °C. The next day, the blots were washed thrice for

10 min each with TBST, and incubated with the respective secondary antibodies (diluted in TBST) for 1 hour at room temperature. The secondary antibodies used were HRP-conjugated. Post-incubation, the membranes were washed thrice with TBST, and further visualized. All primary and secondary antibody dilutions were performed as illustrated in Tables 9 and 10.

4.3.5.6. Protein visualization

The immunoblotted proteins were visualized using an enhanced chemiluminescent substrate in an imager (Vilber). The Super Signal West Femto Maximum Sensitivity Substrate was used, and the images obtained were analyzed and quantified using ImageJ software.

4.4. Immunofluorescence staining

4.4.1. Seeding and fixation of cells on coverslips

Coverslips were sterilized by immersing them briefly in 75% ethanol followed by storage in 100% ethanol. They were then placed vertically into 24-well plates until dry, and further placed completely inside. The coverslips were further coated with 1% gelatin or collagen (or left uncoated for rat Müller cells). The cells were seeded into the wells containing coverslips (or into 4-well chamber slides), and cultured according to the experimental conditions, following which the cells were washed quickly with PBS and fixed using 4% Roti Histofix for 10 min. The cells were washed thrice with PBS, and stored covered with PBS at 4 °C for up to one week before staining.

4.4.2. Immunofluorescence staining in cells

The cells were first permeabilized and blocked with a solution of 2.5% w/v BSA and 0.3% v/v Triton X-100 in PBS for 1 hour at room temperature. Subsequently, 200µl of the primary antibody solution (diluted in PBS) was added to the wells, and the plates were incubated overnight at 4 °C. The following day, the cells were washed thrice with PBS for 5 min each to remove the unbound primary antibody and incubated with 200 µl of the secondary antibody (diluted in PBS) for 1 hour at room temperature in the dark. The cells were further washed thrice with PBS and incubated for 15 min with DAPI at room temperature in the dark, followed by three PBS washes. Using curved forceps, the coverslips were carefully picked out from the wells and placed upside down on glass object slides with mounting medium (Roti-Mount FluorCare). The staining was visualized

using a confocal microscope (Leica SP8), and immunofluorescence intensity was quantified using ImageJ.

4.5. ELISA for VEGF detection

ELISA was performed for the detection of secreted VEGF from HUVECs. HUVECs were cultured and subjected to high glucose and glucosamine stimulation as previously described. Human VEGF DuoSet ELISA kit from R&D systems was used to perform the assay, and all steps were performed according to manufacturer's instructions. First, the capture antibody was diluted to the working concentration in PBS and 100 µl of the solution was applied to coat each well of the supplied 96-well plate, which was further sealed and allowed to incubate at room temperature overnight. The following day, the wells were aspirated of the capture antibody solution and washed three times with wash buffer. The plate was further blocked by adding 300 µl of Reagent Diluent to each well and incubating at room temperature for one hour, followed by three washes with wash buffer to prepare for sample addition. The sample and provided standards were prepared in Reagent Diluent and added to the wells. The plate was covered with an adhesive strip and incubated for two hours at room temperature, following which the aspiration and wash step was repeated. A working solution of Streptavidin-HRP was prepared and 100 µl was added to each well. The plate was covered and incubated for 20 minutes at room temperature away from direct light. After repeating the aspiration and wash step, 100 µl of Substrate solution was added to each well, following which the plate was covered and incubated again for 20 minutes at room temperature away from direct light. Next, 50 µl of Stop solution was added to each well, and the plate was tapped gently to mix the solutions. The optical density of each well was determined immediately using a microplate reader set to 450nm. The results hence obtained were analyzed further, and the level of secreted VEGF determined via comparison with VEGF standards used.

4.6. RNA and qPCR techniques

4.6.1. RNA Isolation from retina

Prior to the isolation, all instruments (forceps, scissors, etc.) and the isolation surface were cleaned with dH₂O, 70% ethanol or RNase remover, and with dH₂O again, and the centrifuge was pre-cooled to 4 °C. The retinas were isolated quickly from unfixed eyes placed on a petri dish on

ice/dry ice. The isolated retinas were placed into a pre-cooled 1.5 ml Eppendorf tube containing 300 μ l of Trizol. At this stage, the retinas could be stored at -80°C , and the RNA isolated at a later time point. In the next stage of the isolation, the retinas were thoroughly homogenized by passing the suspension through syringe needles of decreasing diameters (22G, 25G, 27G), and 700 μ l of Trizol was added to the resultant homogenate to get a final volume of 1 ml. The suspension was allowed to stand at room temperature for 5 min, following which 200 μ l of chloroform was added to the tubes, and the tubes were shaken vigorously for 15 s. The tubes were further incubated at RT for 2 to 3 min, and centrifuged at 12000 g for 30 min, allowing for separation of the layers. The supernatant, or the aqueous layer, containing the RNA was transferred to a fresh 1.5 ml Eppendorf tube, and 500 μ l of isopropanol was added. The tubes were shaken, incubated at RT for 10 min, and centrifuged at 12000 g for 30 min. the supernatant was then carefully discarded, and the pellet washed twice with 1 ml of 75% ethanol, followed by centrifugation at 7500 g for 5 min. After discarding the supernatant, the pellet was dried almost completely of the ethanol, and dissolved in 20 μ l of RNase free dH_2O . The RNA concentration and purity were further measured using a NanoDrop.

4.6.2. RNA isolation from Müller cells

Murine Müller cells were cultured in 6 cm dishes and stimulated with HG and glucosamine as described before. After culture, the dishes were placed immediately on ice. The medium was removed, and the cells were washed quickly twice with ice-cold PBS. 300 μ l of Trizol was added to the cells; the cells were scraped off the dishes using a cell scraper, and the suspension was pipetted up and down with a 1 ml pipette before transferring to an ice-cold 1.5 ml Eppendorf tube. The tubes were then allowed to stand at room temperature for 5 min, and all following steps were performed similar to the isolation of RNA from retinas.

4.6.3. cDNA synthesis

cDNA synthesis from the retinal RNA was performed using Superscript VILO reverse transcriptase enzyme. 1 µg of RNA was added with 4 µl of VILO enzyme, and the final reaction volume was made up to 20 µl using nuclease-free dH₂O.

For cDNA synthesis from Müller cell-derived RNA, GoScript cDNA synthesis kit from Promega was used. The reagents were mixed together according to the manufacturer's instructions and volumes, and added to 1 µg of RNA to create a final reaction volume of 20 µl.

The RNA reaction mixtures from both retina and Müller cells were placed in a thermal cycler and the following program was executed:

Table 22: Program for cDNA synthesis in thermal cycler

Temperature	Time
25 °C	5 min
42 °C	1 hour
70 °C	15 min

The cDNA hence obtained was stored at – 20 °C, and used diluted 1:5 for actin PCR and qPCR.

4.6.4. Actin PCR and agarose gel electrophoresis

To confirm the presence of cDNA in the samples, and to ensure that all samples contained equal amounts, actin PCR was performed with the synthesized cDNA. The components were mixed together as shown in Table 22, and PCR was performed according to the program shown in Table 23.

Table 22: Components and volumes for actin PCR

Components	Volume
PCR master mix	10 μ l
β actin forward primer	1 μ l
β actin reverse primer	1 μ l
cDNA (diluted 1:5)	2 μ l
dH ₂ O	6 μ l

Table 23: Program for actin PCR in thermal cycler

Temperature	Time
95 °C	5 min
95 °C	15 s
62 °C	30 s
72 °C	30 s
72 °C	7 min

} 20 cycles

The amplified products were then subjected to agarose gel electrophoresis. A 1% agarose gel containing ethidium bromide was prepared and immersed in 1X TAE buffer. The samples were loaded on to the gel, and the gel was allowed to run at 100 V for 20-30 min. The resultant DNA bands were visualized using a UV-light imager, and the images obtained used to determine the presence and relative concentration of the DNA between the samples (Fig. 16)

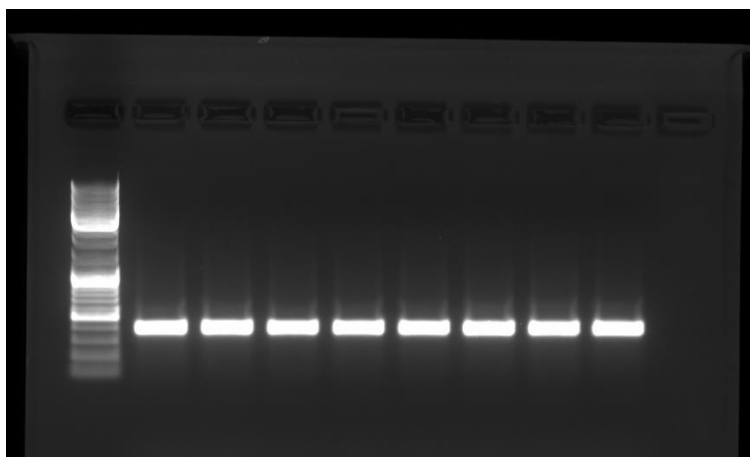


Figure 11: Actin PCR. Example of an image obtained via UV-imaging of agarose gel used to determine the presence and relative concentrations of DNA in different samples after Actin PCR following cDNA synthesis.

4.6.5. qPCR and analysis

Prior to starting the experimental procedure for qPCR, a table was created to formulate the volumes of master mix, primers, water, and cDNA required for the reactions. The samples were further arranged according to their loading order on the qPCR plate. The components were further mixed together in the wells of a qPCR plate (MicroAmp Optical 96-well Reaction plate, Applied Biosystems) according to the volumes given in Table 24. The plate was then covered with a sealing film and spun shortly in a centrifuge. The plate was placed in a Quantstudio 3 machine, and qPCR was performed using the fast reaction setting for 50 cycles. For quantification, the samples were measured in triplets, and analyzed using the $\Delta\Delta C_t$ method, normalizing to the control. The data was further analyzed statistically using GraphPad Prism.

Table 24: Components and volumes for qPCR

Components	Volume
Taqman master mix	10 μ l
Probe primer	1 μ l
Control primer	1 μ l

cDNA (diluted 1:5)	2 μ l
dH ₂ O	6 μ l

4.7. Data quantification and statistical analysis

For immunoblot analysis, the images obtained from visualization of proteins in the imager were quantified using Image J software. The individual bands obtained were selected, and the area adjusted such that minimum background was selected. The intensity of the bands was then calculated by plotting curves of each band and measuring the area under the curve using the 'wand' function. The intensity was normalized against the control housekeeping gene, and the result obtained was used for statistical analysis.

For immunofluorescence staining, the images were also analyzed using Image J. The 'threshold' value was initially set to encapsulate the immunofluorescence intensity for a control image, and the same threshold was used for the measurement of all sample images. The images were loaded on to the software, and the 'measure' function was used to obtain a mean intensity, which was further used for statistical analysis.

All statistical analysis was performed with the GraphPad Prism 6 software (GraphPad, La Jolla). For statistical analysis, the data are presented as mean \pm SD. Statistical significance was established using paired/unpaired student's t-test or one-way ANOVA with Tukey's multiple comparison test, according to the samples. p values <0.05 were considered statistically significant.

5. Results

5.1. Glucosamine supplementation in mice does not alter their metabolic parameters

Male C57Bl/6 mice, one week after undergoing diabetes induction via streptozotocin injection at 8 weeks of age, began treatment with glucosamine (10mg/kg) incorporated into their food. Six months after the commencement of the treatment, the animals were subjected to a metabolic cage to assess their metabolic parameters. During a 16-hour time period in the cage, the water and food intake of the animals as well as the urine and feces output were assessed (Fig. 12).

In comparison with the non-diabetic control animals, diabetic animals showed a significant increase in consumption of water (617%) and food (355%), as well as in the excretion of urine (2268%) and feces (199%), in accordance with the known consequences of diabetes. In the non-diabetic animals, the food and water intake and the urine and feces output were not significantly influenced by glucosamine treatment ($p < 0.05$, $n = 10$). The diabetic animals treated with glucosamine also showed a consistent increase in consumption of water, excretion of urine, the food intake and the feces output, comparable to the diabetic control animals and showing no impact of glucosamine. Hence, this indicates that the consumption of glucosamine along with the food does not alter the metabolic parameters of intake and output in the mice, either with or without diabetes to a larger extent.

5.2. Glucosamine treatment increases its levels in the blood, but is non-toxic

Initially, plasma from the mice was collected and analyzed via UPLC to determine the concentration of glucosamine. Upon measurement of the available glucosamine in the plasma, no differences in the endogenous levels of glucosamine were observed between the control non-diabetic and diabetic animals. The levels of glucosamine in the plasma were significantly increased (49.5%) in the glucosamine treated non-diabetic and diabetic mice (Fig. 13). Surprisingly, the plasma concentration of glucosamine in the diabetic mice was significantly higher than in the non-diabetic mice (323.8%), suggesting a differential metabolism of glucosamine or an altered uptake and distribution in the diabetic mice. It could be speculated

that such an altered uptake could occur due to the fact that glucosamine uptake also occurs via the GLUT glucose transporters.

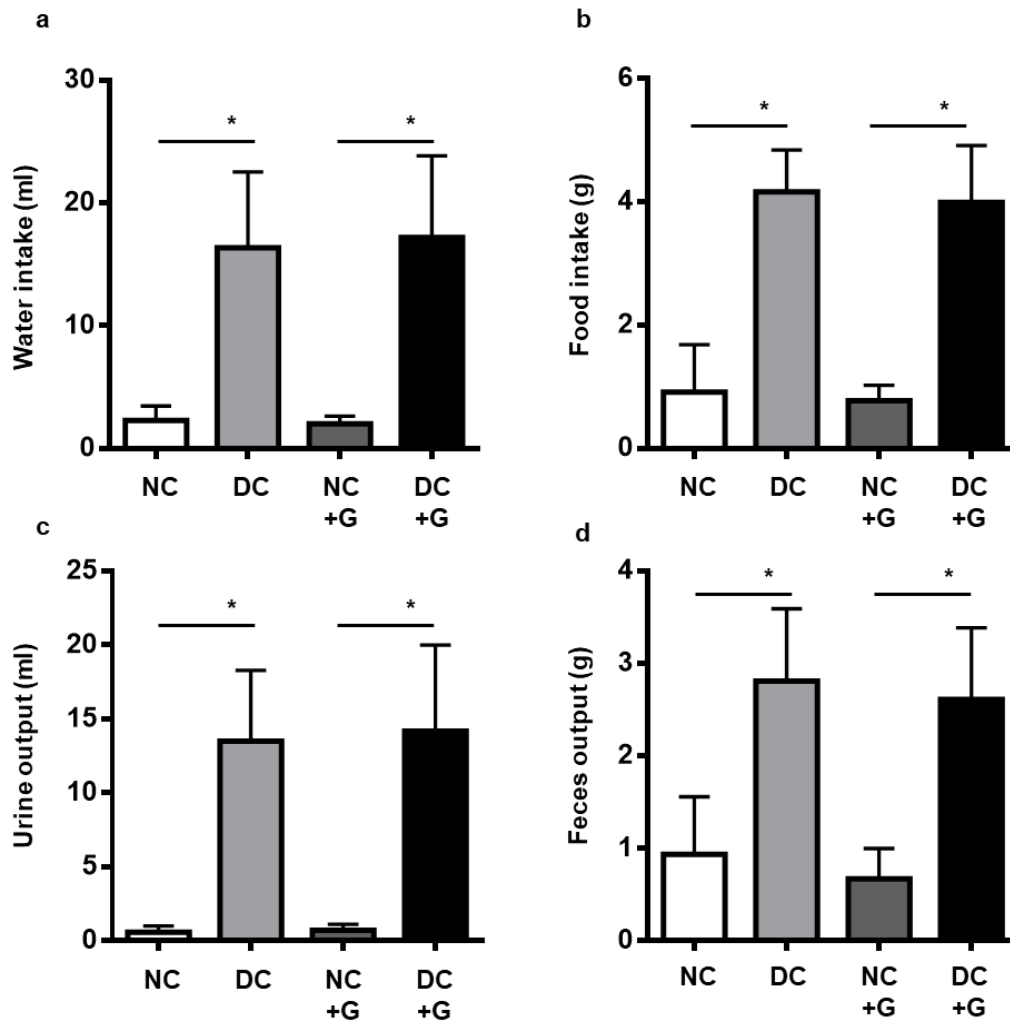


Figure 12: Metabolic parameters of the mice are not impacted by glucosamine. *a*: Water intake, *b*: food intake, *c*: urine output, and *d*: feces output of the mice showing significant increase under diabetic conditions both with and without glucosamine treatment. n=10, *p<0.001. NC: Non-diabetic control, DC: Diabetic control, NC+G: NC supplemented with oral glucosamine, DC+G: DC supplemented with oral glucosamine.

In addition, the influence of glucosamine treatment on liver function was evaluated by measuring the levels of the enzymes glutamic oxaloacetic transaminase (GOT) and glutamic pyruvic transaminase (GPT) in the plasma. These enzymes are produced mainly in the liver, and the concentrations of the enzyme in the plasma are an indication of liver damage. As the amount of

the enzyme in the bloodstream is directly proportional to the extent of liver tissue damage, the enzyme levels in the plasma were measured to determine whether glucosamine can cause liver damage, or result in indirect liver toxicity. No change in the levels of either GOT or GPT enzymes were observed between non-diabetic and diabetic control animals, suggesting no significant influence of hyperglycemia on liver function in the animals. In both diabetic and non-diabetic animals, glucosamine supplementation did not significantly increase the plasma GOT and GPT (Fig. 14), indicating the safety and non-toxicity of the glucosamine treatment.

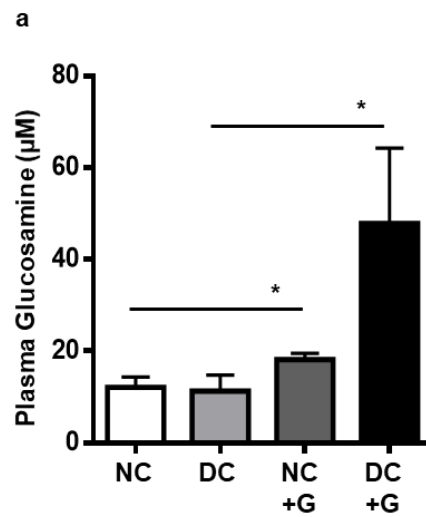


Figure 13: Glucosamine is increased in plasma after supplementation. a: Measurement of glucosamine levels in the plasma shows a significant increase in both non-diabetic and diabetic treated animals. n=5, *p<0.05

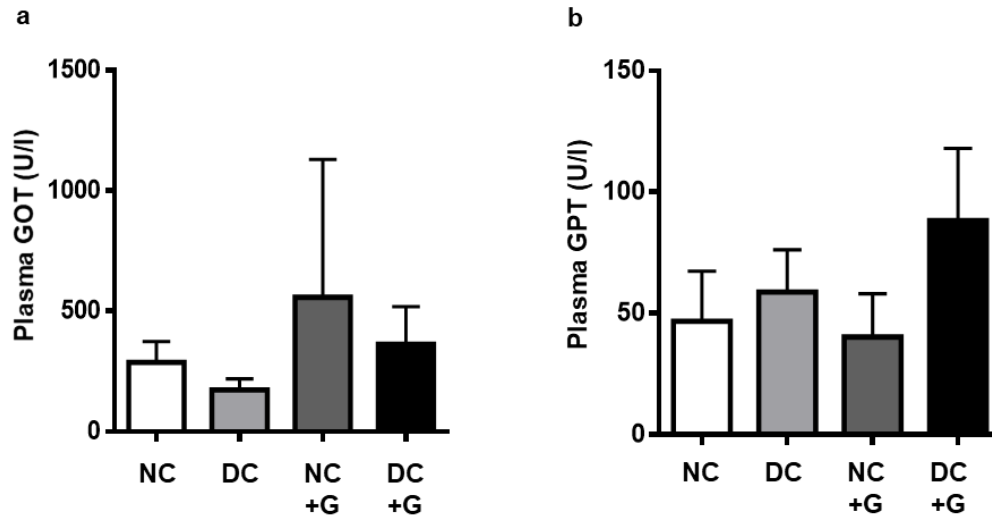


Figure 14: Liver function enzymes in plasma are not influenced by glucosamine. Levels of a: GOT and b: GPT in the plasma of non-diabetic and diabetic mice with or without glucosamine treatment showing no significant differences between the groups. n=6, *p<0.05

5.3. Glucosamine affects neither blood glucose nor HbA1c, but induces body weight gain

In order to assess the influence of glucosamine on the glucose metabolism of the mice, the blood glucose was first measured. In comparison to non-diabetic controls, a significant increase in the levels of blood glucose was observed in the streptozotocin-injected diabetic animals; this is consistent with the diabetic phenotype, and therefore expected. In the non-diabetic animals treated with glucosamine, this supplementation did not lead to changes in the blood glucose level. Similarly, in diabetic animals, glucosamine treatment did not alter the blood glucose levels (Fig. 15a).

Further, the HbA1c levels of the animals was measured. HbA1c values reflect the average blood glucose levels over the past 120 days or 40 days in humans or mice, respectively. Once again conforming to the diabetic phenotype, the STZ-induced hyperglycemia significantly elevated the HbA1c levels measured over the course of the study (Fig. 15b). In both non-diabetic and diabetic animals, no influence of glucosamine treatment was observed in comparison to the controls, suggesting that glucosamine does not have an impact on blood glucose.

Additionally, the impact of glucosamine supply on the body weight of the animals was investigated. Expectedly, a significant decrease in the body weight of diabetic animals compared to non-diabetic animals was observed. In non-diabetic animals, glucosamine supplementation induced a significant 17% body weight gain (Fig. 15c). However, no such body weight change was observed in the diabetic animals with glucosamine treatment, indicating a potential hyperglycemia-independent connotation. The data hence show that despite exerting no influence on the blood glucose level or the general metabolic parameters in the intake of food and water or the excretion of urine and feces in the mice, glucosamine still induced a body weight gain under non-diabetic conditions.

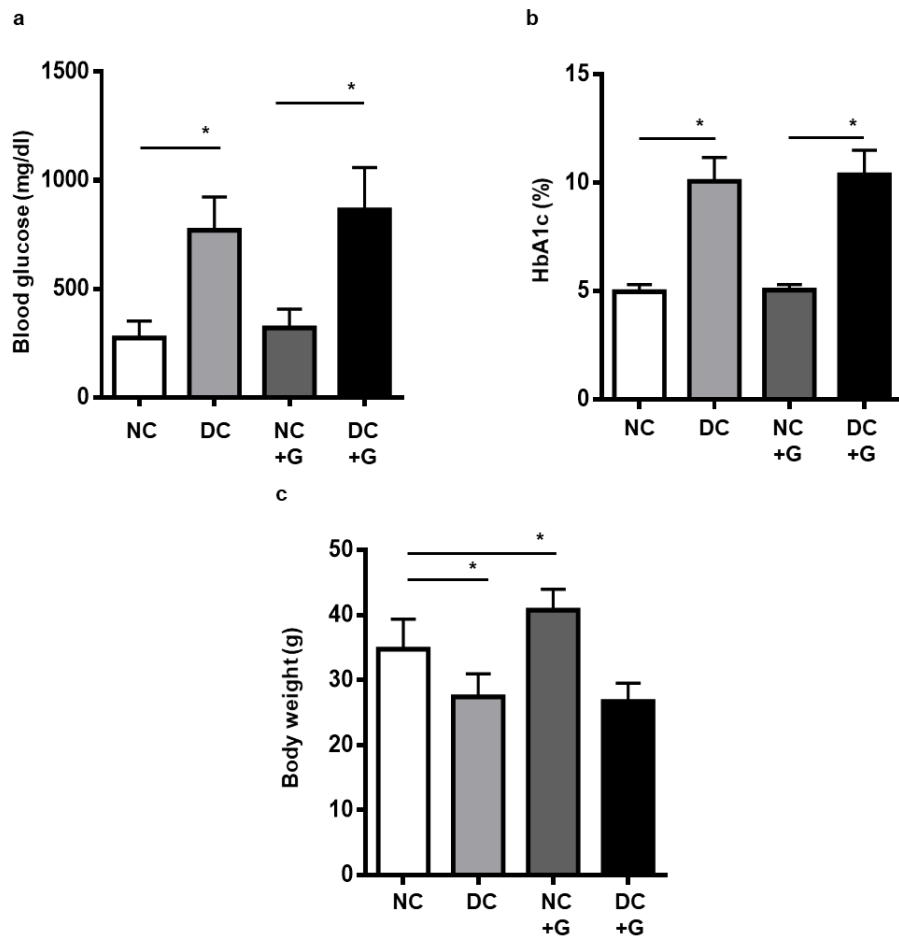


Figure 15: Glucosamine does not affect blood glucose or HbA1c. **a:** Blood glucose and **b:** HbA1c measured show a significant increase in diabetic animals, but no impact of glucosamine. **c:** Body weight of the animals is decreased under diabetic conditions. Glucosamine can increase the body weight in non-diabetic mice. n=6-8, *p<0.05

5.4. Retinal thickness is unaltered by glucosamine

After the initial metabolic parameters of the mice were assessed, the retinas were further examined for the neuronal function to assess the impact of glucosamine on retinal function. Several studies have insinuated that diabetes alters the thickness of the inner and outer layers of the retina, mainly through neuronal cell degeneration in the retina. The retinal thickness hence reduces with disease progression. The total retinal thickness in the mice was measured using optical coherence tomography. No changes in the retinal thickness were observed between the non-diabetic and diabetic animals, suggesting that in this model of diabetes, retinal thickness loss and hence obvious neuronal cell degeneration does not occur. Glucosamine supplementation did not influence the thickness of either the non-diabetic or diabetic retinas, suggesting that it does not cause neuronal degeneration in the retina (Fig 16).

In addition, PAS staining was performed in paraffin sections of mouse eyes in order to verify the OCT findings and assess the thickness of individual retinal layers. The thickness of individual retinal layers was quantified and compared between the groups. Although the inner nuclear cell layer showed a slight reduction in cell number compared to the non-diabetic controls, no significant changes in either cell number or cell layer thickness in the retina were observed either with diabetes or with glucosamine supplementation (Fig 17).

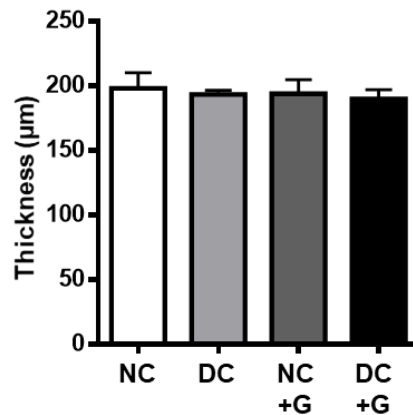


Figure 16: Retinal thickness is unaffected. Measurement of retinal thickness using optical coherence tomography (OCT) showing no changes between non-diabetic and diabetic animals and no influence of glucosamine. n=6-8, *p<0.05

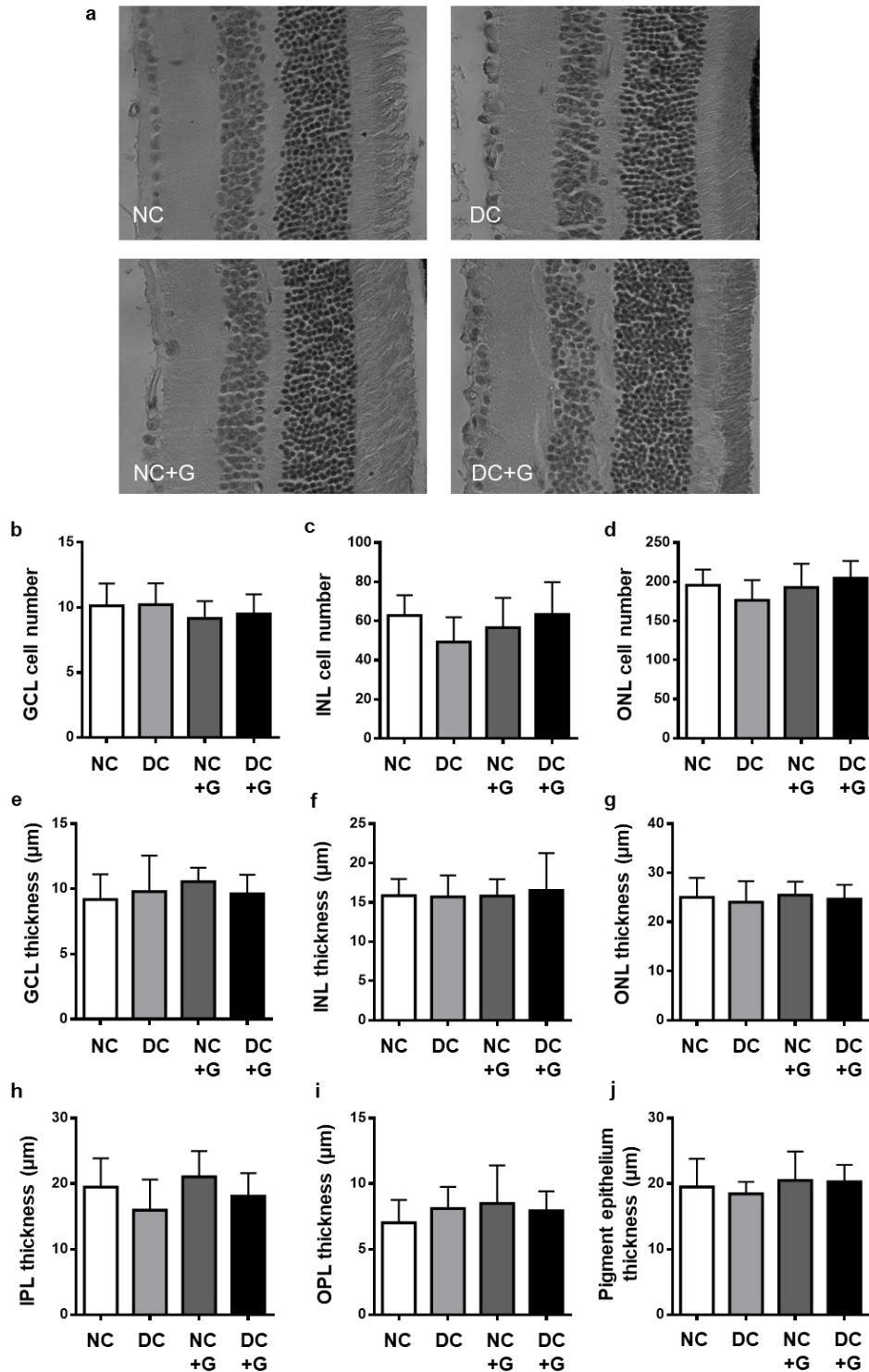


Figure 17: Retinal cell number and layer thickness are unaffected. **a:** Representative images of retinal paraffin sections stained with Periodic Acid-Schiff displaying the layers in the neuroretina. Quantification of cell number in **b:** ganglion cell layer (GCL), **c:** inner nuclear layer (INL), **d:** outer nuclear layer (ONL), and quantification of layer thickness of **e:** GCL, **f:** INL, **g:** ONL, **h:** inner plexiform layer (IPL), **i:** outer plexiform layer (OPL), and **j:** pigment epithelium showing no changes between non-diabetic and diabetic animals, no influence of glucosamine; n=3-4.

5.5. Glucosamine exerts a neuroprotective effect in the retina

Besides vascular dysfunction, early abnormal neuronal function is also a hallmark of diabetic retinopathy. In fact, it is insinuated that neuronal damage can even begin before, and hence contribute towards, vascular regression in the retina. To investigate the influence of glucosamine on the neuronal aspect of the retina, a functional test was performed. The electrical activity of the retina in response to light stimulus was measured using multifocal electroretinogram (mfERG) in order to assess the neuronal function of the retina. The different waveforms generated in the mfERG correspond to the activity of different cell types in the retina. In this study, the N1- and P1-waves of the mfERG were investigated.

The amplitude of the N1-wave seen in the mfERG corresponds to the activity of the photoreceptors in the retina. The N1-wave amplitude showed a reduced extent but no significant change in diabetic animals compared to the non-diabetic controls, suggesting that there is no major photoreceptor damage in this model of streptozotocin-induced diabetes in mice, and the overall photoreceptor activity is largely maintained. Glucosamine treatment showed a tendency to increase the N1-wave amplitude in both non-diabetic and diabetic animals compared to their respective controls but this also did not reach statistical significance. The data therefore indicate that the photoreceptor function remains largely unaltered by glucosamine supplementation (Fig. 18a).

The P1-wave of the ERG, generated by Müller cells and ON-bipolar cells, was significantly reduced in the diabetic retinas compared to non-diabetic controls, conforming to previously published data, substantiating that this model of diabetes shows signs of changes in neuron-glial response in the retina. This response most likely corresponds first to the activation and/or dysfunction of Müller cells due to the chronic hyperglycemia. In the non-diabetic animals, glucosamine did not affect the P1-wave. However, under diabetic conditions glucosamine rescued the P1-wave amplitude, increasing it to the level of the non-diabetic controls (Fig. 18b), suggesting that it could play a role in the restoration of neuron-glial function in the retina via its action on Müller or ON-bipolar cells.

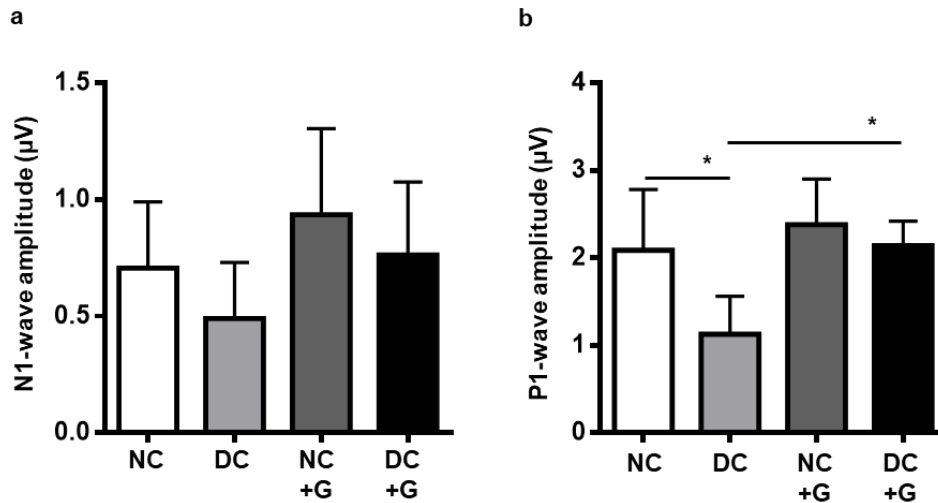


Figure 18: Glucosamine is neuroprotective in the retina. *a*: N1-wave amplitude of the ERG showing no changes between any of the groups. *b*: P1-wave amplitude of the ERG showing a decrease in diabetic animals, and amelioration with glucosamine treatment. n=6-8, *p<0.05

5.6. Astrocyte coverage in the retina is unaffected by glucosamine

In order to further investigate the effects of glucosamine on the macroglial aspect of the retina, whole retinas from the mice were subjected to immunofluorescence staining against GFAP which is expressed by astrocytes and Müller cells in the retina. An increase in GFAP expression indicates an activation of macroglial cells. The GFAP-stained retina was examined using confocal microscope, wherein the superficial layer displayed GFAP expression in the astrocytes. Astrocytes are mainly found in the nerve fiber layer in the retina and, like Müller cells, their processes are involved in the formation of the blood retinal barrier in the superficial retinal layer.

In non-diabetic retinas, the astrocytes displayed normal morphology and are distributed evenly but sparsely throughout the retina. In the diabetic retinas, the astrocytes displayed a slightly more ramified structure. In the glucosamine-treated retinas, the astrocyte morphology resembles the normal phenotype. The astrocyte number, however, was unaltered in the diabetic animals, suggesting that hyperglycemia, while altering the morphology of the astrocytes, does not change their numbers. This hence indicates that no astrocyte degeneration or proliferation occurs during progression of diabetic retinopathy. Further, glucosamine supplementation did not

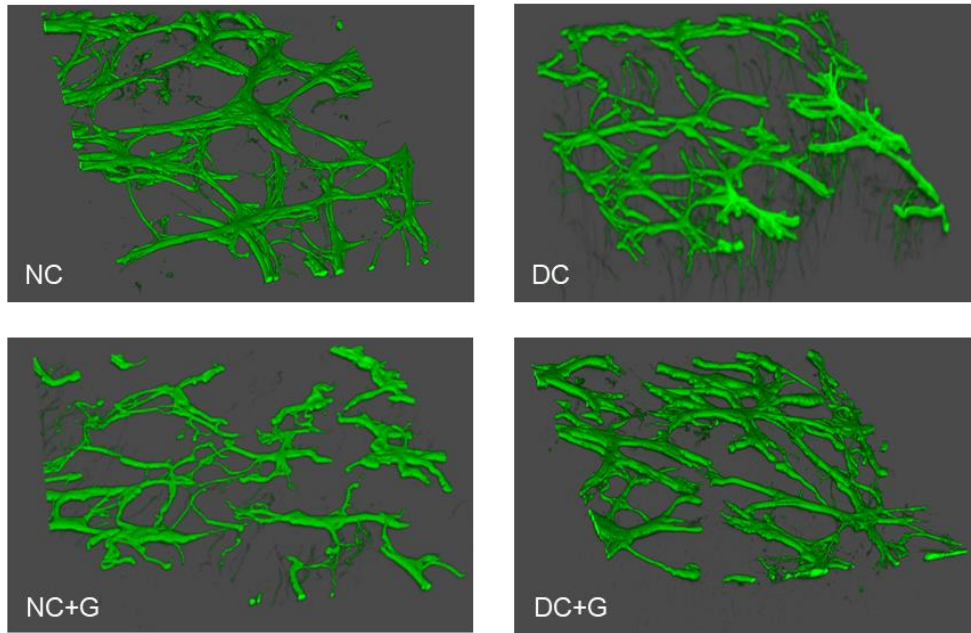
have an effect on the astrocyte numbers in the superficial layer of the retina, in either the non-diabetic or diabetic animals (Fig. 19b).

5.7. Müller cell activation in the diabetic retina is reduced by glucosamine

Müller cells span the entire length of the retina and play a major role in the modulation of the neurovascular microenvironment. Since the activity of Müller cells is the primary contributor to the P1-wave of the ERG, their activation in the retina was studied further using GFAP immunofluorescence. The activation of Müller cells can be seen via increased GFAP levels in the cells. Hence, examining the GFAP immunofluorescence in the retina further, GFAP protein expression was observed in the endfeet of Müller cells, visible in the superficial layer in the diabetic animals and, rarely, in the other groups. Following this GFAP expression from the endfeet down through the retina into the deep retinal layer, increased GFAP expression was seen throughout the Müller cells in the diabetic retinas, a phenotype of Müller cell activation.

In contrast, the retinas from non-diabetic animals displayed minimal GFAP expression in the Müller cells, with the expression descending only a fraction of that seen in the diabetic retinas. In the non-diabetic animals, glucosamine had no visible effect in comparison to the control retinas, whereas glucosamine supplementation reduced the GFAP expression, and therefore the activation of the Müller cells, in the diabetic animals, showing a significant reduction of GFAP staining beyond the superficial layer (Fig. 20). This hence indicates that glucosamine can suppress the activation of Müller cells in the retina caused by chronic hyperglycemia, and suggests a potential mechanism for the neuroprotective effects seen in the mfERG.

a



b

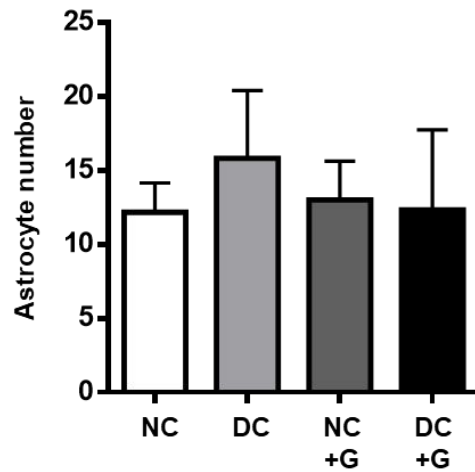


Figure 19: Astrocyte coverage in the retina is unaffected. *a*: Confocal 3D image of GFAP immunofluorescence staining of astrocytes in the retinas of non-diabetic and diabetic mice with and without glucosamine treatment showing no difference between the groups. *b*: Quantification of the astrocyte number also shows no variations between the groups. $n=3$, $*p<0.05$

5.8. Glucosamine decreases activation of Müller cells and reduces the expression of VEGF *in vitro*

In order to investigate the effect of glucosamine on Müller cells, an *in vitro* approach was used. Using a rat Müller cell line, the protein expression of GFAP was examined. A high glucose concentration (30 mM) was used to mimic diabetic conditions, and normal glucose (5 mM) was used as control. Both conditions were stimulated with glucosamine, and the GFAP protein expression was detected via immunoblotting. A rather strong GFAP expression was detected in the cultured rMCs in basal conditions already. High glucose, interestingly, did not have a significant effect on the GFAP levels. This is contradictory to other studies that show increase in GFAP expression [165], and hence Müller cell activation, under high glucose conditions. Glucosamine stimulation resulted in a significant decrease in GFAP protein levels in both normal and high-glucose stimulated cells, indicating a reduced activation of the rMCs with its treatment (Fig. 21a, b).

Moreover, the GFAP expression in the rMCs was examined via immunofluorescence. Similar to the immunoblot, GFAP expression in the rMCs was not induced by high glucose concentrations. However, glucosamine treatment showed a consistent decrease in the GFAP expression in the rMCs, confirming that glucosamine can indeed reduce GFAP expression in the rMCs (Fig. 21d, e).

In addition to contributing to the formation of the blood retinal barrier, Müller cells are also one of the major secretors of VEGF and Ang2 in the retina, suggesting that they can also regulate endothelial cell survival signaling. VEGF, produced by glial cells and endothelial cells in the retina, is overexpressed and harmful in diabetic retinas, leading to progression of diabetic retinopathy [166]. Therefore, the VEGF expression in the rMCs was further investigated following the assessment of GFAP expression.

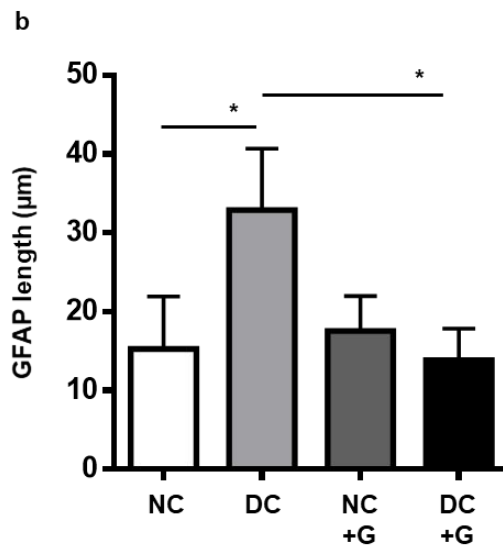
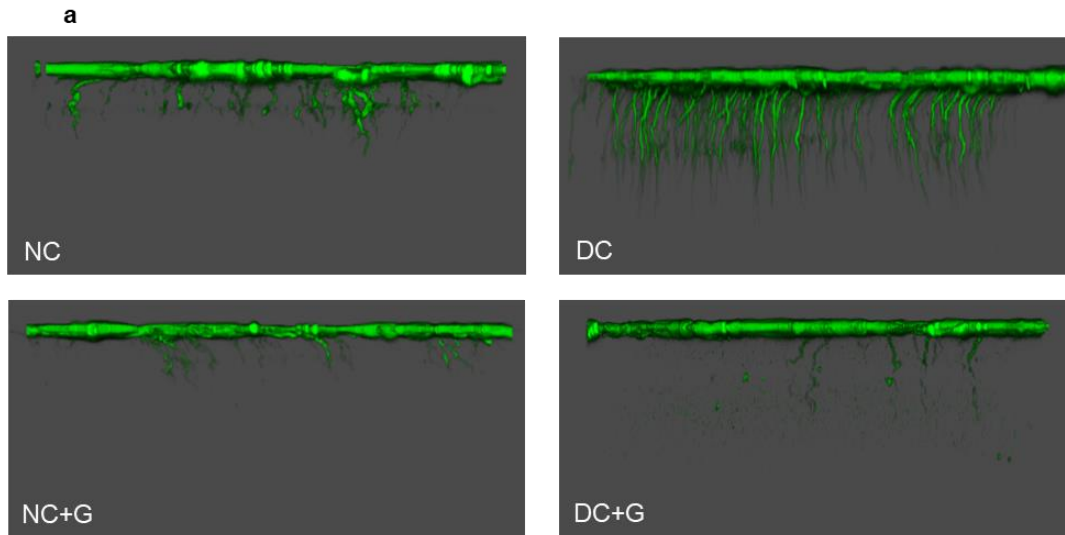


Figure 20: Glucosamine reduces Müller cell activation in the retina. **a:** Confocal 3D images of GFAP immunofluorescence staining spanning the depth of the retina showing Müller cells in green. Under diabetic conditions, the Müller cells display GFAP to a greater depth compared to non-diabetic retinas. Diabetic mice treated with glucosamine show reduced GFAP lengths in Müller cells. **b:** Quantification of activated Müller cell length shows a significant decrease of GFAP staining with glucosamine treatment in diabetic retinas. $n=3$, $*p<0.05$

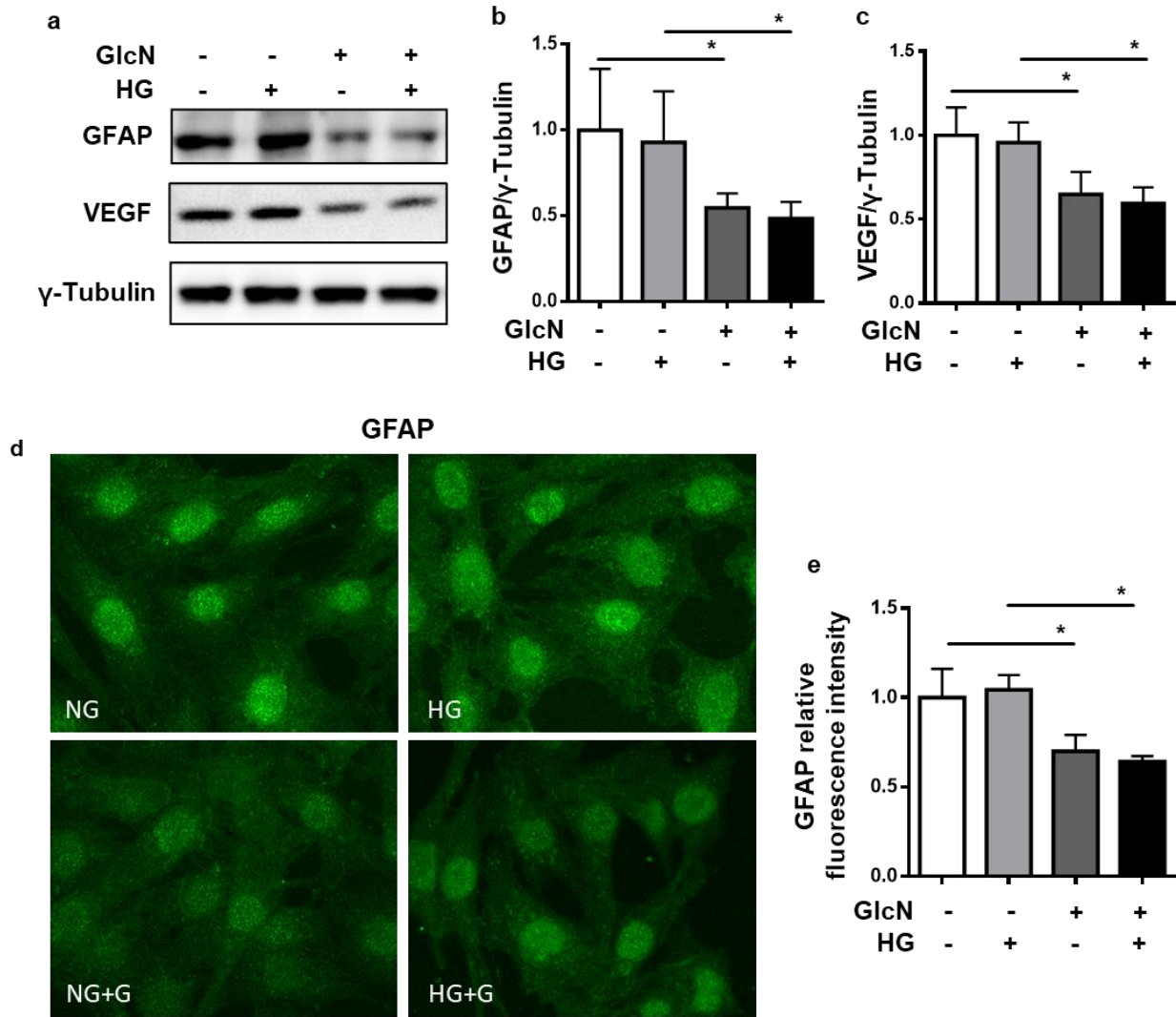


Figure 21: Glucosamine reduces rat Müller cell activation. **a:** Immunoblot analysis in rat Müller cells treated with HG and glucosamine showing a decrease in GFAP and VEGF expression with glucosamine stimulation. Quantification of **b:** GFAP and **c:** VEGF with respect to γ -Tubulin, n=6. **d:** Immunofluorescence staining of GFAP in rat Müller cells and **e:** quantification of GFAP fluorescence intensity showing a significant decrease with glucosamine. n=4, *p<0.05. NG: Normal glucose (5mM), HG: High glucose (30mM), NG+G: NG treated with 10mM glucosamine, HG+G: HG treated with 10mM glucosamine.

High glucose did not alter the VEGF expression in the retina compared to the NG controls, similar to the effect seen on GFAP. Glucosamine treatment, however, significantly reduced the VEGF protein content in the rMCs, in both normal and high glucose concentrations (Fig. 21a, c). As judged by GFAP expression, Müller cells are apparently activated in the *in vitro* culture. In line with this interpretation, the VEGF expression is regulated similarly as GFAP. Since VEGF signaling

plays a role also in the regulation for survival signals in endothelial cells, it is possible that the regulation of the Müller cell secretome, such as inhibition of VEGF release, via glucosamine could also have an impact on endothelial cells.

5.9. Glucosamine does not alter expression of neurotrophic factors in Müller cells

Müller cells produce neurotrophic factors such as GDNF and BDNF in order to regulate the neuronal microenvironment and protect neuronal cells. To determine their levels in Müller cells in the retinas from the experimental animals, total mRNA from the mouse retinas was isolated and reverse transcribed into cDNA, further to which qPCR was performed with specific primers for neurotrophic factors and GFAP. The expression of neurotrophic factors was influenced neither by hyperglycemia, nor by glucosamine treatment, leaving their expression unaltered at the transcriptional level (Fig. 22a, b). Similarly, no change in GFAP mRNA expression was seen, either due to diabetes or glucosamine (Fig. 22c). Since the effect of glucosamine on GFAP protein expression in the retina is clearly visible, the data hence suggest that the regulation in retinal GFAP occurs at a post-transcriptional level, exhibiting itself as a marker of the activation of Müller cells.

In addition to the retina, mRNA expression of the neurotrophic factors was also examined in mouse Müller cells isolated from the retinas of mice. The Müller cells were cultured and stimulated with glucose and glucosamine before RNA isolation and subsequent qPCR. Identical to their expression in the retinas *in vivo*, no difference was seen in the expression of GDNF and BDNF at the transcriptional level in the Müller cells *in vitro* (Fig. 22d, e), indicating the presence of other mechanisms involved in the protective/beneficial effect of inhibited Müller cell activation by glucosamine.

5.10. Inflammatory and angiogenic factors are not influenced at the transcriptional level by glucosamine

Based on the potential anti-inflammatory characteristics of glucosamine, the mRNA expression of inflammatory factors such as IL-1 β , IL-6, TNF- α , and ICAM-1 in the retina were additionally examined. Surprisingly, no significant change in the inflammatory factors was detected in the diabetic retinas compared to non-diabetic controls (Fig. 23a, b, c, d). Glucosamine treatment had no effect on the inflammatory factors at the transcriptional level. Furthermore, the expression of the inflammatory factors TNF- α and IL-6 was investigated in the mouse Müller cells, yielding similar results (Fig. 23e, f), indicating that these factors are not changed at the transcriptional level in our models *in vivo* and *in vitro* by glucosamine.

In addition, the expression of angiogenic factors such as Ang2 and of recipient receptors such as VEGFR2 also contribute to the regulation of neurovascular unit. These factors were accordingly examined in the retina via qPCR. No changes in the mRNA expression of Ang2 and VEGFR2 was seen either with diabetes or with glucosamine treatment (Fig. 24a, b). Upon investigating the expression of Ang2 and VEGFR2 in mouse Müller cells, similar results were observed. While there was a tendency of increased mRNA expression of Ang2 seen in the mouse Müller cells cultured in high glucose concentration, overall, no significant effect of either high glucose or glucosamine was observed on Ang2 or VEGFR2 (Fig. 24c, d), suggesting that glucosamine does not affect these factors at the transcriptional level.

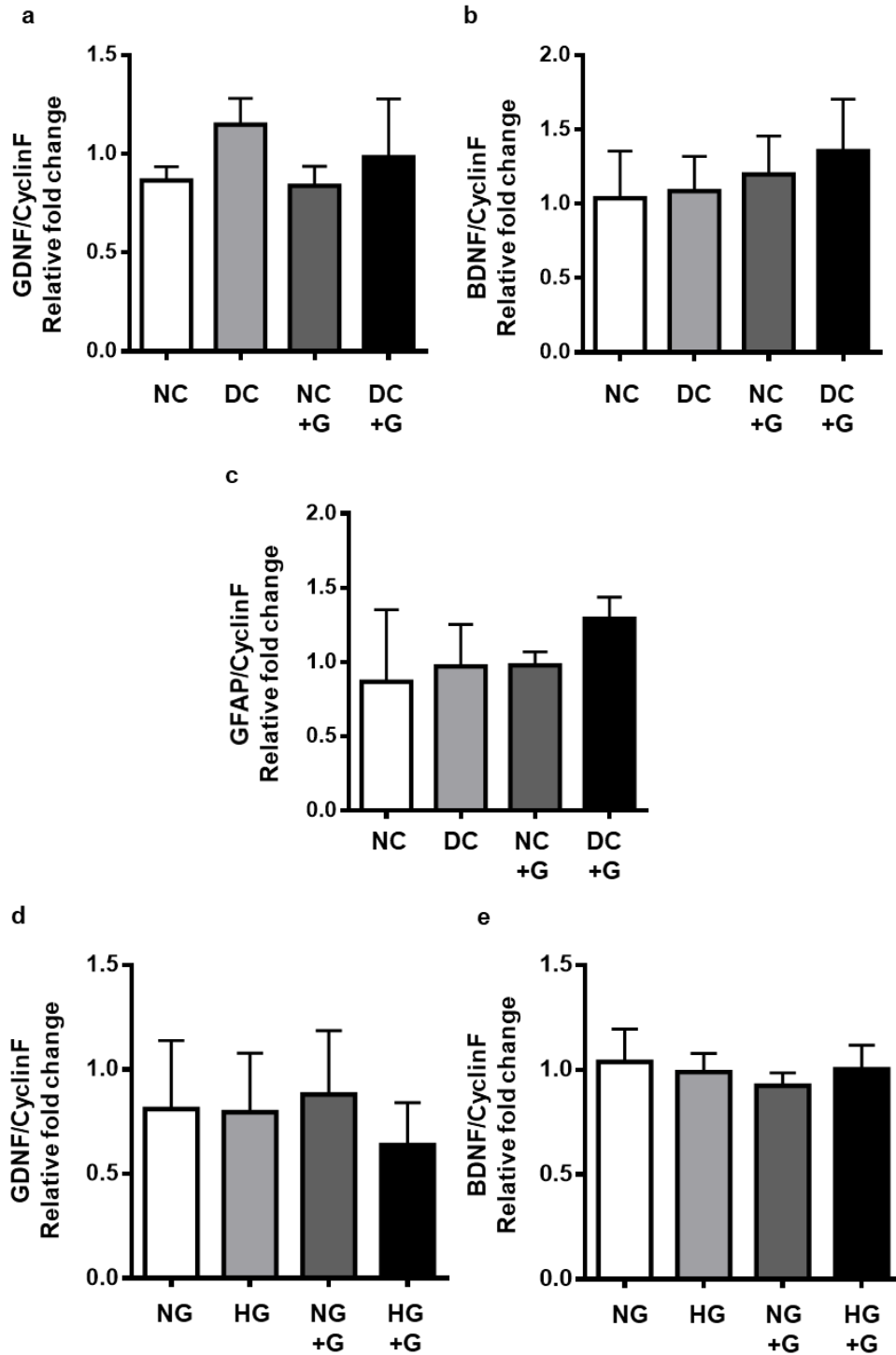


Figure 22: Neurotrophic factor mRNA expression is uninfluenced by glucosamine. qPCR done using RNA isolated from retinas of diabetic and non-diabetic mice treated with or without glucosamine showing relative fold change of **a**: GDNF, **b**: BDNF, and **c**: GFAP compared to Cyclophilin F housekeeping gene exhibiting no changes between any of the groups. qPCR with mRNA from rMCs treated with or without HG and glucosamine showing no changes in relative fold changes of **d**: GDNF and **e**: BDNF compared to Cyclophilin F between the groups. n=3

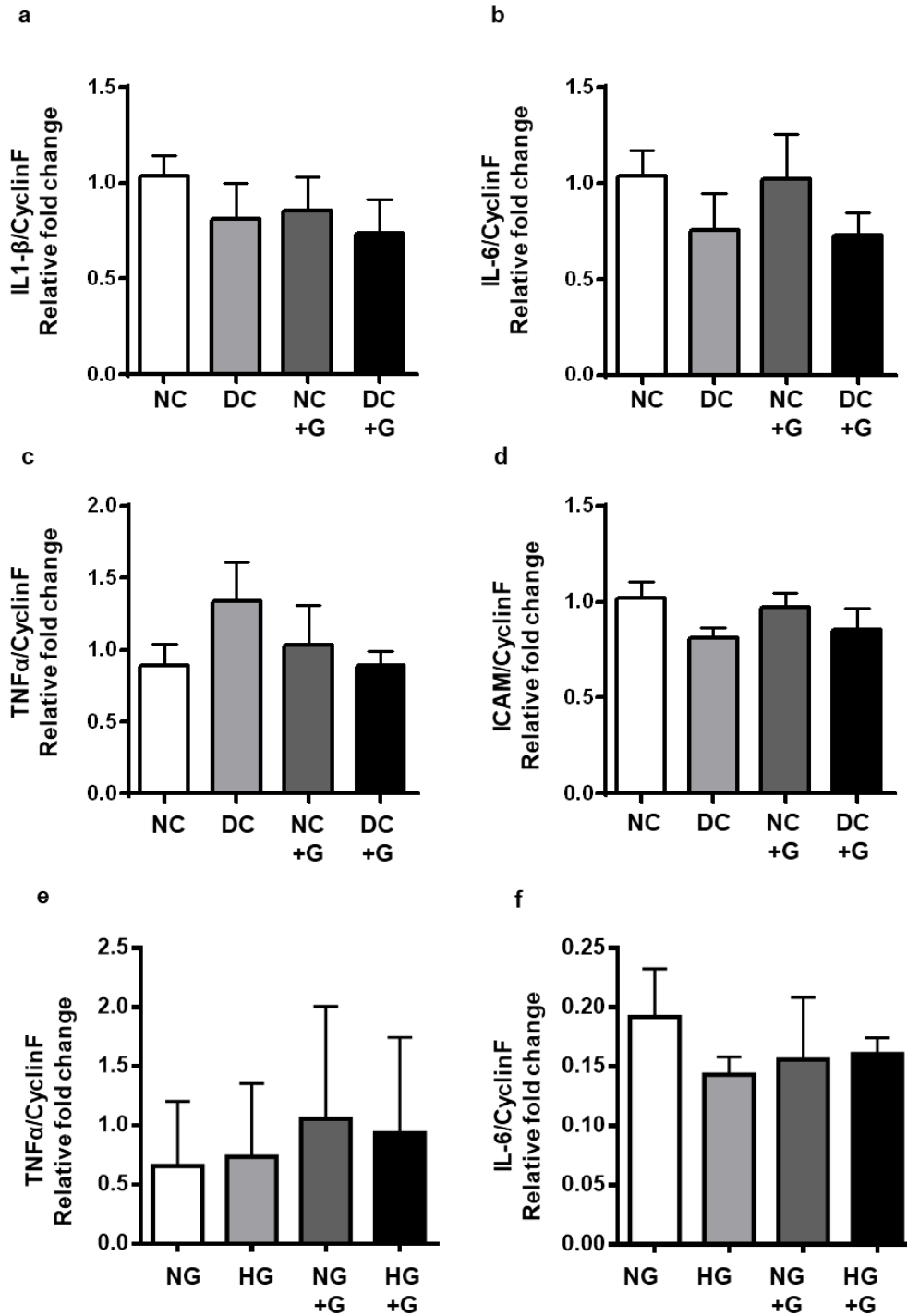


Figure 23: Inflammatory factors in the retina and mouse Müller cells are not impacted by glucosamine. qPCR relative fold change in the retinas of diabetic and non-diabetic animals supplemented with and without glucosamine of **a**: IL-1 β , **b**: IL-6, **c**: TNF- α , and **d**: ICAM-1 compared to Cyclin F showing no changes between the groups. Relative fold change of **e**: TNF- α and **f**: IL-6 in mouse Müller cells also showing no changes with either high glucose or glucosamine stimulation. n=3

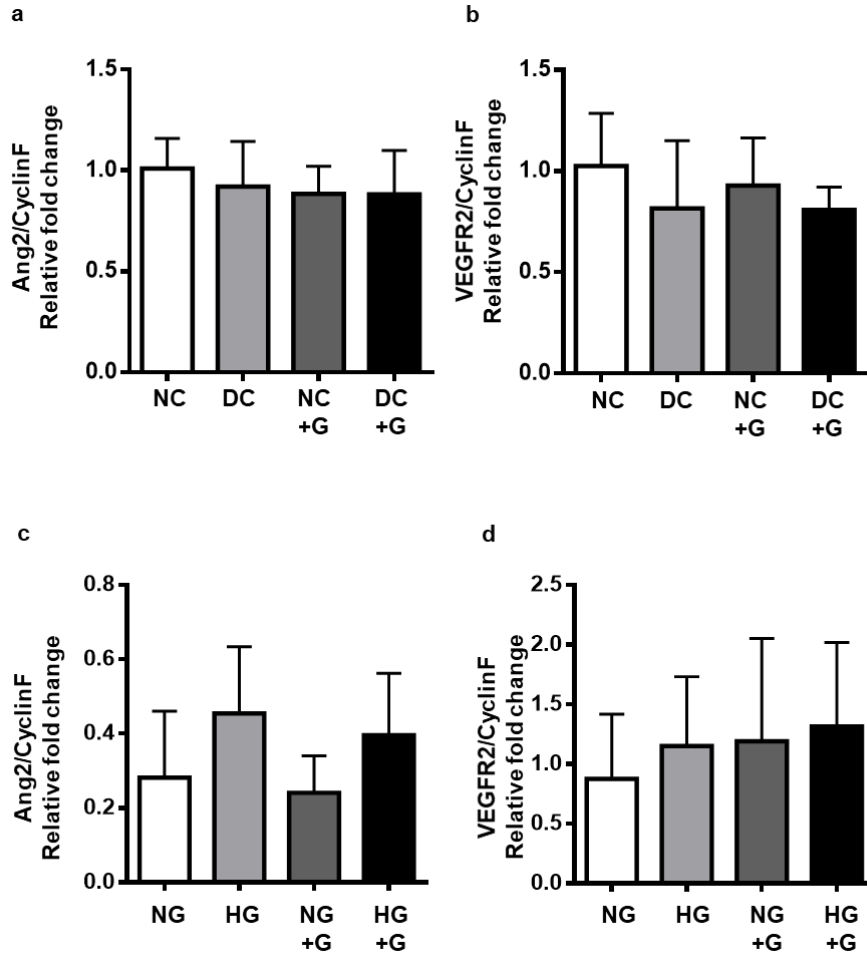


Figure 24: Angiogenic and survival factors are not influenced at transcriptional level by glucosamine. qPCR analysis of **a**: Ang2 and **b**: VEGFR2 in the mouse retinas showing no influence of glucosamine on relative fold change compared to Cyclophilin F. Similar analysis of **c**: Ang2 and **d**: VEGFR2 in mouse Müller cells also showing no impact of glucosamine on these factors. n=3

5.11. Glucosamine aggravates vascular damage in the retina

Further to examining the effect of glucosamine on the neuronal aspect of the retina, its impact on vascular damage in the retina was analyzed. Diabetic retinopathy manifests early via pericyte dropout and the formation of acellular capillaries, two features that are considered the hallmarks of vascular damage in the retina. The quantification of the pericyte coverage and acellular capillary formation in the retina provides an indication of the extent and severity of vascular injury. Therefore, in order to assess the vascular damage in the retina, the numbers of pericytes and acellular capillaries were quantified in retinal digest preparation stained with PAS.

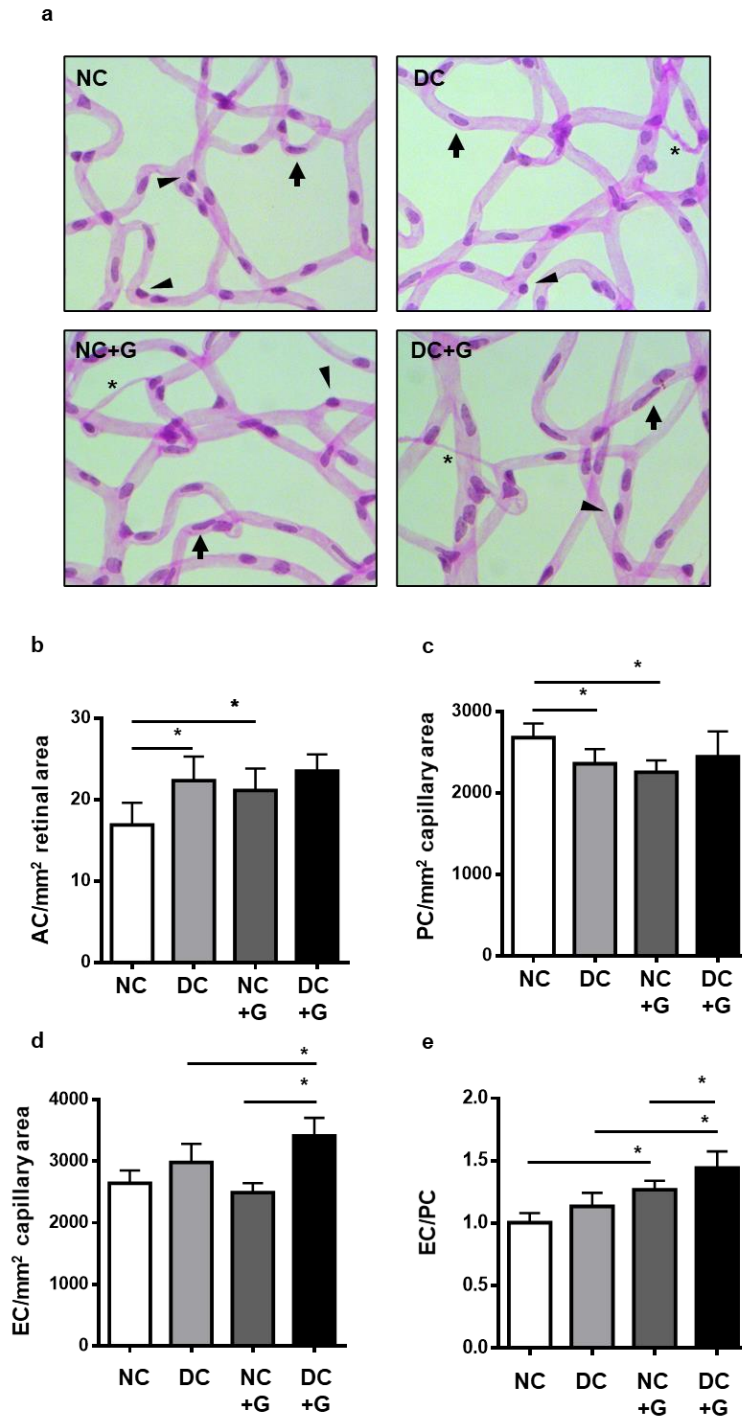


Figure 25: Glucosamine aggravates vascular damage in the retina. **a:** Representative images of Periodic Acid-Schiff staining in retinal vasculature following retinal digestion in non-diabetic and diabetic animals supplemented with and without glucosamine. Arrows indicate endothelial cells (ECs), arrowheads indicate pericytes (PCs), and stars mark acellular capillaries (ACs). Quantification of **b:** ACs and **c:** PCs showing increase and decrease in numbers, respectively, with glucosamine treatment in non-diabetic animals. Quantification of **d:** ECs and **e:** EC to PC ratio showing increase in both parameters with glucosamine treatment in both diabetic and non-diabetic conditions. n=6-8, *p<0.05

Compared to the non-diabetic controls, the diabetic animals displayed a significant reduction in the number of pericytes (-12%) and a significant increase in the formation of acellular capillaries (+32%), confirming the occurrence of an early diabetic retinopathy phenotype of vascular damage. Surprisingly, under non-diabetic conditions, glucosamine supplementation induced a dropout of pericytes (-16%) and an increase in acellular capillary formation (+26%) similar to that observed in diabetic animals (Fig. 25b, c). Compared to diabetic animals and to non-diabetic animals treated with glucosamine, the supplementation with glucosamine in diabetic animals did not further increase the loss of pericytes, nor the formation of acellular capillaries.

The total number of endothelial cells and the endothelial cell to pericyte ratio remained unaltered between non-diabetic and diabetic control animals. Interestingly, glucosamine treatment led to a significant increase in the total number of endothelial cells in the diabetic animals, and an increase in the endothelial cell to pericyte ratio in both non-diabetic and diabetic retinas (Fig. 25d, e).

5.12. Glucosamine suppresses survival signaling in endothelial cells

To gain further insight into the apparent vascular damage caused by glucosamine supplementation *in vivo*, the impact of glucosamine on endothelial cells was assessed further *in vitro*. Initially, the influence of glucosamine on cell survival, toxicity, and apoptosis was assessed to determine optimal working concentrations for the experiments. Endothelial cells were treated with increasing concentrations of glucosamine and subjected to analysis with the ApoTox-Glo Triplex assay kit (Promega) according to the manufacturer's instructions. With 5 and 10 mM concentrations of glucosamine, no significant changes in either cell viability, resistance to toxicity, or apoptosis was observed. Under 25 mM concentration of glucosamine, both cell viability and resistance to toxicity were significantly reduced, while cell apoptosis tended to increase, suggesting that glucosamine at 25 mM is harmful to the cells (Fig. 26). Thus, for further experiments, 5 and 10 mM concentrations of glucosamine were used.

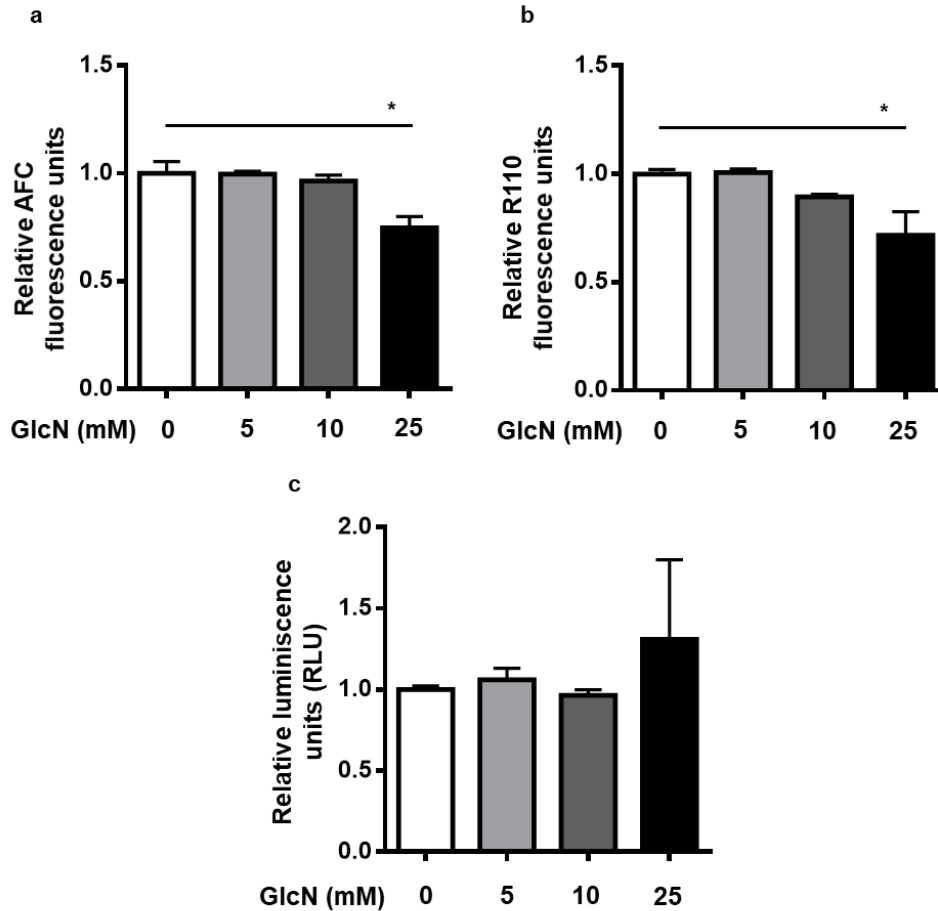


Figure 26: Glucosamine is harmful to endothelial cells in higher concentrations. Measurement of cell viability, toxicity, and apoptosis with glucosamine treatment using ApoTox-Glo Triplex assay kit (Promega). Quantification of relative fluorescence units of **a**: AFC (aminofluorocoumarin) as an indicator of cell viability, **b**: R110 (rhodamine 110) as an indicator of resistance to cell toxicity, and **c**: quantification of relative luminescence units proportional to caspase activity as an indicator of cell apoptosis, n=3-4, *p<0.05

In endothelial cells, VEGF-VEGFR2 signaling is crucial to their survival. In addition, Ang2, a key growth factor that mediates pericyte loss, is produced by endothelial cells. Therefore, the protein regulation of these two factors was analyzed in detail.

Initially, cultured HUVECs were used as a cell model. To determine whether glucosamine treatment could have an effect on VEGFR2 and Ang2 protein levels, and to pinpoint the concentrations of glucosamine that could bring about this hypothesized effect, HUVECs were treated with increasing concentration of glucosamine in cell culture, and the protein expression was further analyzed via immunoblot. With increasing glucosamine concentrations, a dose-

dependent decrease in the VEGFR2 protein level was observed. In addition, a slight shift in the apparent molecular mass of the band representing VEGFR2 in SDS-PAGE was observed in the groups treated with glucosamine (Fig. 27a, b). A similar concentration-dependent decrease was observed in Ang2 protein levels, along with an observed shift in the apparent molecular mass (Fig. 27a, c). Glucosamine concentrations over 5 mM significantly suppressed VEGFR2 and Ang2 expression in HUVECs, suggesting a potential regulation of endothelial signaling under these conditions. The level of protein O-GlcNAcylation in the cells was also assessed via immunoblot, since exogenous glucosamine supplementation can increase the flux through the HBP and hence influence the downstream process of protein O-GlcNAcylation. Interestingly, glucosamine supplementation did not appear to affect the level of protein O-GlcNAcylation in the HUVECs.

To mimic diabetic conditions, HUVECs were treated with 30mM glucose along with glucosamine (5 and 10 mM). In both normal and high glucose concentrations, glucosamine could once again reduce the protein levels of VEGFR2 and Ang2, in addition to the slight shift in molecular mass (Fig. 28a, b, c). Significant reduction in the protein levels was observed at both 5 mM and 10 mM concentrations of glucosamine, indicating a possible interference with VEGF-VEGFR2 signaling and Ang2 secretion upon treatment of endothelial cells with concentrations of glucosamine higher than 5 mM. Although high glucose concentrations did not alter the VEGFR2 protein content, it did increase Ang2 protein content in HUVECs. This is in accordance with previously published data, which attribute this increase to enhanced protein O-GlcNAcylation in the cells treated with high glucose (30 mM). No significant difference in the level of protein O-GlcNAcylation in the HUVECs was however observed upon glucosamine treatment, either in normal or high glucose conditions, although high glucose increased the protein O-GlcNAcylation compared to the normal glucose controls.

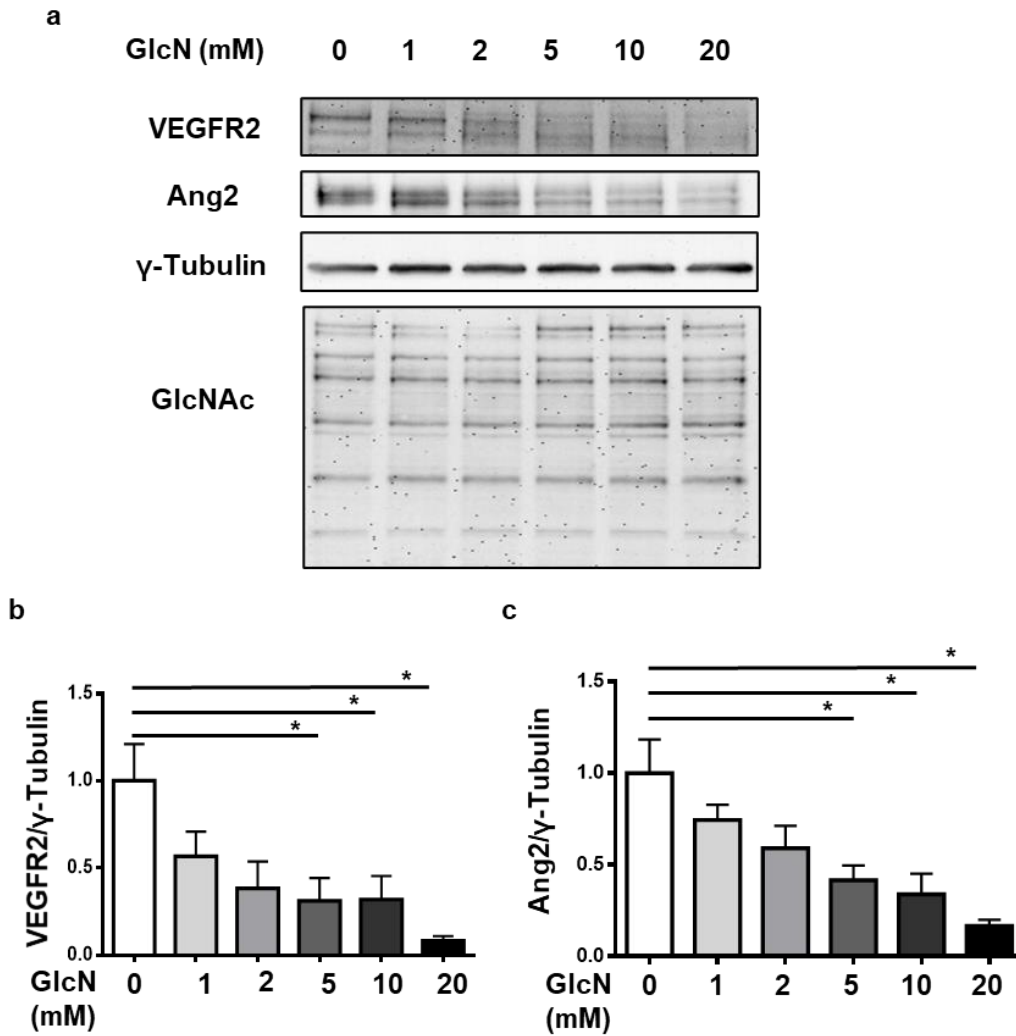


Figure 27: Glucosamine alters Ang2 and VEGFR2 content in HUVECs. *a*: Immunoblot analysis of VEGFR2, Ang2, and protein O-GlcNAcylation protein levels with increasing glucosamine stimulation. Quantification of *b*: VEGFR2 and *c*: Ang2 with respect to γ -Tubulin. n=7, *p<0.05

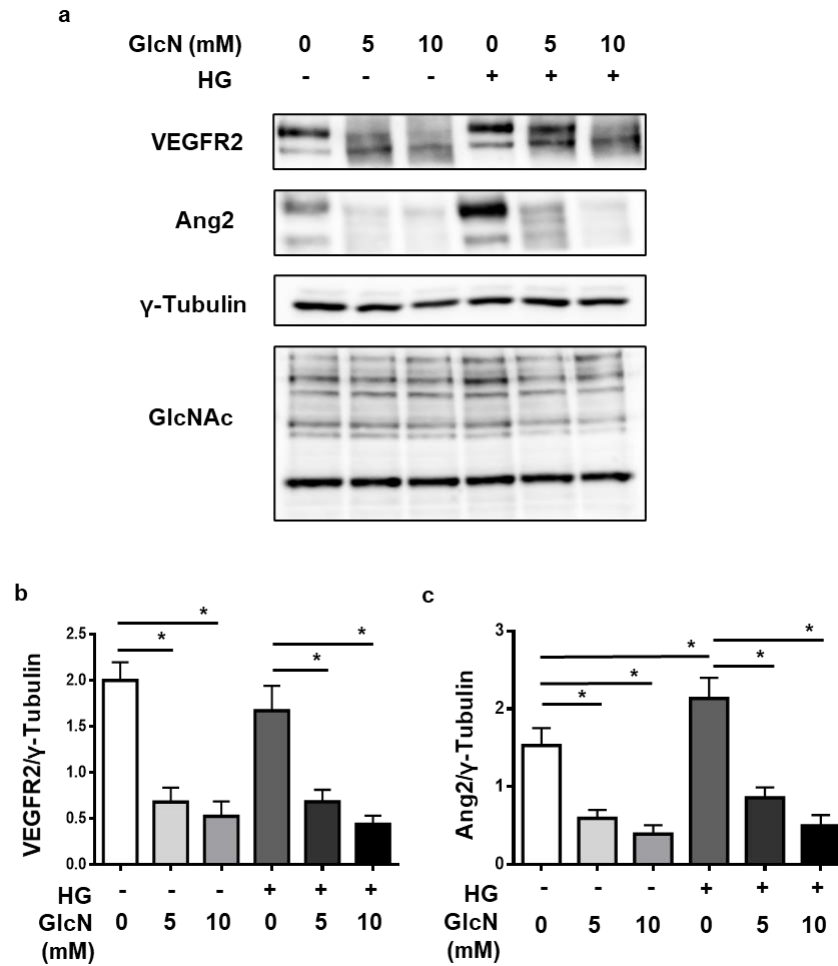


Figure 28: Glucosamine alters Ang2 and VEGFR2 content independently of the glucose concentration. a: Immunoblot analysis in normal and high glucose conditions showing VEGFR2 and Ang2 protein expression and protein O-GlcNAcylation with glucosamine treatment. Quantification of **b:** VEGFR2 and **c:** Ang2 with respect to γ -Tubulin. n=7, *p<0.05

These findings were further substantiated by immunofluorescence staining of VEGFR2 and Ang2 in HUVECs under normal and high glucose conditions. Similar to the immunoblot data, no changes in VEGFR2 content were observed with high glucose concentrations, whereas the Ang2 immunofluorescence intensity was significantly increased. Confirming the immunoblot data, glucosamine treatment significantly diminished the immunofluorescence signal of both VEGFR2 and Ang2, confirming the regulation of these factors by glucosamine treatment observed by immunoblotting (Fig. 29a, b, c).

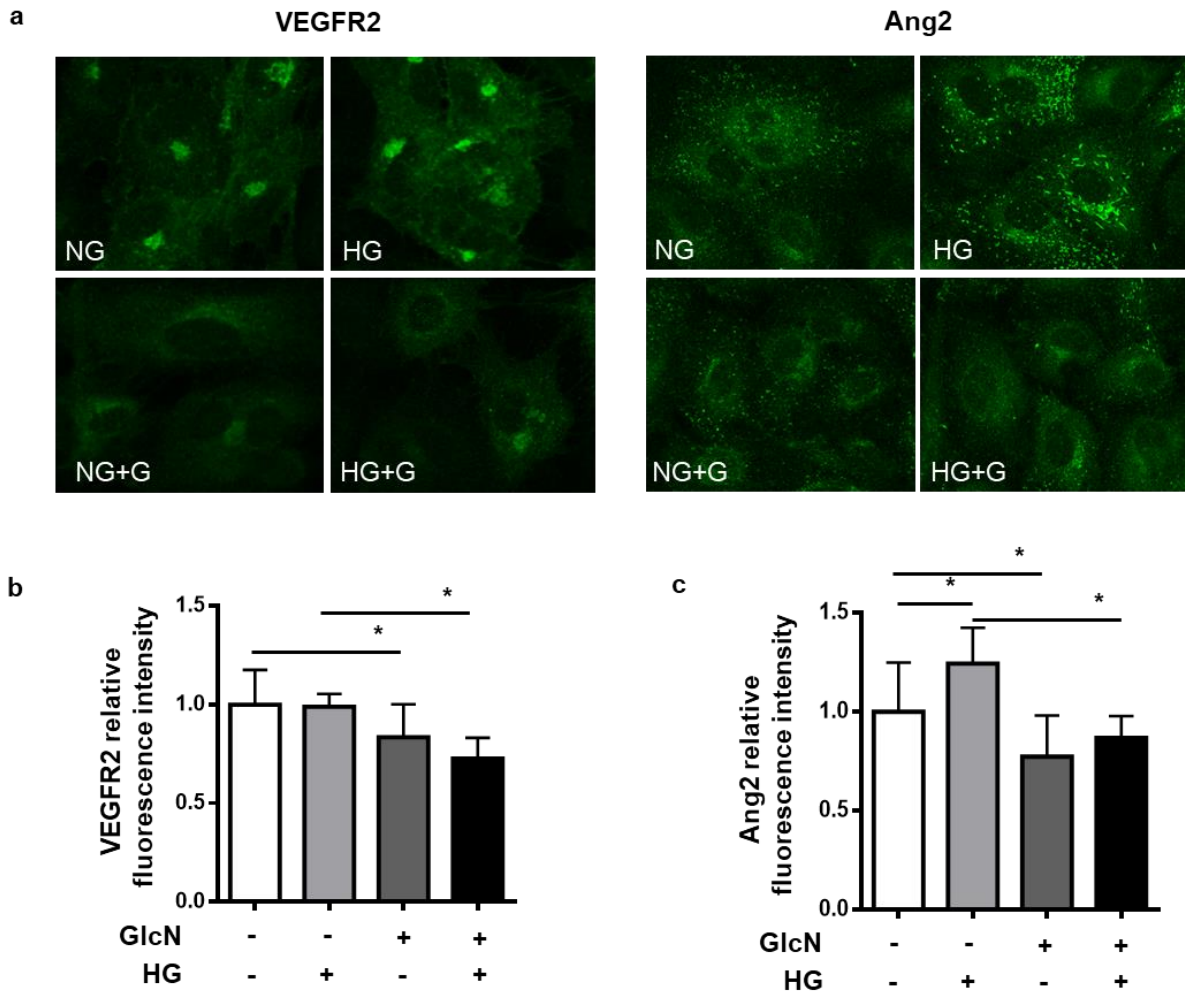


Figure 29: Glucosamine alters Ang2 and VEGFR2 content in HUVECs. *a*: Immunofluorescence staining of VEGFR2 and Ang2 in HUVECs. Quantification of *b*: VEGFR2 and *c*: Ang2 relative immunofluorescence intensity. n=4, *p<0.05

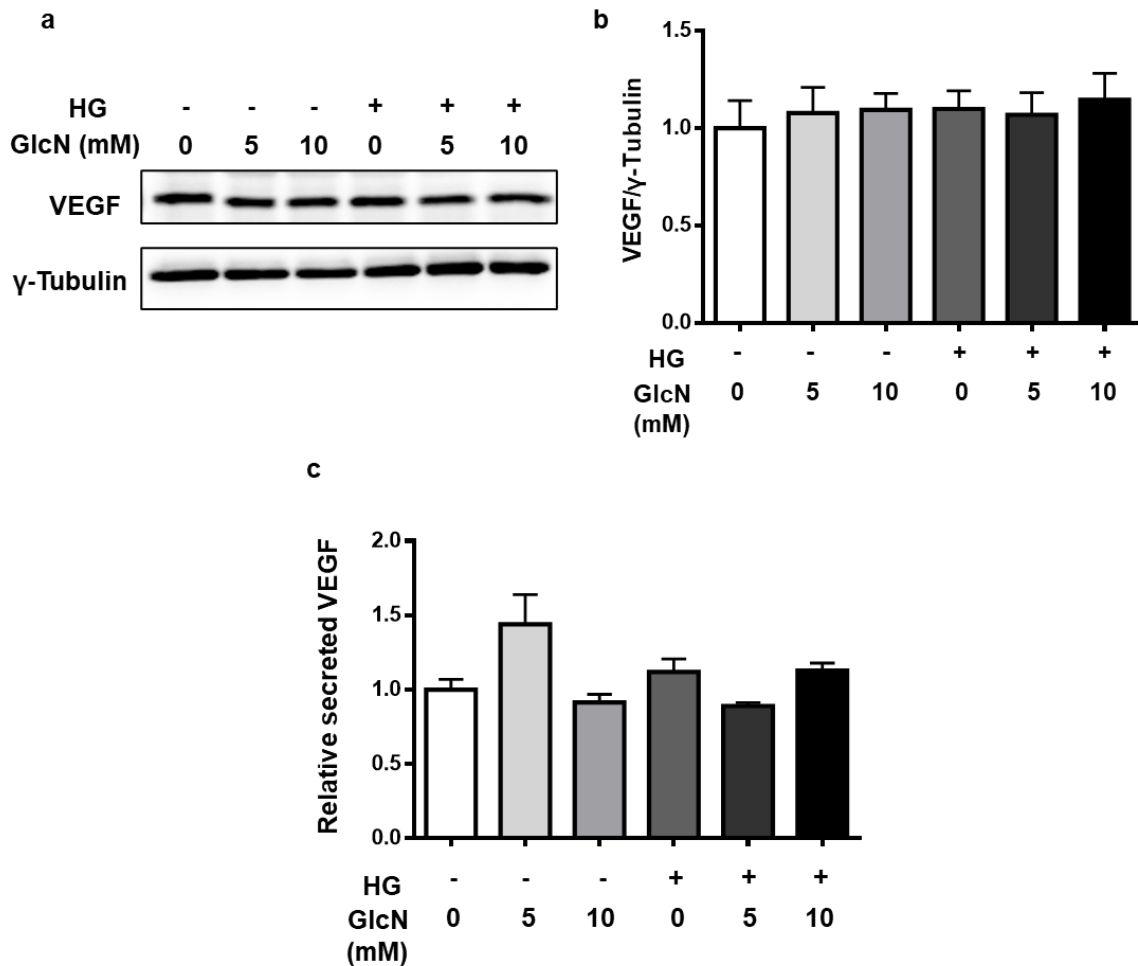


Figure 30: Glucosamine does not influence VEGF protein content or secretion. *a*: Immunoblot analysis showing VEGF protein expression with high glucose and glucosamine stimulation, *b*: Quantification of VEGF with respect to γ -Tubulin, *c*: VEGF ELISA analysis showing no significant changes between the groups, n=3-4.

In order to further investigate the mechanisms behind the decrease in VEGFR2 protein expression seen with glucosamine treatment, a possible regulation via VEGF was examined. VEGF protein content was analyzed via immunoblot in HUVECs, but revealed no changes with either high glucose or glucosamine treatment (Fig. 30a, b). In order to determine whether VEGF secretion from the cells could be influenced by glucosamine, an ELISA was performed using supernatants from cultured cells treated with high glucose concentrations and glucosamine. This, too, revealed no significant alterations in VEGF secretion, again suggesting that VEGF-induced autocrine signaling might not be involved in the effects of glucosamine (Fig. 30c). Thus, further signaling

cascades involved in endothelial signaling cells were also examined. The analysis of the phosphorylation and total protein content of AKT and ERK1/2 did not reveal any significant changes associated with high glucose and glucosamine treatment (Fig 31), suggesting a different mechanism of action of glucosamine in endothelial cells.

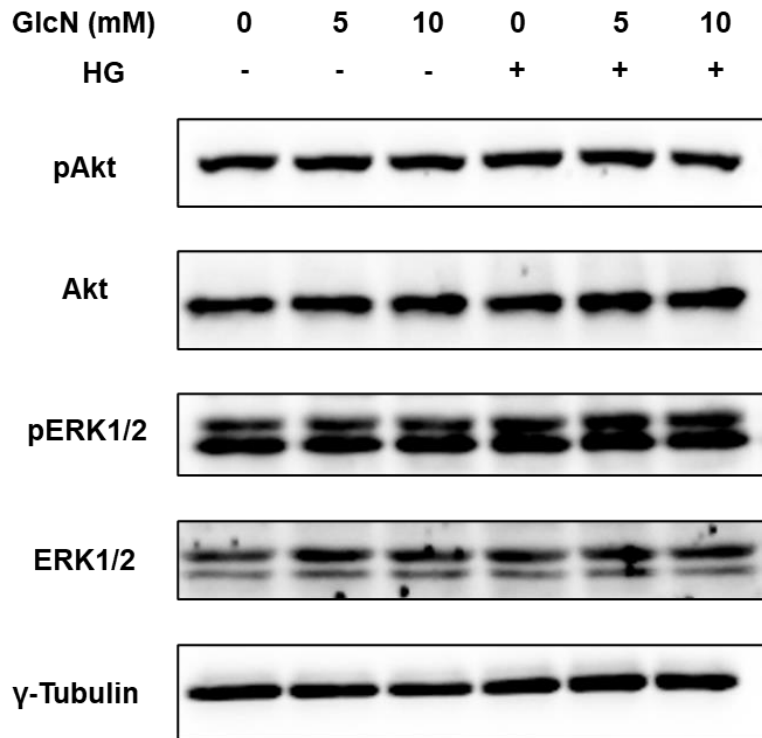


Figure 31: Glucosamine does not influence AKT and ERK1/2 phosphorylation a: Immunoblot analysis showing protein expression and phosphorylation status of AKT and ERK1/2 with high glucose and glucosamine stimulation, with γ -Tubulin as loading control.

HUVECs are macrovascular cells, while the endothelial cells in the retina are microvascular in nature. Therefore, the findings in the HUVECs were also corroborated in human retinal microvascular endothelial cells (HRMVECs). The HRMVECs were treated with increasing concentrations of glucosamine showing, similar to the HUVECs, a decrease in VEGFR2 and Ang2 protein content along with a corresponding band shift in a dose-dependent manner (Fig. 32a, b, c).

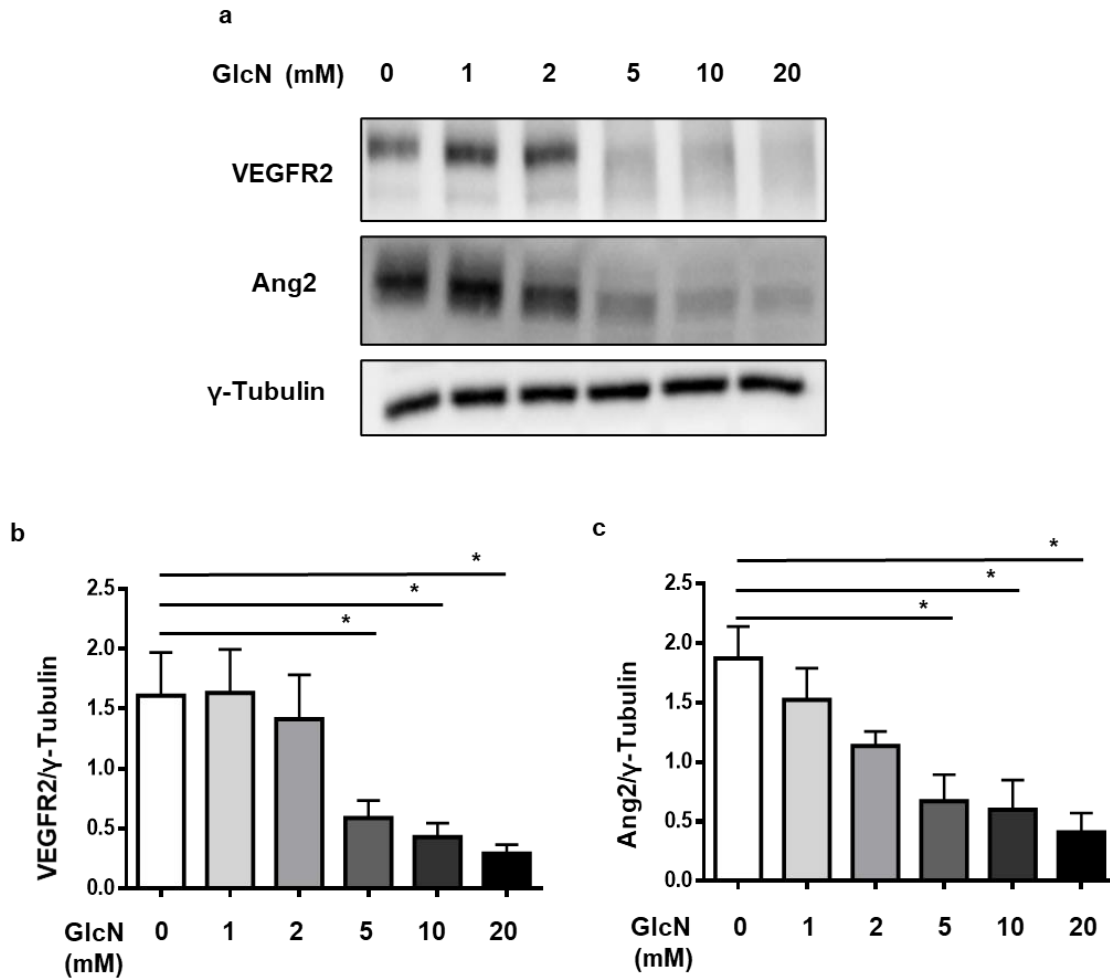


Figure 32: Glucosamine Glucosamine alters Ang2 and VEGFR2 content in HRMVECs. **a:** Immunoblot analysis showing VEGFR2 and Ang2 protein levels with increasing glucosamine concentrations in HRMVECs. Quantification of **b:** VEGFR2 and **c:** Ang2 with respect to γ -Tubulin. n=4-5, *p<0.05

Upon treatment with high glucose concentration, while VEGFR2 expression showed no change, the Ang2 protein level was again significantly increased, suggesting similar regulation in the HRMVECs as in the HUVECs. Glucosamine treatment reduced the VEGFR2 and Ang2 protein expression in both normal and high glucose conditions at concentrations higher than 2 mM, accompanied by a shift in molecular mass (Fig. 33a, b, c). This indicates that the effect of glucosamine in endothelial cells is conserved across different endothelial beds, macro- and microvascular. In addition, since the HRMVECs are retinal in origin, the data allow the speculation that a similar mechanism of action could occur in the endothelial cells in the retina, perhaps

contributing the observed vascular damage in the retina of glucosamine-supplemented non-diabetic mice.

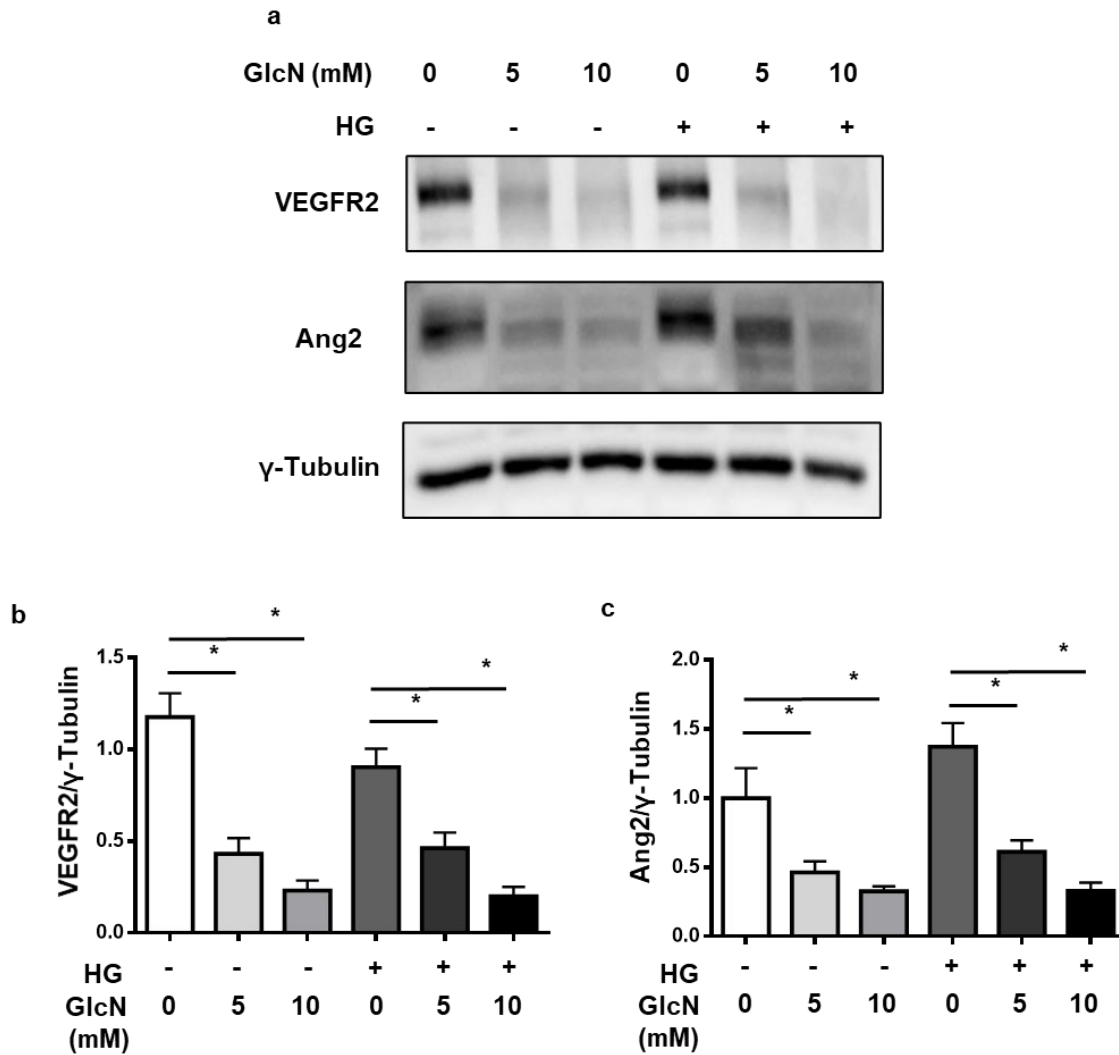


Figure 33: Glucosamine suppresses survival signaling in HRMVECs. **a:** Immunoblot analysis in normal and high glucose conditions showing VEGFR2 and Ang2 protein expressions with glucosamine stimulation. Quantification of **b:** VEGFR2 and **c:** Ang2 with respect to γ -Tubulin. n=4-5, *p<0.05

6. Discussion

In this study, mice with and without experimental diabetic retinopathy were treated with glucosamine, and its consequences were analyzed. A beneficial effect could be demonstrated in the suppression of activated Müller cells in the diabetic retinas treated with glucosamine compared to the diabetic controls. In addition, glucosamine ameliorated the activation of Müller cells *in vitro*, and alter growth factor expression. However, in the retinal vasculature, glucosamine supplementation in the non-diabetic animals induced vasoregression to a similar extent as that seen in the control diabetic animals. In the diabetic animals, glucosamine did not further exacerbate the vasoregression. Furthermore, in cultured endothelial cells, glucosamine treatment altered VEGFR2 content, hinting at altered signaling mechanisms that could result in the observed vascular damage.

6.1. Glucosamine-induced neuroprotection and related mechanisms

Although still being heavily disputed, the deterioration of the neuronal function in the retina that occurs during the very early stages of DR likely precedes or parallels the vascular damage [13, 167]. Several studies suggest that neuronal degeneration may even influence vascular regression that occurs in DR via crosstalk between the neuronal and vascular compartments in the retina [14, 15].

In DR, the neuronal damage is assessed by analyzing the electrical activity in the retina in response to a light stimulus using multi-focal electroretinography (ERG), and the amplitude of the waves produced serve as an indicator for the level of damage. Specific components (N1, P1, and N2) correspond to activities of specific cell types in the retina. The most commonly analyzed waves are the N1 and P1 waves. The initial negative component, N1, of the ERG corresponds to the activity of the photoreceptor cells. Photoreceptor damage is a controversially observed characteristic of DR, and can occur at 12 weeks after STZ-induced diabetes in mice [168]. In accordance with these data, we also see a tendency towards a reduction in P1 in diabetic animals compared to non-diabetic controls.

Müller cells and ON-bipolar cells are involved sequentially in the generation of the positive component, the P1-wave [169]. In accordance with previous studies [170-172], a decrease in the P1-wave amplitude was observed in the diabetic animals compared to their non-diabetic controls, sustaining the neuronal damage characteristic in the diabetic retina. In the diabetic animals treated with glucosamine, a significant increase in the P1-wave amplitude was observed, raising it to the level of the non-diabetic animals, and suggesting that glucosamine can rescue the neuronal deterioration in the diabetic retina. In the non-diabetic animals treated with glucosamine, no effect towards the P1-wave amplitude was observed. The data hence indicate that an improvement in neuronal function could occur with glucosamine treatment in diabetic mouse retinas, and hints towards neuroprotective properties of glucosamine. This finding supports previously published reports; in 2010, Hwang et al conducted a study in a rat model of brain injury where they demonstrated that glucosamine can exert a neuroprotective effect by suppressing the activation of microglial cells and inhibiting the release of inflammatory molecules [173]. Furthermore, Chen et al studied the effect of glucosamine in an ischemia/reperfusion-induced rat glaucoma model. In their study, they found that glucosamine can protect the retina against neuronal injury by hampering the damage to retinal ganglion cells [174].

Other studies, however, show contrarily that glucosamine can result in the apoptosis of R28 cells, a retinal neuronal cell model, *in vitro* [175]. This suggests that the effect of glucosamine may not be a result of direct interaction with neuronal cells, but rather a modulation of the neuronal microenvironment by regulation of the signaling pathways in retinal cells such as glial cells. Examination of astrocytes, a glial cell type in the retina, showed a more ramified structure in the diabetic retina, however no changes were observed with glucosamine supplementation, suggesting a cell-specific modulation by glucosamine.

Since the P1-wave of the ERG is generated primarily by Müller cells in the retina, further experiments focused on Müller cells both *in vivo* and *in vitro*. In DR, Müller cells are strongly activated in the retina [18, 176]. Reactive gliosis in Müller cells is discernible through the upregulation of GFAP, and is often associated with increased expression of VEGF and pro-inflammatory cytokines [177]. In the diabetic mice in this study, the activation of Müller cells could be seen clearly through visualization of the GFAP protein expression in the retina through

immunofluorescence and 3D confocal scanning. GFAP expression in the superficial retinal layer was observed prominently in astrocytes. Müller cell endfeet were discernible in the superficial ganglion cell layer as pinpoints of GFAP immunofluorescence, completely unattached to the astrocytes. These points, when followed through the depth of the retina, revealed increased GFAP expression throughout Müller cells spanning the retinal layers, indicating their activated state. In contrast, in non-diabetic retinas, although some Müller cell endfeet were still visible in the superficial layer, GFAP expression in the Müller cells was confined to just below the superficial layer and did not extend to all retinal layers, hence showing that the cells are currently inactive. Glucosamine treatment in the non-diabetic animals did not influence GFAP expression, whereas in the diabetic animals, glucosamine starkly reduced the extent of GFAP expression, and hence Müller cell activation, in the retina compared to the diabetic control animals.

These data indicate that glucosamine can influence Müller cell gliosis in the retina, and hence play a role in the modulation of the neuronal microenvironment in the retina. Surprisingly, the data here are in contrast with a study conducted in 2009 showing increase in GFAP expression in Müller cell processes along the inner plexiform layer with continuous cerebral glucosamine infusion [178]. This change could be due to the different animal model (mice vs. rats), or due to the mode and concentration of glucosamine supplementation. As such, further studies are required to conclusively state the effect of glucosamine on Müller cells and neuronal modulation in diabetic retinopathy.

As mentioned earlier, Müller cell gliosis or activation can have both beneficial and detrimental effects on the retinal neurons [61, 179]. Under gliotic conditions, regular cell-cell communication in the retina is disrupted, and neurodegeneration can occur via downregulation of cellular retinaldehyde-binding protein [180], glutamine synthase [181], carbonic anhydrase [182], and inward rectifying potassium channels [183, 184], resulting in the dysregulation of neurotransmitter recycling and ion and water homeostasis [61]. In addition, reactive Müller cells can increase immune and inflammatory response, recruiting macrophages and microglial cells to the retina [185, 186], leading to increase in free oxygen species and toxic cytokines, further exacerbating neurodegeneration. On the contrary, activated Müller cells can also release neurotrophic factors such as GDNF and BDNF, which can protect photoreceptors and ganglion

cells [187, 188]. Additionally, antioxidants such as glutathione, pyruvate, and α -ketoglutarate can be released by the gliotic Müller cells [186, 189, 190].

In this study, the potential modulations by activated Müller cells were investigated by analyzing mRNA expression of neurotrophic, inflammatory, and angiogenic factors in the retina. Surprisingly, no changes in the expression of BDNF, GDNF, IL1- β , IL-6, TNF- α , ICAM, Ang2, and VEGFR2 were observed in the retina, neither with diabetes nor glucosamine supplementation. It is possible that the regulation occurs at the post-transcriptional level, and hence changes in the mRNA level are non-existent.

Further elucidation of the mechanisms of glucosamine influence on Müller cell reactivity and signaling was accomplished using Müller cells cultured and stimulated *in vitro* with high glucose and glucosamine. In rat Müller cells (rMCs), treatment with glucosamine in concentrations ≥ 5 mM significantly reduced the GFAP expression, and hence Müller cell activation, in both normal and high glucose concentrations. Combined with the *in vivo* data from the mfERG and retinal immunofluorescence, these data suggest that glucosamine can ameliorate neuronal function in the diabetic retina by improving the function of Müller cells. This is therefore the first study that demonstrates an effect of glucosamine on Müller cell function, and hence neuronal environment regulation.

In addition to GFAP, VEGF protein expression was also investigated in the rat Müller cells. Müller cells are one of the primary secretors of VEGF in the retina, alongside endothelial cells. In this manner, they are involved in the regulation of vascular signaling in the retina. In the rat Müller cells, glucosamine treatment markedly reduced the VEGF content in both normal and high glucose concentrations, suggesting that glucosamine could have a role in the modulation of survival signaling via Müller cells. Since in diabetes, the expression of VEGF is increased in the retina, contributing to the breakdown of the BRB, inhibition of VEGF content, and thereby also likely its secretion, by glucosamine suggests a potential therapeutic effect in the treatment of diabetic retinopathy. However, further effects of glucosamine on other cell types in the retina and other organs must be studied before translation into humans is considered.

Contrary to previous studies [191], no changes in GFAP or VEGF protein expression were observed by treatment with high glucose concentrations. The expression of GFAP and VEGF in Müller cells under hyperglycemic conditions is, however, controversial; published reports indicate no changes in GFAP and/or VEGF expression in Müller cells *in vivo* and *in vitro*, supporting the findings in this study [66, 192]. The rat Müller cells used in this study are an immortalized cell line that are already activated to an extent in cell culture, which might explain why high glucose concentrations could not further increase GFAP and VEGF expression. Nevertheless, the effect of glucosamine was clearly observed, suggesting that even in a pre-activated cell status, which is as most likely present in diabetes [103, 165], glucosamine treatment could normalize glial cell activation.

Furthermore, the mRNA expression of neurotrophic, inflammatory, and angiogenic survival factors was also examined in cultured mouse Müller cells. Similar to the retina, no changes in these factors were seen in the Müller cells, further suggesting a post-transcriptional regulation in the factors that could influence the neuronal microenvironment.

6.2. Glucosamine-induced vascular damage and related mechanisms

Contrary to the protective effect of glucosamine seen in the neuroretina, the effects on the retinal vasculature appear to be more detrimental. In the non-diabetic mice, glucosamine induced a loss of pericytes and the formation of acellular capillaries to a similar extent as seen in the control diabetic animals. In diabetic animals, glucosamine treatment did however not further exacerbate these parameters. These data indicate that glucosamine can negatively impact the retinal vasculature in a hyperglycemia-independent manner to a similar extent as chronic hyperglycemia. The damaging effect of glucosamine on the vasculature and endothelial cell function has been demonstrated previously in correlation with the development of arteriosclerosis and cardiovascular (CVD) risk and mortality, where endothelial dysfunction upon glucosamine supplementation could play a role [193].

The mechanisms underlying this effect on the vasculature were investigated using cultured endothelial cells. In diabetic retinas, pericyte loss is triggered by increasing levels of Ang2, released by endothelial or Müller cells [5]. However, in HUVECs and HRMVECs *in vitro*, glucosamine in millimolar concentrations reduced Ang2 protein expression significantly, despite the well-known increase in Ang2 observed at high glucose concentrations. Corroboration of the immunoblot findings by immunofluorescence visualization of Ang2 in endothelial cells also displayed an increase in Ang2 at high glucose concentrations, and a decrease with glucosamine treatment (≥ 2 mM) both at normal and high glucose concentrations. This indicates that the glucosamine-induced vascular damage in the retina is presumably not initiated by pericyte loss due to increased Ang2 levels. Another possibility is that glucosamine increases the Ang2 secretion by endothelial cells, despite reducing protein content within the cell. Further investigation of the secreted Ang2 upon glucosamine stimulation needs to be conducted to definitively state the effect on Ang2 in the vasculature. Ang2 regulation is also controlled by the cellular O-GlcNAc cycle [194]. A previous publication shows that Ang2 can be modified by the post-translational protein modification of O-GlcNAcylation. Increased protein O-GlcNAcylation by suppression of the O-GlcNAcase activity caused an increase Ang2 protein content in endothelial cells, suggesting that O-GlcNAcylation of Ang2 could possibly prevent the protein from degradation, or otherwise increase or stabilize its content in endothelial cells [107, 195]. It can thus be hypothesized that increased O-GlcNAcylation due to hyperglycemia or through increased flux through the HBP via glucosamine could increase Ang2 protein levels. Surprisingly, however, in this study no evidence of an increased or altered protein O-GlcNAcylation was observed in endothelial cells with glucosamine treatment, indicating that the effect of glucosamine on Ang2 and the vascular damage in the retina is likely independent of protein O-GlcNAcylation.

Vascular damage in the retina, combined with decreased Ang2 protein expression, could denote the impairment of survival signals by glucosamine in endothelial cells. As a component of one of the major survival signaling pathways in endothelial cells in the retina, the protein expression of the VEGF receptor VEGFR2 was further investigated. Similar to Ang2, VEGFR2 protein content was also starkly reduced by treatment with glucosamine in concentrations ≥ 2 mM under both normal and high glucose concentrations. It might therefore be speculated that glucosamine in

the retina could interfere with VEGFR2-mediated survival signals in endothelial cells, hence contributing to vascular damage. Nevertheless, glucosamine influenced neither the protein content of VEGF in nor its secretion from endothelial cells, suggesting a VEGF-independent regulation of VEGFR2 level. VEGFR2 can be regulated, in addition to VEGF, via its transcription, translation, interaction with its co-receptors, phosphorylation, endocytosis, and glycosylation. Therefore, other mechanisms should be additionally analyzed to determine how glucosamine can influence VEGFR2 content in endothelial cells. Moreover, glucosamine did not influence the phosphorylation status of AKT and ERK1/2, or cell viability in the concentrations used in this study, suggesting that glucosamine, under these experimental conditions does not suppress survival signaling to significantly decrease cell viability.

The decrease in Ang2 and VEGFR2 protein levels were seen in endothelial cells of macrovascular (HUVECs) and microvascular (HRMVECs) origin, suggesting that the effect of glucosamine is conserved across different endothelial beds.

In addition to the reduction in protein level, glucosamine also induced a band shift of the proteins as detected by immunoblot, suggesting an altered mobility of the proteins in the SDS gel that could be due to the alteration of covalent protein modifications by glucosamine treatment. It has been previously published that glucosamine can alter N-glycosylation of proteins, conferring an anti-cancer effect through this mechanism [196]. Additionally, glucosamine has been shown to inhibit the activity of COX2 by preventing COX2 co-translational N-glycosylation [197, 198], and modulates T-cell differentiation through decrease in N-glycosylation of CD25 [199]. However, contrarily, a study from 2004 also showed that glucosamine can increase the N-glycosylation of F₁-F₀-ATP-synthase in pancreatic islet cells, hence altering its function in the mitochondria [200]. It is thus likely that glucosamine exerts differential effects on different proteins in several cell types.

6.3. Glucosamine effect on blood glucose, HbA1c, and body weight

In this study, the effect of glucosamine on the blood glucose and HbA1c levels in the mice was examined. Since glucosamine is a part of the HBP and hence a part of glucose metabolism, and glucose and glucosamine share the same transport systems for uptake into mammalian cells, it would be possible that exogenous glucosamine supply alters glucose metabolism in mice. The diabetic animals showed marked increase in blood glucose and HbA1c, as expected, but no influence of glucosamine on these parameters was observed, suggesting that glucosamine does not interfere with glucose metabolism. Previously, several studies have been conducted that show no adverse effect of glucosamine on blood glucose and glucose metabolism [201] or HbA1c [202] in humans hence concurring with the results in this study in mice. Interestingly, glucosamine has been implicated in increase in insulin resistance *in vivo* in insulin sensitive tissues via activation of the HBP [203, 204].

The impact on glucosamine on body weight is controversial. In 2006, a clinical study done on lean and obese human subjects found no correlation between oral glucosamine supplementation and insulin resistance or endothelial dysfunction [205]. Additionally, no change in body weight in mice was reported with glucosamine treatment by Ryczko et al in 2016 [206]. However, in 2015, Hwang et al showed a weight gain along with increased white adipose tissue in mice with glucosamine treatment, hence demonstrating that chronic activation of the HBP controls fat accumulation and insulin sensitivity [207]. The findings in this study corroborate the weight gain recorded by Hwang et al. A significant body weight gain was observed in non-diabetic mice treated with glucosamine. No changes in the body weight of diabetic animals with glucosamine supplementation was observed; this could be due to the prominent body weight reducing effect of diabetes that glucosamine could not overcome.

6.4. Limitations of the study

Although this study helped gain insight into the role of glucosamine in the neuronal and vascular function in diabetic retinopathy, some aspects require further investigation. In the animal model of experimental diabetic retinopathy, glucosamine uptake into the cells as well as the excretion of glucosamine was not measured. Only the level of glucosamine in the plasma was examined, exhibiting a much higher level in the diabetic animals compared to the non-diabetic animals. Additionally, in the *in vitro* experiments, the uptake of glucosamine into the cells was not monitored. In pharmacological convention, relatively high concentrations of glucosamine treatment in the cells were required to illicit a response, even though it is unclear how much glucosamine is taken up into the cells and hence is actually required for the regulation observed. It would be interesting to examine whether there is differential uptake of glucosamine in the presence of high glucose.

Furthermore, since all the research in this study was conducted on mice and cultured cells, translation of the data to human subjects must be performed with care. Although investigation of survival signals with glucosamine influence was performed in human-derived endothelial cells, further studies need to be done to confirm similar regulation in humans *in vivo*. So far, only the overall safety of glucosamine and its influence on osteoarthritis and pain has been studied *in vivo*; hence only a limited pool of data has been obtained, and a very small population of diabetic patients studied in this aspect. More data needs to be collected and assessed to determine the effects of glucosamine in humans *in vivo*.

Additionally, this study focused on glucosamine influence in the retina. However, glucosamine could potentially influence endothelial cells in other organ systems, including the kidney and heart. Moreover, Müller cells in the brain could be similarly affected, as could other cell types not in focus in this study. Therefore, further investigation into the impact of glucosamine in other organs is essential to obtain a clearer picture of the overall safety and efficacy of glucosamine in humans.

7. Conclusion

In examining the role of glucosamine in diabetic retinopathy, this study has shown the potential of glucosamine to ameliorate neuronal damage in diabetic animals. Both *in vivo* and *in vitro*, glucosamine reduced Müller cell activation, suggesting a mechanism for the proposed neuroprotective action. Contrarily, it has also demonstrated that glucosamine by itself can exert debilitating effects on the retinal vasculature, damaging it similar to hyperglycemia in experimental diabetic retinopathy. These might indicate that regular glucosamine oral supplementation such as that prescribed to osteoarthritis patients may have previously unknown side-effects. The effect on the vasculature, possibly caused by interference of glucosamine with endothelial signaling, could also possibly affect not only the retinal but also the vasculature in other organ systems. Therefore, glucosamine exerts multi-faceted effects, and its supplementation, especially in osteoarthritis patients suffering concomitantly from diabetes, should be taken with care.

References

1. Fong, D.S., et al., *Retinopathy in diabetes*. Diabetes Care, 2004. **27 Suppl 1**: p. S84-7.
2. Duh, E.J., J.K. Sun, and A.W. Stitt, *Diabetic retinopathy: current understanding, mechanisms, and treatment strategies*. JCI Insight, 2017. **2**(14).
3. Lechner, J., O.E. O'Leary, and A.W. Stitt, *The pathology associated with diabetic retinopathy*. Vision Res, 2017. **139**: p. 7-14.
4. Antonetti, D.A., R. Klein, and T.W. Gardner, *Diabetic retinopathy*. N Engl J Med, 2012. **366**(13): p. 1227-39.
5. Hammes, H.P., et al., *Diabetic retinopathy: targeting vasoregression*. Diabetes, 2011. **60**(1): p. 9-16.
6. Hussein, K.A., et al., *Bone morphogenetic protein 2: a potential new player in the pathogenesis of diabetic retinopathy*. Exp Eye Res, 2014. **125**: p. 79-88.
7. Gardner, T.W., et al., *Diabetic retinopathy: more than meets the eye*. Surv Ophthalmol, 2002. **47 Suppl 2**: p. S253-62.
8. Shin, E.S., C.M. Sorenson, and N. Sheibani, *Diabetes and retinal vascular dysfunction*. J Ophthalmic Vis Res, 2014. **9**(3): p. 362-73.
9. Korn, C. and H.G. Augustin, *Mechanisms of Vessel Pruning and Regression*. Dev Cell, 2015. **34**(1): p. 5-17.
10. Pfister, F., et al., *Retinal overexpression of angiopoietin-2 mimics diabetic retinopathy and enhances vascular damages in hyperglycemia*. Acta Diabetol, 2010. **47**(1): p. 59-64.
11. Stitt, A.W., et al., *Substrates modified by advanced glycation end-products cause dysfunction and death in retinal pericytes by reducing survival signals mediated by platelet-derived growth factor*. Diabetologia, 2004. **47**(10): p. 1735-46.
12. Nian, S., et al., *Neurovascular unit in diabetic retinopathy: pathophysiological roles and potential therapeutical targets*. Eye Vis (Lond), 2021. **8**(1): p. 15.
13. Lieth, E., et al., *Retinal neurodegeneration: early pathology in diabetes*. Clin Exp Ophthalmol, 2000. **28**(1): p. 3-8.
14. Lynch, S.K. and M.D. Abramoff, *Diabetic retinopathy is a neurodegenerative disorder*. Vision Res, 2017. **139**: p. 101-107.
15. Barber, A.J., T.W. Gardner, and S.F. Abcouwer, *The significance of vascular and neural apoptosis to the pathology of diabetic retinopathy*. Invest Ophthalmol Vis Sci, 2011. **52**(2): p. 1156-63.
16. El-Remessy, A.B., et al., *Neuroprotective and blood-retinal barrier-preserving effects of cannabidiol in experimental diabetes*. Am J Pathol, 2006. **168**(1): p. 235-44.
17. Feng, Y., et al., *Vasoregression linked to neuronal damage in the rat with defect of polycystin-2*. PLoS One, 2009. **4**(10): p. e7328.
18. Simo, R., et al., *Fenofibrate: a new treatment for diabetic retinopathy. Molecular mechanisms and future perspectives*. Curr Med Chem, 2013. **20**(26): p. 3258-66.
19. Davalli, A.M., C. Perego, and F.B. Folli, *The potential role of glutamate in the current diabetes epidemic*. Acta Diabetol, 2012. **49**(3): p. 167-83.
20. Barber, A.J. and B. Baccouche, *Neurodegeneration in diabetic retinopathy: Potential for novel therapies*. Vision Res, 2017. **139**: p. 82-92.

21. Ng, J.S., et al., *Local diabetic retinopathy prediction by multifocal ERG delays over 3 years*. Invest Ophthalmol Vis Sci, 2008. **49**(4): p. 1622-8.
22. Kowluru, R.A. and P.S. Chan, *Oxidative stress and diabetic retinopathy*. Exp Diabetes Res, 2007. **2007**: p. 43603.
23. Li, J., et al., *Inhibition of reactive oxygen species by Lovastatin downregulates vascular endothelial growth factor expression and ameliorates blood-retinal barrier breakdown in db/db mice: role of NADPH oxidase 4*. Diabetes, 2010. **59**(6): p. 1528-38.
24. Baynes, J.W., *Role of oxidative stress in development of complications in diabetes*. Diabetes, 1991. **40**(4): p. 405-12.
25. Roy, S., S. Amin, and S. Roy, *Retinal fibrosis in diabetic retinopathy*. Exp Eye Res, 2016. **142**: p. 71-5.
26. Ueno, M., *Molecular anatomy of the brain endothelial barrier: an overview of the distributional features*. Curr Med Chem, 2007. **14**(11): p. 1199-206.
27. Mizutani, M., T.S. Kern, and M. Lorenzi, *Accelerated death of retinal microvascular cells in human and experimental diabetic retinopathy*. J Clin Invest, 1996. **97**(12): p. 2883-90.
28. Barber, A.J., et al., *The Ins2Akita mouse as a model of early retinal complications in diabetes*. Invest Ophthalmol Vis Sci, 2005. **46**(6): p. 2210-8.
29. Pfister, F., et al., *Pericyte migration: a novel mechanism of pericyte loss in experimental diabetic retinopathy*. Diabetes, 2008. **57**(9): p. 2495-502.
30. Thurston, G. and C. Daly, *The complex role of angiopoietin-2 in the angiopoietin-tie signaling pathway*. Cold Spring Harb Perspect Med, 2012. **2**(9): p. a006550.
31. Rangasamy, S., et al., *A potential role for angiopoietin 2 in the regulation of the blood-retinal barrier in diabetic retinopathy*. Invest Ophthalmol Vis Sci, 2011. **52**(6): p. 3784-91.
32. Daly, C., et al., *Angiopoietin-2 functions as a Tie2 agonist in tumor models, where it limits the effects of VEGF inhibition*. Cancer Res, 2013. **73**(1): p. 108-18.
33. Fiedler, U., et al., *The Tie-2 ligand angiopoietin-2 is stored in and rapidly released upon stimulation from endothelial cell Weibel-Palade bodies*. Blood, 2004. **103**(11): p. 4150-6.
34. Matsumura, T., et al., *Hyperglycemia Increases Angiopoietin-2 Expression in Retinal Muller Cells through Superoxide-Induced Overproduction of [Alpha]-Oxaldehyde AGE Precursors, in Diabetes*. 2000. p. A55.
35. Hammes, H.P., et al., *Angiopoietin-2 causes pericyte dropout in the normal retina: evidence for involvement in diabetic retinopathy*. Diabetes, 2004. **53**(4): p. 1104-10.
36. Park, S.W., et al., *Angiopoietin 2 induces pericyte apoptosis via alpha3beta1 integrin signaling in diabetic retinopathy*. Diabetes, 2014. **63**(9): p. 3057-68.
37. Whitehead, M., et al., *Angiopoietins in Diabetic Retinopathy: Current Understanding and Therapeutic Potential*. J Diabetes Res, 2019. **2019**: p. 5140521.
38. Das, A., et al., *Angiopoietin/Tek interactions regulate mmp-9 expression and retinal neovascularization*. Lab Invest, 2003. **83**(11): p. 1637-45.
39. Hackett, S.F., et al., *Angiopoietin-2 plays an important role in retinal angiogenesis*. J Cell Physiol, 2002. **192**(2): p. 182-7.
40. Feng, Y., et al., *Impaired pericyte recruitment and abnormal retinal angiogenesis as a result of angiopoietin-2 overexpression*. Thromb Haemost, 2007. **97**(1): p. 99-108.

41. Cai, J., et al., *The angiopoietin/Tie-2 system regulates pericyte survival and recruitment in diabetic retinopathy*. Invest Ophthalmol Vis Sci, 2008. **49**(5): p. 2163-71.
42. Feng, Y., et al., *Angiopoietin-2 deficiency decelerates age-dependent vascular changes in the mouse retina*. Cell Physiol Biochem, 2008. **21**(1-3): p. 129-36.
43. Qiu, Y., et al., *Nucleoside diphosphate kinase B deficiency causes a diabetes-like vascular pathology via up-regulation of endothelial angiopoietin-2 in the retina*. Acta Diabetol, 2016. **53**(1): p. 81-9.
44. Bharadwaj, A.S., et al., *Role of the retinal vascular endothelial cell in ocular disease*. Prog Retin Eye Res, 2013. **32**: p. 102-80.
45. Yao, D., et al., *High glucose increases angiopoietin-2 transcription in microvascular endothelial cells through methylglyoxal modification of mSin3A*. J Biol Chem, 2007. **282**(42): p. 31038-45.
46. Shan, S., et al., *O-GlcNAcylation of FoxO1 mediates nucleoside diphosphate kinase B deficiency induced endothelial damage*. Sci Rep, 2018. **8**(1): p. 10581.
47. Abhinand, C.S., et al., *VEGF-A/VEGFR2 signaling network in endothelial cells relevant to angiogenesis*. J Cell Commun Signal, 2016. **10**(4): p. 347-354.
48. Kendall, R.L., et al., *Vascular endothelial growth factor receptor KDR tyrosine kinase activity is increased by autophosphorylation of two activation loop tyrosine residues*. J Biol Chem, 1999. **274**(10): p. 6453-60.
49. Karar, J. and A. Maity, *PI3K/AKT/mTOR Pathway in Angiogenesis*. Front Mol Neurosci, 2011. **4**: p. 51.
50. Yamamizu, K., et al., *Convergence of Notch and beta-catenin signaling induces arterial fate in vascular progenitors*. J Cell Biol, 2010. **189**(2): p. 325-38.
51. Zhao, X. and J.L. Guan, *Focal adhesion kinase and its signaling pathways in cell migration and angiogenesis*. Adv Drug Deliv Rev, 2011. **63**(8): p. 610-5.
52. Saint-Geniez, M., et al., *Endogenous VEGF is required for visual function: evidence for a survival role on muller cells and photoreceptors*. PLoS One, 2008. **3**(11): p. e3554.
53. Wang, J.J., M. Zhu, and Y.Z. Le, *Functions of Muller cell-derived vascular endothelial growth factor in diabetic retinopathy*. World J Diabetes, 2015. **6**(5): p. 726-33.
54. Fu, S., et al., *Muller Glia Are a Major Cellular Source of Survival Signals for Retinal Neurons in Diabetes*. Diabetes, 2015. **64**(10): p. 3554-63.
55. Bringmann, A., et al., *Muller cells in the healthy and diseased retina*. Prog Retin Eye Res, 2006. **25**(4): p. 397-424.
56. Reichenbach, A., et al., *What do retinal muller (glial) cells do for their neuronal 'small siblings'? J Chem Neuroanat, 1993. **6**(4): p. 201-13.*
57. Poitry-Yamate, C.L., S. Poitry, and M. Tsacopoulos, *Lactate released by Muller glial cells is metabolized by photoreceptors from mammalian retina*. J Neurosci, 1995. **15**(7 Pt 2): p. 5179-91.
58. Kofuji, P., et al., *Kir potassium channel subunit expression in retinal glial cells: implications for spatial potassium buffering*. Glia, 2002. **39**(3): p. 292-303.
59. Nagelhus, E.A., et al., *Aquaporin-4 water channel protein in the rat retina and optic nerve: polarized expression in Muller cells and fibrous astrocytes*. J Neurosci, 1998. **18**(7): p. 2506-19.
60. Matsui, K., N. Hosoi, and M. Tachibana, *Active role of glutamate uptake in the synaptic transmission from retinal nonspiking neurons*. J Neurosci, 1999. **19**(16): p. 6755-66.

61. Bringmann, A., et al., *Cellular signaling and factors involved in Muller cell gliosis: neuroprotective and detrimental effects*. Prog Retin Eye Res, 2009. **28**(6): p. 423-51.
62. Pow, D.V. and S.R. Robinson, *Glutamate in some retinal neurons is derived solely from glia*. Neuroscience, 1994. **60**(2): p. 355-66.
63. Stevens, E.R., et al., *D-serine and serine racemase are present in the vertebrate retina and contribute to the physiological activation of NMDA receptors*. Proc Natl Acad Sci U S A, 2003. **100**(11): p. 6789-94.
64. Newman, E.A. and K.R. Zahs, *Modulation of neuronal activity by glial cells in the retina*. J Neurosci, 1998. **18**(11): p. 4022-8.
65. Newman, E.A., *Glial cell inhibition of neurons by release of ATP*. J Neurosci, 2003. **23**(5): p. 1659-66.
66. Eichler, W., et al., *VEGF release by retinal glia depends on both oxygen and glucose supply*. Neuroreport, 2000. **11**(16): p. 3533-7.
67. Ikeda, T., et al., *Expression of transforming growth factor-beta s and their receptors by human retinal glial cells*. Curr Eye Res, 1998. **17**(5): p. 546-50.
68. Schutte, M. and P. Werner, *Redistribution of glutathione in the ischemic rat retina*. Neurosci Lett, 1998. **246**(1): p. 53-6.
69. Reichelt, W., et al., *The glutathione level of retinal Muller glial cells is dependent on the high-affinity sodium-dependent uptake of glutamate*. Neuroscience, 1997. **77**(4): p. 1213-24.
70. Silver, I.A., J. Deas, and M. Erecinska, *Ion homeostasis in brain cells: differences in intracellular ion responses to energy limitation between cultured neurons and glial cells*. Neuroscience, 1997. **78**(2): p. 589-601.
71. Harada, T., et al., *Microglia-Muller glia cell interactions control neurotrophic factor production during light-induced retinal degeneration*. J Neurosci, 2002. **22**(21): p. 9228-36.
72. Bringmann, A. and A. Reichenbach, *Role of Muller cells in retinal degenerations*. Front Biosci, 2001. **6**: p. E72-92.
73. Eisenfeld, A.J., A.H. Bunt-Milam, and P.V. Sarthy, *Muller cell expression of glial fibrillary acidic protein after genetic and experimental photoreceptor degeneration in the rat retina*. Invest Ophthalmol Vis Sci, 1984. **25**(11): p. 1321-8.
74. Bignami, A. and D. Dahl, *The radial glia of Muller in the rat retina and their response to injury. An immunofluorescence study with antibodies to the glial fibrillary acidic (GFA) protein*. Exp Eye Res, 1979. **28**(1): p. 63-9.
75. Erickson, P.A., et al., *Glial fibrillary acidic protein increases in Muller cells after retinal detachment*. Exp Eye Res, 1987. **44**(1): p. 37-48.
76. Osborne, N.N., F. Block, and K.H. Sontag, *Reduction of ocular blood flow results in glial fibrillary acidic protein (GFAP) expression in rat retinal Muller cells*. Vis Neurosci, 1991. **7**(6): p. 637-9.
77. Lieth, E., et al., *Glial reactivity and impaired glutamate metabolism in short-term experimental diabetic retinopathy*. Penn State Retina Research Group. Diabetes, 1998. **47**(5): p. 815-20.
78. Grosche, J., W. Hartig, and A. Reichenbach, *Expression of glial fibrillary acidic protein (GFAP), glutamine synthetase (GS), and Bcl-2 protooncogene protein by Muller (glial) cells in retinal light damage of rats*. Neurosci Lett, 1995. **185**(2): p. 119-22.

79. Linser, P. and A.A. Moscona, *Induction of glutamine synthetase in embryonic neural retina: localization in Muller fibers and dependence on cell interactions*. Proc Natl Acad Sci U S A, 1979. **76**(12): p. 6476-80.
80. Pow, D.V. and D.K. Crook, *Direct immunocytochemical evidence for the transfer of glutamine from glial cells to neurons: use of specific antibodies directed against the d-stereoisomers of glutamate and glutamine*. Neuroscience, 1996. **70**(1): p. 295-302.
81. Lieth, E., et al., *Diabetes reduces glutamate oxidation and glutamine synthesis in the retina. The Penn State Retina Research Group*. Exp Eye Res, 2000. **70**(6): p. 723-30.
82. Xi, X., et al., *Chronically elevated glucose-induced apoptosis is mediated by inactivation of Akt in cultured Muller cells*. Biochem Biophys Res Commun, 2005. **326**(3): p. 548-53.
83. Paulson, O.B. and E.A. Newman, *Does the release of potassium from astrocyte endfeet regulate cerebral blood flow?* Science, 1987. **237**(4817): p. 896-8.
84. Tretiach, M., et al., *Effect of Muller cell co-culture on in vitro permeability of bovine retinal vascular endothelium in normoxic and hypoxic conditions*. Neurosci Lett, 2005. **378**(3): p. 160-5.
85. Aiello, L.P., et al., *Suppression of retinal neovascularization in vivo by inhibition of vascular endothelial growth factor (VEGF) using soluble VEGF-receptor chimeric proteins*. Proc Natl Acad Sci U S A, 1995. **92**(23): p. 10457-61.
86. Eichler, W., et al., *PEDF derived from glial Muller cells: a possible regulator of retinal angiogenesis*. Exp Cell Res, 2004. **299**(1): p. 68-78.
87. Igarashi, Y., et al., *Expression of receptors for glial cell line-derived neurotrophic factor (GDNF) and neurturin in the inner blood-retinal barrier of rats*. Cell Struct Funct, 2000. **25**(4): p. 237-41.
88. Du, Y., V.P. Sarthy, and T.S. Kern, *Interaction between NO and COX pathways in retinal cells exposed to elevated glucose and retina of diabetic rats*. Am J Physiol Regul Integr Comp Physiol, 2004. **287**(4): p. R735-41.
89. Goureau, O., F. Regnier-Ricard, and Y. Courtois, *Requirement for nitric oxide in retinal neuronal cell death induced by activated Muller glial cells*. J Neurochem, 1999. **72**(6): p. 2506-15.
90. Gerhardinger, C., et al., *Expression of acute-phase response proteins in retinal Muller cells in diabetes*. Invest Ophthalmol Vis Sci, 2005. **46**(1): p. 349-57.
91. Busik, J.V., S. Mohr, and M.B. Grant, *Hyperglycemia-induced reactive oxygen species toxicity to endothelial cells is dependent on paracrine mediators*. Diabetes, 2008. **57**(7): p. 1952-65.
92. Bai, Y., et al., *Muller cell-derived VEGF is a significant contributor to retinal neovascularization*. J Pathol, 2009. **219**(4): p. 446-54.
93. Wang, J., et al., *Muller cell-derived VEGF is essential for diabetes-induced retinal inflammation and vascular leakage*. Diabetes, 2010. **59**(9): p. 2297-305.
94. Hammes, H.P., et al., *Differential accumulation of advanced glycation end products in the course of diabetic retinopathy*. Diabetologia, 1999. **42**(6): p. 728-36.
95. Hirata, C., et al., *Advanced glycation end products induce expression of vascular endothelial growth factor by retinal Muller cells*. Biochem Biophys Res Commun, 1997. **236**(3): p. 712-5.
96. Mignatti, P., et al., *In vitro angiogenesis on the human amniotic membrane: requirement for basic fibroblast growth factor-induced proteinases*. J Cell Biol, 1989. **108**(2): p. 671-82.
97. Unemori, E.N., et al., *Vascular endothelial growth factor induces interstitial collagenase expression in human endothelial cells*. J Cell Physiol, 1992. **153**(3): p. 557-62.

98. Majka, S., P.G. McGuire, and A. Das, *Regulation of matrix metalloproteinase expression by tumor necrosis factor in a murine model of retinal neovascularization*. Invest Ophthalmol Vis Sci, 2002. **43**(1): p. 260-6.
99. Giebel, S.J., et al., *Matrix metalloproteinases in early diabetic retinopathy and their role in alteration of the blood-retinal barrier*. Lab Invest, 2005. **85**(5): p. 597-607.
100. Behzadian, M.A., et al., *TGF-beta increases retinal endothelial cell permeability by increasing MMP-9: possible role of glial cells in endothelial barrier function*. Invest Ophthalmol Vis Sci, 2001. **42**(3): p. 853-9.
101. Berka, J.L., et al., *Renin-containing Muller cells of the retina display endocrine features*. Invest Ophthalmol Vis Sci, 1995. **36**(7): p. 1450-8.
102. Fletcher, E.L., J.A. Phipps, and J.L. Wilkinson-Berka, *Dysfunction of retinal neurons and glia during diabetes*. Clin Exp Optom, 2005. **88**(3): p. 132-45.
103. Coughlin, B.A., D.J. Feenstra, and S. Mohr, *Muller cells and diabetic retinopathy*. Vision Res, 2017. **139**: p. 93-100.
104. Fantus, I.G., et al., *The Hexosamine Biosynthesis Pathway*, in *The Diabetic Kidney*, P. Cortes and C.E. Mogensen, Editors. 2006, Humana Press: Totowa, NJ. p. 117-133.
105. Qin, C.X., et al., *Insights into the role of maladaptive hexosamine biosynthesis and O-GlcNAcylation in development of diabetic cardiac complications*. Pharmacol Res, 2017. **116**: p. 45-56.
106. Semba, R.D., et al., *The role of O-GlcNAc signaling in the pathogenesis of diabetic retinopathy*. Proteomics Clin Appl, 2014. **8**(3-4): p. 218-31.
107. Yang, X. and K. Qian, *Protein O-GlcNAcylation: emerging mechanisms and functions*. Nat Rev Mol Cell Biol, 2017. **18**(7): p. 452-465.
108. Housley, M.P., et al., *O-GlcNAc regulates FoxO activation in response to glucose*. J Biol Chem, 2008. **283**(24): p. 16283-92.
109. Golks, A. and D. Guerini, *The O-linked N-acetylglucosamine modification in cellular signalling and the immune system. 'Protein modifications: beyond the usual suspects' review series*. EMBO Rep, 2008. **9**(8): p. 748-53.
110. Wells, L., et al., *Mapping sites of O-GlcNAc modification using affinity tags for serine and threonine post-translational modifications*. Mol Cell Proteomics, 2002. **1**(10): p. 791-804.
111. Luo, B., Y. Soesanto, and D.A. McClain, *Protein modification by O-linked GlcNAc reduces angiogenesis by inhibiting Akt activity in endothelial cells*. Arterioscler Thromb Vasc Biol, 2008. **28**(4): p. 651-7.
112. Akella, N.M., L. Ciraku, and M.J. Reginato, *Fueling the fire: emerging role of the hexosamine biosynthetic pathway in cancer*. BMC Biol, 2019. **17**(1): p. 52.
113. Copeland, R.J., J.W. Bullen, and G.W. Hart, *Cross-talk between GlcNAcylation and phosphorylation: roles in insulin resistance and glucose toxicity*. Am J Physiol Endocrinol Metab, 2008. **295**(1): p. E17-28.
114. Marshall, S., V. Bacote, and R.R. Traxinger, *Complete inhibition of glucose-induced desensitization of the glucose transport system by inhibitors of mRNA synthesis. Evidence for rapid turnover of glutamine:fructose-6-phosphate amidotransferase*. J Biol Chem, 1991. **266**(16): p. 10155-61.
115. Rossetti, L., et al., *In vivo glucosamine infusion induces insulin resistance in normoglycemic but not in hyperglycemic conscious rats*. J Clin Invest, 1995. **96**(1): p. 132-40.

116. Gurel, Z., et al., *Retinal O-linked N-acetylglucosamine protein modifications: implications for postnatal retinal vascularization and the pathogenesis of diabetic retinopathy*. Mol Vis, 2013. **19**: p. 1047-59.
117. Gurel, Z., et al., *Identification of O-GlcNAc modification targets in mouse retinal pericytes: implication of p53 in pathogenesis of diabetic retinopathy*. PLoS One, 2014. **9**(5): p. e95561.
118. Du, X.L., et al., *Hyperglycemia-induced mitochondrial superoxide overproduction activates the hexosamine pathway and induces plasminogen activator inhibitor-1 expression by increasing Sp1 glycosylation*. Proc Natl Acad Sci U S A, 2000. **97**(22): p. 12222-6.
119. Schleicher, E.D. and C. Weigert, *Role of the hexosamine biosynthetic pathway in diabetic nephropathy*. Kidney Int Suppl, 2000. **77**: p. S13-8.
120. Marshall, S., W.T. Garvey, and R.R. Traxinger, *New insights into the metabolic regulation of insulin action and insulin resistance: role of glucose and amino acids*. FASEB J, 1991. **5**(15): p. 3031-6.
121. Salazar, J., et al., *Glucosamine for osteoarthritis: biological effects, clinical efficacy, and safety on glucose metabolism*. Arthritis, 2014. **2014**: p. 432463.
122. Laczy, B., et al., *Acute regulation of cardiac metabolism by the hexosamine biosynthesis pathway and protein O-GlcNAcylation*. PLoS One, 2011. **6**(4): p. e18417.
123. Ren, J., et al., *High extracellular glucose impairs cardiac E-C coupling in a glycosylation-dependent manner*. Am J Physiol, 1997. **273**(6): p. H2876-83.
124. Buse, M.G., *Hexosamines, insulin resistance, and the complications of diabetes: current status*. Am J Physiol Endocrinol Metab, 2006. **290**(1): p. E1-E8.
125. Marshall, S., O. Nadeau, and K. Yamasaki, *Dynamic actions of glucose and glucosamine on hexosamine biosynthesis in isolated adipocytes: differential effects on glucosamine 6-phosphate, UDP-N-acetylglucosamine, and ATP levels*. J Biol Chem, 2004. **279**(34): p. 35313-9.
126. Miller, K.L. and D.O. Clegg, *Glucosamine and chondroitin sulfate*. Rheum Dis Clin North Am, 2011. **37**(1): p. 103-18.
127. Rovati, L.C., F. Girolami, and S. Persiani, *Crystalline glucosamine sulfate in the management of knee osteoarthritis: efficacy, safety, and pharmacokinetic properties*. Ther Adv Musculoskelet Dis, 2012. **4**(3): p. 167-80.
128. Zhang, L.J., et al., *Determination of glucosamine sulfate in human plasma by precolumn derivatization using high performance liquid chromatography with fluorescence detection: its application to a bioequivalence study*. J Chromatogr B Analyt Technol Biomed Life Sci, 2006. **842**(1): p. 8-12.
129. Zhu, Y., et al., *Bioequivalence of two formulations of glucosamine sulfate 500-mg capsules in healthy male Chinese volunteers: an open-label, randomized-sequence, single-dose, fasting, two-way crossover study*. Clin Ther, 2009. **31**(7): p. 1551-8.
130. Persiani, S., et al., *Glucosamine oral bioavailability and plasma pharmacokinetics after increasing doses of crystalline glucosamine sulfate in man*. Osteoarthritis Cartilage, 2005. **13**(12): p. 1041-9.
131. Aghazadeh-Habashi, A., et al., *Single dose pharmacokinetics and bioavailability of glucosamine in the rat*. J Pharm Pharm Sci, 2002. **5**(2): p. 181-4.
132. Anderson, J.W., R.J. Nicolosi, and J.F. Borzelleca, *Glucosamine effects in humans: a review of effects on glucose metabolism, side effects, safety considerations and efficacy*. Food Chem Toxicol, 2005. **43**(2): p. 187-201.

133. Kelly, G.S., *The role of glucosamine sulfate and chondroitin sulfates in the treatment of degenerative joint disease*. *Altern Med Rev*, 1998. **3**(1): p. 27-39.
134. Uldry, M., et al., *GLUT2 is a high affinity glucosamine transporter*. *FEBS Lett*, 2002. **524**(1-3): p. 199-203.
135. Simon, R.R., et al., *A comprehensive review of oral glucosamine use and effects on glucose metabolism in normal and diabetic individuals*. *Diabetes Metab Res Rev*, 2011. **27**(1): p. 14-27.
136. Reginster, J.Y., et al., *Long-term effects of glucosamine sulphate on osteoarthritis progression: a randomised, placebo-controlled clinical trial*. *Lancet*, 2001. **357**(9252): p. 251-6.
137. Bruyere, O., et al., *Total joint replacement after glucosamine sulphate treatment in knee osteoarthritis: results of a mean 8-year observation of patients from two previous 3-year, randomised, placebo-controlled trials*. *Osteoarthritis Cartilage*, 2008. **16**(2): p. 254-60.
138. Pavelka, K., et al., *Glucosamine sulfate use and delay of progression of knee osteoarthritis: a 3-year, randomized, placebo-controlled, double-blind study*. *Arch Intern Med*, 2002. **162**(18): p. 2113-23.
139. Yan, Y., et al., *The antioxidative and immunostimulating properties of D-glucosamine*. *Int Immunopharmacol*, 2007. **7**(1): p. 29-35.
140. Mendis, E., et al., *Sulfated glucosamine inhibits oxidation of biomolecules in cells via a mechanism involving intracellular free radical scavenging*. *Eur J Pharmacol*, 2008. **579**(1-3): p. 74-85.
141. Jamialahmadi, K., et al., *Protective effects of glucosamine hydrochloride against free radical-induced erythrocytes damage*. *Environ Toxicol Pharmacol*, 2014. **38**(1): p. 212-9.
142. Azuma, K., et al., *Anti-inflammatory effects of orally administered glucosamine oligomer in an experimental model of inflammatory bowel disease*. *Carbohydr Polym*, 2015. **115**: p. 448-56.
143. Nagaoka, I., et al., *Recent aspects of the anti-inflammatory actions of glucosamine*. *Carbohydrate polymers*, 2011. **84**(2): p. 825-830.
144. Nagaoka, I., M. Igarashi, and K. Sakamoto, *Biological activities of glucosamine and its related substances*. *Adv Food Nutr Res*, 2012. **65**: p. 337-52.
145. NAGAOKA, I., *Recent aspects of the chondroprotective and anti-inflammatory actions of glucosamine, a functional food*. *Juntendo Medical Journal*, 2014. **60**(6): p. 580-587.
146. Quastel, J.H. and A. Cantero, *Inhibition of tumour growth by D-glucosamine*. *Nature*, 1953. **171**(4345): p. 252-4.
147. Brasky, T.M., et al., *Use of glucosamine and chondroitin and lung cancer risk in the VITamins And Lifestyle (VITAL) cohort*. *Cancer Causes Control*, 2011. **22**(9): p. 1333-42.
148. Kantor, E.D., et al., *Use of glucosamine and chondroitin supplements and risk of colorectal cancer*. *Cancer Causes Control*, 2013. **24**(6): p. 1137-46.
149. Zahedipour, F., et al., *Molecular mechanisms of anticancer effects of Glucosamine*. *Biomed Pharmacother*, 2017. **95**: p. 1051-1058.
150. Masuda, S., et al., *Anti-tumor properties of orally administered glucosamine and N-acetyl-D-glucosamine oligomers in a mouse model*. *Carbohydr Polym*, 2014. **111**: p. 783-7.
151. Koch, H.U., *Über die Mechanismen der Hemmung der Virusvermehrung durch D-Glucosamin*. 1978.
152. Weimer, S., et al., *D-Glucosamine supplementation extends life span of nematodes and of ageing mice*. *Nat Commun*, 2014. **5**: p. 3563.
153. Shintani, T., Y. Kosuge, and H. Ashida, *Glucosamine Extends the Lifespan of Caenorhabditis elegans via Autophagy Induction*. *J Appl Glycosci (1999)*, 2018. **65**(3): p. 37-43.

154. Gueniche, A. and I. Castiel-Higounenc, *Efficacy of Glucosamine Sulphate in Skin Ageing: Results from an ex vivo Anti-Ageing Model and a Clinical Trial*. *Skin Pharmacol Physiol*, 2017. **30**(1): p. 36-41.
155. Fulop, N., R.B. Marchase, and J.C. Chatham, *Role of protein O-linked N-acetyl-glucosamine in mediating cell function and survival in the cardiovascular system*. *Cardiovasc Res*, 2007. **73**(2): p. 288-97.
156. Liu, J., et al., *Increased hexosamine biosynthesis and protein O-GlcNAc levels associated with myocardial protection against calcium paradox and ischemia*. *J Mol Cell Cardiol*, 2006. **40**(2): p. 303-12.
157. Champattanachai, V., R.B. Marchase, and J.C. Chatham, *Glucosamine protects neonatal cardiomyocytes from ischemia-reperfusion injury via increased protein-associated O-GlcNAc*. *Am J Physiol Cell Physiol*, 2007. **292**(1): p. C178-87.
158. Rossetti, L., *Perspective: Hexosamines and nutrient sensing*. *Endocrinology*, 2000. **141**(6): p. 1922-5.
159. Wang, J., et al., *A nutrient-sensing pathway regulates leptin gene expression in muscle and fat*. *Nature*, 1998. **393**(6686): p. 684-8.
160. Hawkins, M., et al., *Role of the glucosamine pathway in fat-induced insulin resistance*. *J Clin Invest*, 1997. **99**(9): p. 2173-82.
161. Cooksey, R.C. and D.A. McClain, *Increased hexosamine pathway flux and high fat feeding are not additive in inducing insulin resistance: evidence for a shared pathway*. *Amino Acids*, 2011. **40**(3): p. 841-6.
162. Yki-Jarvinen, H., et al., *Insulin and glucosamine infusions increase O-linked N-acetyl-glucosamine in skeletal muscle proteins in vivo*. *Metabolism*, 1998. **47**(4): p. 449-55.
163. Wirtz, M., M. Droux, and R. Hell, *O-acetylserine (thiol) lyase: an enigmatic enzyme of plant cysteine biosynthesis revisited in Arabidopsis thaliana*. *J Exp Bot*, 2004. **55**(404): p. 1785-98.
164. Dutescu, R.M., et al., *Multifocal ERG recordings under visual control of the stimulated fundus in mice*. *Invest Ophthalmol Vis Sci*, 2013. **54**(4): p. 2582-9.
165. Picconi, F., et al., *Activation of retinal Muller cells in response to glucose variability*. *Endocrine*, 2019. **65**(3): p. 542-549.
166. Hammes, H.P., *Diabetic retinopathy: hyperglycaemia, oxidative stress and beyond*. *Diabetologia*, 2018. **61**(1): p. 29-38.
167. Abcouwer, S.F. and T.W. Gardner, *Diabetic retinopathy: loss of neuroretinal adaptation to the diabetic metabolic environment*. *Ann N Y Acad Sci*, 2014. **1311**: p. 174-90.
168. Becker, S., L.S. Carroll, and F. Vinberg, *Diabetic photoreceptors: Mechanisms underlying changes in structure and function*. *Vis Neurosci*, 2020. **37**: p. E008.
169. Dettoraki, M. and M.M. Moschos, *The Role of Multifocal Electroretinography in the Assessment of Drug-Induced Retinopathy: A Review of the Literature*. *Ophthalmic Res*, 2016. **56**(4): p. 169-177.
170. Simao, S., et al., *Development of a Normative Database for Multifocal Electroretinography in the Context of a Multicenter Clinical Trial*. *Ophthalmic Res*, 2017. **57**(2): p. 107-117.
171. Bresnick, G.H. and M. Palta, *Oscillatory potential amplitudes. Relation to severity of diabetic retinopathy*. *Arch Ophthalmol*, 1987. **105**(7): p. 929-33.
172. Prager, T.C., et al., *The pattern electroretinogram in diabetes*. *Am J Ophthalmol*, 1990. **109**(3): p. 279-84.

173. Hwang, S.Y., et al., *Glucosamine exerts a neuroprotective effect via suppression of inflammation in rat brain ischemia/reperfusion injury*. *Glia*, 2010. **58**(15): p. 1881-92.
174. Chen, Y.J., et al., *Protective effects of glucosamine on oxidative-stress and ischemia/reperfusion-induced retinal injury*. *Invest Ophthalmol Vis Sci*, 2015. **56**(3): p. 1506-16.
175. Nakamura, M., et al., *Excessive hexosamines block the neuroprotective effect of insulin and induce apoptosis in retinal neurons*. *J Biol Chem*, 2001. **276**(47): p. 43748-55.
176. Fletcher, E.L., et al., *Neuronal and glial cell abnormality as predictors of progression of diabetic retinopathy*. *Curr Pharm Des*, 2007. **13**(26): p. 2699-712.
177. Bringmann, A. and P. Wiedemann, *Müller glial cells in retinal disease*. *Ophthalmologica*, 2012. **227**(1): p. 1-19.
178. Soyong, J., et al., *Dysfunction of retinal cell and optic nerve by continuous cerebroventricular infusion of glucosamine*. *The Korean Society of Applied Pharmacology*, 2009. **17**(4): p. 362-369.
179. Reichenbach, A. and A. Bringmann, *Müller cells in the healthy and diseased retina*. 2010: Springer Science & Business Media.
180. Muniz, A., et al., *A novel cone visual cycle in the cone-dominated retina*. *Exp Eye Res*, 2007. **85**(2): p. 175-84.
181. Lewis, G.P., et al., *Changes in the expression of specific Müller cell proteins during long-term retinal detachment*. *Exp Eye Res*, 1989. **49**(1): p. 93-111.
182. Lewis, G., et al., *Limiting the proliferation and reactivity of retinal Müller cells during experimental retinal detachment: the value of oxygen supplementation*. *Am J Ophthalmol*, 1999. **128**(2): p. 165-72.
183. Pannicke, T., et al., *A potassium channel-linked mechanism of glial cell swelling in the postischemic retina*. *Mol Cell Neurosci*, 2004. **26**(4): p. 493-502.
184. Wurm, A., et al., *Purinergic signaling involved in Müller cell function in the mammalian retina*. *Prog Retin Eye Res*, 2011. **30**(5): p. 324-42.
185. Nakazawa, T., et al., *Characterization of cytokine responses to retinal detachment in rats*. *Mol Vis*, 2006. **12**: p. 867-78.
186. Hollborn, M., et al., *Early activation of inflammation- and immune response-related genes after experimental detachment of the porcine retina*. *Invest Ophthalmol Vis Sci*, 2008. **49**(3): p. 1262-73.
187. Harada, C., et al., *Potential role of glial cell line-derived neurotrophic factor receptors in Müller glial cells during light-induced retinal degeneration*. *Neuroscience*, 2003. **122**(1): p. 229-35.
188. Koeberle, P.D. and M. Bahr, *The upregulation of GLAST-1 is an indirect antiapoptotic mechanism of GDNF and neurturin in the adult CNS*. *Cell Death Differ*, 2008. **15**(3): p. 471-83.
189. Woodford, B.J., M.O. Tso, and K.W. Lam, *Reduced and oxidized ascorbates in guinea pig retina under normal and light-exposed conditions*. *Invest Ophthalmol Vis Sci*, 1983. **24**(7): p. 862-7.
190. Ulyanova, T., et al., *Oxidative stress induces heme oxygenase-1 immunoreactivity in Müller cells of mouse retina in organ culture*. *Invest Ophthalmol Vis Sci*, 2001. **42**(6): p. 1370-4.
191. Matteucci, A., et al., *Neuroprotection by rat Müller glia against high glucose-induced neurodegeneration through a mechanism involving ERK1/2 activation*. *Exp Eye Res*, 2014. **125**: p. 20-9.
192. Li, Q., et al., *Diabetic eNOS-knockout mice develop accelerated retinopathy*. *Invest Ophthalmol Vis Sci*, 2010. **51**(10): p. 5240-6.

193. Dang, V., et al., *Glucosamine-induced ER stress accelerates atherogenesis: A potential link between diabetes and cardiovascular disease*. J Mol Genet Med, 2015. **9**(197): p. 10.4172.
194. Chatterjee, A., et al., *Involvement of NDPK-B in Glucose Metabolism-Mediated Endothelial Damage via Activation of the Hexosamine Biosynthesis Pathway and Suppression of O-GlcNAcase Activity*. Cells, 2020. **9**(10).
195. Ruan, H.B., Y. Nie, and X. Yang, *Regulation of protein degradation by O-GlcNAcylation: crosstalk with ubiquitination*. Mol Cell Proteomics, 2013. **12**(12): p. 3489-97.
196. Chesnokov, V., et al., *Anti-cancer activity of glucosamine through inhibition of N-linked glycosylation*. Cancer Cell Int, 2014. **14**: p. 45.
197. Park, S.H., et al., *Nonsteroidal anti-inflammatory drugs (NSAID) sparing effects of glucosamine hydrochloride through N-glycosylation inhibition; strategy to rescue stomach from NSAID damage*. J Physiol Pharmacol, 2013. **64**(2): p. 157-65.
198. Jang, B.C., et al., *Glucosamine hydrochloride specifically inhibits COX-2 by preventing COX-2 N-glycosylation and by increasing COX-2 protein turnover in a proteasome-dependent manner*. J Biol Chem, 2007. **282**(38): p. 27622-32.
199. Chien, M.W., et al., *Glucosamine Modulates T Cell Differentiation through Down-regulating N-Linked Glycosylation of CD25*. J Biol Chem, 2015. **290**(49): p. 29329-44.
200. Anello, M., et al., *Glucosamine-induced alterations of mitochondrial function in pancreatic beta-cells: possible role of protein glycosylation*. Am J Physiol Endocrinol Metab, 2004. **287**(4): p. E602-8.
201. Dostrovsky, N.R., et al., *The effect of glucosamine on glucose metabolism in humans: a systematic review of the literature*. Osteoarthritis Cartilage, 2011. **19**(4): p. 375-80.
202. Scroggie, D.A., A. Albright, and M.D. Harris, *The effect of glucosamine-chondroitin supplementation on glycosylated hemoglobin levels in patients with type 2 diabetes mellitus: a placebo-controlled, double-blinded, randomized clinical trial*. Arch Intern Med, 2003. **163**(13): p. 1587-90.
203. Virkamaki, A., et al., *Activation of the hexosamine pathway by glucosamine in vivo induces insulin resistance in multiple insulin sensitive tissues*. Endocrinology, 1997. **138**(6): p. 2501-7.
204. Hawkins, M., et al., *The tissue concentration of UDP-N-acetylglucosamine modulates the stimulatory effect of insulin on skeletal muscle glucose uptake*. J Biol Chem, 1997. **272**(8): p. 4889-95.
205. Muniyappa, R., et al., *Oral glucosamine for 6 weeks at standard doses does not cause or worsen insulin resistance or endothelial dysfunction in lean or obese subjects*. Diabetes, 2006. **55**(11): p. 3142-50.
206. Ryczko, M.C., et al., *Metabolic Reprogramming by Hexosamine Biosynthetic and Golgi N-Glycan Branching Pathways*. Sci Rep, 2016. **6**: p. 23043.
207. Hwang, J.S., et al., *Glucosamine enhances body weight gain and reduces insulin response in mice fed chow diet but mitigates obesity, insulin resistance and impaired glucose tolerance in mice high-fat diet*. Metabolism, 2015. **64**(3): p. 368-79.